CONTENTS

Contents

Summary/Samenvatting	1
Preface	3
1 Introduction	5
2 Canopy hot-spot reflectance characteristics	7
2.1 Principles of the hot-spot reflectance meter HSM	7
2.2 hot-spot reflectance and crop characteristics	9
3 Measurement programme and ground truth collection	11
3.1 Experiments	11
3.2 Ground truth collection	11
3.3 Instrumentation	12
3.3.1 The hot-spot reflectance meter HSM	12
3.3.2 The CABO hand-held reflectance meter	13
Figures	15
4 Crop growth and IR/R reflectance ratios	19
4.1 Winter wheat	19
4.2 Oats and barley	20
4.3 Maize	21
4.4 Beans	21
4.5 Beets	22
4.6 Potatoes	22
4.7 Grass	23
4.8 Bare soil	23
4.9 Summary	23
Figures	25
5 IR/R reflectance ratios versus LAI and biomass	31
5.1 Crops in 1982	31
5.2 Crops in 1983	31
5.3 Summary	32
Figures	34
6 Linear regression between HSM IR/R reflectance and LAI	37
6.1 Crops in 1982	37
6.2 Crops in 1983	40
6.3 Cereals in 1982 and 1983	42
6.4 Summary	42
Figures	45
7 Linear regression between CABO IR/R reflectance and LAI	51
7.1 Small grain cereals	51
7.2 Non-cereal crops and maize	54
7.3 Summary	55
Figures	57

8 Summary and discussion 61
8.1 IR/R reflectance and crop parameters 61
8.1.1 Leaf Area Index 61
8.1.2 Canopy biomass 61
8.2 The HSM and the CABO reflectance meter 62
8.3 Recommandations 64
Figures 67

References

Appendix I: Derivation of the canopy hot-spot reflectance properties from a radiative transfer model

Appendix II: HSM calibration algorithms

Appendix III: Test field designs

SUMMARY

In this report, the results of agricultural field experiments using the prototype active hot-spot reflectance meter (HSM) are presented. The prototype HSM is compared with a passive hemispherical reflectance meter. For both instruments, the measured infrared/red ratio throughout the growing season is related to crop growth and development. Using linear regression, relationships are established between this reflectance ratio and the crop parameter Leaf Area Index (LAI). This is done for individual crops and for groups of crops of increasing magnitude. The coefficient of correlation and the standard error of estimate SEE are used to quantify and compare the merits of both reflectance meters. The emphasis of this report is on the comparison of the two instruments and not on the determination of the relationships between canopy reflectance and LAI itself.
It is concluded that the HSM performs better than the passive reflectance meter when a) only individual crops and varieties are considered, and b) only the small grain cereals (wheat, oats, barley) are grouped. For all other clusters of crops, the passive reflectance meter performs better. Using the hot-spot concept, the expected increase in correlation between the infrared/red ratio and the LAI for groups of crops with different canopy structure, is not clearly demonstrated.

SAMENVATTING

In dit rapport worden de resultaten van veldproeven met het prototype van de actieve Heiligenschijnmeter (HSM) gepresenteerd. De prototype HSM is vergeleken met een passieve reflectiemeter. Voor beide instrumenten is de gemeten infrarood/rood ratio in de loop van het groeiseizoen gerelateerd aan de groei en ontwikkeling van het gewas. Lineaire regressie is gebruikt om de relatie tussen deze reflectieratio en de bladoppervlakte-index LAI te beschrijven. Dit is gedaan voor gewassen afzonderlijk en voor gewassen gegroepeerd in groepen van oplopende grootte. De correlatie-coëfficient en een maat voor de afwijking in de schatting (SEE) zijn gebruikt om het verschil in resultaat voor beide instrumenten kwantitatief te beoordelen. De nadruk van dit rapport ligt op de vergelijking van de twee instrumenten en niet op de bepaling van de relaties tussen gewas reflectie en de LAI zelf.
Het resultaat met de Heiligenschijnmeter is beter dan met de passieve reflectiemeter als a) enkel gewassen en gewasvariëteiten afzonderlijk beschouwd worden, en b) bij de groep van kleine granen (wintertarwe, haver, gerst). Voor alle andere groepen van gewassen is het resultaat beter met de passieve reflectiemeter. De verwachte toename in correlatie tussen de infrarood/rood-ratio en de LAI bij groepen van gewassen met verschillende gewasarchitectuur bij gebruikmaking van het heiligenschijnconcept is niet duidelijk aangetoond.

PREFACE

In 1982 and 1983 the hot-spot ('Heiligenschijn' in Dutch) reflectance from agricultural targets was measured in field experiments. The purpose of these experiments was to test the prototype Heiligenschijn reflectance meter (HSM meter) and its underlying physical concepts. The research was a joint project of the Institute of Applied Physics (TNO-TPD), the National Aerospace Laboratory (NLR) and the Centre for Agrobiological Research (CABO). The TNO-TPD designed and manufactured the prototype HSM instrument and the NLR took care of HSM instrumentation requirements, data processing and theoretic reflection modelling. The CABO took care of experimental design, ground truth collection and data interpretation. A large number of investigators and assistents was involved in the project:
NLR: N.J.J. Bunnik, R.W. de Jongh, W. Verhoef
CABO: Th. de Boer, R. Geerts, H.J.W van Kasteren, G. Noordman and D. Uenk.

Preliminary results of the experiments were reported by Bunnik et al. (1983, 1984). At the end of 1987, an effort was undertaken to summarize the results of the project, which led to the current report. The emphasis of this report is on the comparison of the active HSM with a passive hand-held reflectance meter for the monitoring of crop parameters. To quantify the differences, reflectance ratios obtained by both instruments are related to Leaf Area Index (LAI) and canopy biomass. The choice of the crop parameters is based on the importance in agricultural field research and potential monitoring applications.

This report is necessarily limited and does not provide a detailed analysis of all aspects involved in the concept of the hot-spot reflectance. However, it does provide an analysis of the comparative merits of the HSM for specific agricultural purposes.

1 INTRODUCTION

In crop and vegetation science, knowledge about the growth rate of biomass and phenological phases is important to various research approaches. Leaf area per ground area (leaf area index = LAI) is a major parameter in modelling the intercepted solar energy for estimating photosynthetic activity. As yet, the biomass and LAI in plant growth experiments are measured several times during the growing cycle, after sampling by cutting. Because this procedure is laborious and demands a rather large area for field experiments, research workers are interested in non-destructive measurements of these parameters.

Experiments with field spectrometers have shown possibilities to measure crop parameters on the basis of the reflection of incoming solar energy (N.J.J. Bunnik, 1978; J.G.P.W. Clevers, 1986). In the visible and near infrared part of the spectrum, absorption and internal reflection are related to physiological processes and plant anatomy. The morphology and geometry of a crop also have an influence on the multispectral canopy reflectance. Striking features in canopy reflectance spectra are the relatively high absorption in the blue and red parts, the local maximum in reflectance in the green part, and the high reflectance in the near infrared. For application purposes, this means that canopy reflection in these bands of the spectrum can give information about relevant botanical parameters.

In 1979, the development of a series of hand-held reflectance meters was initiated at the Centre for Agrobiological Research. Design specifications were in accordance with requirements for easy portability and direct read-out data (H.W.J.v. Kasteren, 1981; D. Uenk, 1982). However, one of the drawbacks of such passive instruments is the dependence on the momentaneous illumination conditions, e.g. cloud cover and solar elevation angle. Changes in illumination conditions induce variability in the measurements. This variability depends in particular on the canopy geometry and the chosen direction of observation. From theoretical studies it was concluded that on the one hand the measurement of directional variation of reflectance could be used as an additional feature, and that on the other hand, a standardization of the geometry of illumination and observation could be applied to eliminate variables introduced as described above. This second solution has been worked out by Bunnik (1978) and resulted in the 'Heiligenschijnmeter' (= Hot-spot reflectance meter) concept. In this concept, the canopy is actively irradiated with a flash light, and reflectance measurements are performed in the canopy hot-spot under oblique view angle of 52° off nadir. In the hot-spot centre, the direction of observation is the same as the direction of irradiant flux, and only directly irradiated canopy components and soil are observed. This new method combines the advantage of the independence of solar illumination conditions with a decreased sensitivity for the leaf angle distribution of the crop. Also, a a drastic simplification of the mathematical description of the canopy hot-spot reflectance for an oblique view angle of 52° is reached.

To evaluate the above mentioned concept, a research project was started in 1982, with a grant from the Ministry of Science Policy and the Ministry of Agriculture and Fisheries. A prototype hot-spot

reflectance meter (HSM) was built by the Institute of Applied Physics (TPD), Delft, with a grant from the Central Organization for Applied Scientific Research (TNO).
The research approach was to measure HSM reflectance of a variety of crops at regular intervals during the growing season. To quantify the advantages of the HSM, canopy reflectance was also measured using the passive, hand-held reflectance meter developed at the CABO (CABO meter). HSM measurements in the hot-spot were made at 52° off nadir viewing angle and passive measurements with the CABO meter were made at vertical viewing angle.
In 1982, the measurements were carried out at the experimental research farm 'Droevendaal' at Wageningen. Only one variety of winter wheat (Tundra) was chosen for this first test year. In order to obtain differences in growth pattern and yield, different nitrogen and fungicide levels were applied. In 1983, the measurements were carried out at the research farm 'De Schreef' at Dronten. That year, a variety of crops was chosen which included grass, beets, potatoes, beans, wheat, barley, oats and corn. Both years, HSM reflectance measurements were performed for some crops at view angles perpendicular as well as parallel to the row direction. Besides reflectance measurements, various botanical parameters were measured. Dry biomass of the crop, LAI and soil cover were measured as parameters of interest to agricultural researchers. Visual observations were made of the phenological stage, leaf colour and anomalities in growth and development.
First results of the project have been reported by Bunnik et al. (1983; 1984).

The current report deals with the comparison between the HSM and a hand-held, passive reflectance meter (CABO reflectance meter) for the determination of crop parameters. For both instruments the infrared/red reflectance ratio is studied in relation to LAI and canopy biomass during the growing season. It should be stressed that the emphasis of this report is on the comparison of the two instruments and not on the determination of the relationships between canopy reflectance and the mentioned crop parameters themselves.
The principles of the hot-spot concept are given in Chapter 2, together with theoretical considerations on relationships between HSM reflectance and crop parameters. A description of the experiments and the HSM and CABO hand-held reflectance meter is given in Chapter 3. A discussion on the HSM and CABO infrared/red reflectance ratio in relation to the development of the crops is given in Chapter 4. In Chapter 5, 6 and 7, relationships between the infrared/red reflectance ratios and the crop parameters LAI and biomass are studied for both the HSM and the CABO reflectance meter. A summary and discussions is given in Chapter 8. An evaluation is made of the specific characteristics of the HSM concept and a comparison is made between the merits of both reflectance instruments.

2 CANOPY HOT-SPOT REFLECTANCE CHARACTERISTICS

2.1 Principles of the hot-spot reflectance meter HSM

The multispectral reflectance of solar radiation by plant canopies is a complex function of the following factors:

- the optical properties of the canopy components (leaves, stalks, etc.) and of the bounding soil
- the canopy geometrical structure
- the ratio between direct solar irradiance and diffuse sky irradiance
- the sun elevation angle
- the angle of observation

Over the years, remote sensing investigators have developed a variety of passive multispectral reflectance meters for agricultural purposes. One of the drawbacks of the use of such passive instruments is the dependence on the momentaneous illumination conditions, i.e. solar elevation and cloud cover. The measured reflectance is defined as the ratio between the detected radiation of all scattering elements within the field of view, and the irradiance at the top of the canopy. The radiation from a crop canopy is composed of the single scattering of direct solar radiation by sunlit plant components and the sunlit fraction of the soil, and the components and soil observed in the internal shadow. The variability introduced by possible changes in the illumination depends in particular on the canopy geometry and the chosen direction of observation.

Standardization of the geometry of illumination and observation could be a means to eliminate variables introduced as described above. When the direction of observation is the same as the direction of irradiant flux, the resulting reflectance of non-Lambertian extended scattering volumes will increase. One cause can be the Fresnel backscatter of droplets of spherical particles present at the cuticle of leaves. In case of diffuse scattering by plant components and the bounding soil, only directly irradiated components will be observed. This results into an increase in reflectance due to the absence of internal shadow. This well-known effect is called the hot-spot ('Heiligenschijn' in Dutch) and can be observed under favourable conditions by eye by observers in the field. When the direction of observation coincides with the direction of solar irradiance, a bright circular zone is visible around the shadow of the head on the canopy. G.H Suits (1972) described the effect of the hot-spot configuration on the different scattering terms of his analytical model. This has been further elaborated by using the SAIL model developed by Verhoef (1983) as an extension of the Suits model. The canopy scattering and extinction coefficients are described as a function of the actual leaf inclination distribution function. It was found (Bunnik, 1978) that for view angles between 50° and 60°, the reflectance becomes nearly independent of the different leaf inclination distribution functions. Similar results have been reported by Warren Wilson (1965) in studies on stand structure and light penetration. He found that a particular angle exists (view angle of 57.5°), where the proportion of gap within the canopy for a given value of the leaf area index does not depend on the inclination angle of point quadrats (leaves, stems, etc.).

The development of an instrument suitable for measuring the reflectance of extended objects in the hot-spot requires the use of an active radiant source. This requirement provides another advantage of equal importance. In in-situ conditions measurements can be performed independent of (changing) illumination conditions. When an active radiant source is applied, the total radiance is equal to the radiance in the hot-spot (active) added to the radiance caused by solar and sky irradiance (passive). The hot-spot radiance itself is found by subtracting the passive radiance from the total radiance measured during illumination by the active radiant source.
The use of an artificial radiant source for a ground-based reflectance meter however, requires several adaptations of the reflectance model. The active irradiance at the canopy top is inversely proportional to the square of the distance between the radiant source and the canopy top. This is because of the divergent nature of the flashlight, compared with the parallel rays of the incoming solar radiation. A measurement in a single spectral band will therefore depend on the distance. To eliminate this distance effect as much as possible, ratios of radiance values measured in different spectral bands are taken. Such ratios provide yet another advantage. The sensitivity of the measurement to changes in the optical characteristics of the soil background caused by varying soil moisture conditions is reduced. The reflectances in the optical and near infrared part of the spectrum are about equally affected by variations in soil moisture.

Summarizing, the active HSM concept should offer the following advantages for canopy reflectance measurements over passive instrumentation used so far:

- the use of an artificial radiant source eliminates the variability due to changes in illumination conditions, e.g cloud cover, solar elevation angle
- the angle of observation between 50° and 60° view angle reduces the influence of the leaf inclination distribution function, i.e. canopy geometry
- the measurement in the hot-spot greatly simplifies the mathematical description of the canopy reflectance

This means that HSM reflectance values depend mainly on the optical properties of the scattering plant components and the bounding soil. By taking the ratios of reflectance values in different spectral bands, the sensitivity to varying soil moisture conditions is greatly reduced.
Curves of HSM reflectance values versus crop parameters in time, like biomass, soil cover or LAI, are expected to be smoother in appearance than similar curves of passive reflectance values. Furthermore, relationships between HSM reflectance and plant characteristics are easier to model on a mathematical basis.

In appendix I, the canopy hot-spot reflectance properties are derived from a radiative transfer model. The model applied by Bunnik (1978) is the same as developed by Suits (1972), and a further elaboration of the hot-spot reflectance is based on an extended model for arbitrary inclined leaves developed by Verhoef (1983). The implementation of the adaptations in the reflectance model, due to the use of an artificial radiant source, is also described.

2.2 HSM reflectance and crop characteristics.

Canopy reflectance in the visible light region can be approximated by the single scattering contribution. Reflectance will decrease with increasing soil cover until the fraction of the directly irradiated soil can be neglected. Measurements in the combined green and red parts of the visible light region will provide information on changes of the concentration of absorbing pigments. In the near infrared part of the spectrum, the contribution of multiple scattering increases. This will result in a further increase of reflectance after complete soil cover, until the asymptotic maximum reflectance is reached. Based on these considerations, three spectral passbands were chosen for the prototype HSM:

1: 870 nm: minimum value of green leaf absorption
2: 670 nm: maximum value of green leaf absorption
3: 550 nm: relative minimum of green leaf absorption

From the mathematical description in appendix I, the following relations between HSM reflectance and crop characteristics can be expected:

- the near infrared/red reflectance ratio will be a monotone increasing function of the LAI.
- the green/red reflectance ratio will (for green leaf canopies) increase until maximum soil cover is reached.
- if a high correlation exists between LAI and biomass, the reflectance ratios can be used to estimate the biomass.
- for the oblique view angle of 52°, the canopy reflectance should be uniquely related to apparent soil cover. By oblique observation, the apparant soil cover will reach its maximum before the perpendicular soil cover will be maximum. However, the observation in the hot-spot will provide a deeper penetration of the lines of sight since they coincide with the penetrating radiant flux.
- By the single scattering approach, the green/red reflectance ratio for dense crop canopies becomes equal to the ratio of the single leaf reflectance values. Since this last parameter is a function of leaf colour only, this ratio will be an estimator of variations of the concentration of absorbing pigments.

Bunnik et al. (1984) confirmed some of these expectations in a first analysis of the measurement results. They concluded that the sensitivity of the HSM infrared/red ratio to the increase in canopy biomass and LAI is high during the whole vegetative stage for winter wheat, potatoes and sugar beets. During the generative stage of cereals, the increase in biomass is detected because of the change of the plant colour in the ripening and senescing phase. The green/red ratio can be applied as an estimator of the colour of the plant components.

In this report, relationships are studied between canopy infrared/red reflectance and the crop parameters LAI and dry canopy biomass of all above-ground plant material. For this purpose, simple linear regression techniques are used. Both HSM and CABO reflectance measurements are included in the analysis to enable the comparison of the merits of both instruments. Because of the reduced influence of the canopy geometry (leaf angle distribution function) at 52° view

angle, various crops of different geometrical structure but with similar optical characteristics (e.g. leaf colour) are expected to have similar relationships between HSM reflectance and the mentioned crop parameters. Differences in relationships will be mainly due to differences in optical properties of the canopy components. Deviations from derived relationships may occur at any part of the growing season due to variations in nutriental status or to the presence of diseases or water stress when they affect the optical properties of the canopy components.

3 MEASUREMENT PROGRAMME

3.1 Experiments

In 1982, six plots of 10 x 10 meter each were sown with one variety of winter wheat Tundra at test farm 'Droevendaal' in Wageningen. To obtain biomass and yield differences, the following treatments in nitrogen were given to the six plots of Tundra: plots 1 and 4 received a single dose of 50 kg/ha (treatment 1), plots 3 and 6 one dose of 50 and another dose of 150 kg/ha (treatment 2), and plots 2 and 5 three doses of 50 kg/ha (treatment 3). Furthermore, plots 4, 5 and 6 were treated with fungicide, while plots 1, 2 and 3 were left untreated. A design of the test site is given in Appendix III.
During the growing season from April to August, HSM reflectance was measured twice a week, both across and along the row direction of the crops. The CABO reflectance meter was used only on plot 1 during the first three months of the growing season. CABO reflectance measurements were made at vertical viewing angle.

In 1983, the hypothesis of the insensitivity of HSM reflectance for differences between leaf inclination distribution and the application to other crop types was tested. At test farm 'De Schreef' near Dronten, fourteen test fields of 18 x 19 meter were prepared. A design of the test site is given in Appendix III. The selected crops were: sugar beet, potato, stembean, grass, maize, oats, spring barley and four winter wheat varieties with different canopy structure (Arminda, Okapi, Donjon, Durin). One field was kept bare during the whole growing season. All crops had a row direction across the view direction of the HSM. For potatoes and the winter wheat variety Arminda, extra fields with row direction along the HSM-view direction were added.
To increase the speed and the accuracy of the measurement procedure, the HSM was moved along the test plots by means of a rail system (Fig. 3.1). HSM reflectance was measured twice a week. Six measurements were made in one part of each test field. The HSM head was situated at about 4.0 meter above ground level which resulted in an irradiated spot at ground level of about 3 m2. The remaining part of the field was used for ground truth determination. CABO reflectance was measured during the whole growing season for all crops except for maize. After the 5th of August this crop was too tall to make measurements with the CABO meter.

3.2 Ground truth collection

Visual observations on crop growth and development were recorded on all dates of measurement. For a more quantitative description, various crop parameters were measured during the growing season. For all crops, the mean canopy height was measured in the field. The apparent soil cover was estimated from visual observations and from slides taken at perpendicular view angle. Biomass and LAI were measured on a crop specific base:

- For cereals (winter wheat, spring barley, oats), a sample of 2 rows of 1 meter length (0.5 m2) was taken every week. A subsample of 100 stems was used for dry biomass and LAI assessment. After heading, the subsample was split into ears, stems and leaves for individual determination of biomass and LAI. The development of the cereals was

described on a decimal scale.

- For maize, samples of 3 m2, and later of 1.5 m2, were taken for determination of LAI and biomass The same measurement procedure was followed as for cereals.

- For potatoes and beets, 10 sample plants were harvested every week to measure above and underground fresh biomass. Three representative plants were divided in leaf blade and leaf stem for determination of dry biomass and LAI.

- In the stembean field, a row of 4 meter length (2 m2), and later of 2 meter (1 m2), was harvested for fresh biomass determination. From these samples, 10 representative plants were divided in stems, leaves and pods for individual dry biomass and LAI assessment.

- For the determination of the fresh biomass of grass, samples of 0.25 or 0.50 m2 were harvested. LAI was not measured.

Since reflectance was measured twice a week and ground truth was collected once a week, the ground truth data were interpolated and smoothed in time. The weighed average over a period of 10 days before and after measurement was used to assess the ground truth parameters for each date of measurement. This also served the purpose of smoothing the relatively large fluctuations in the measured values. In 1982, the differences between the six fields of winter wheat were rather small, and the variation in measured crop parameters within each field quite large. Soil cover and growth stage were taken as an average for all fields during the whole growing season. The fresh and dry biomass, crop height and LAI were measured for each individual field only after May 21st and June 1st (LAI). During the first part of the growing season an average value was taken for these parameters as well (Fig. 3.2).

Meteorological data (temperature, irradiance, rainfall, speed and direction of wind) were collected in both years from local meteorological stations. The wetness of the soil surface was estimated in the field and expressed as a value on a 1 (very dry) to 5 (very wet) scale. In 1982, the wetness of the soil surface was taken as an average for all fields.

For easy analysis and interpretation of the measurements, a database containing the ground truth information as well as the calibrated reflectance measurements was set up. A software package was developed to produce graphical and numerical output of selected information stored in the database.

Detailed reports on the ground truth collection are given by R. Geerts (1982) and H. Noordman (1983).

3.3 Instrumentation

3.3.1 The hot-spot reflectance meter HSM

A prototype hot-spot reflectance meter, based on the use of an active radiation source has been designed and built by the Institute of Applied Physics TPD in the Netherlands (Fig. 3.1). A commercially

available flashlamp with the required spectral range has been selected as radiation source. The reflector of the flashlamp has been replaced by an especially designed reflector providing a diverging radiant flux. The imaging system of the sensor is a modified photographic camera. Two beam splitters and three band filters have been used to measure the reflected radiation in three spectral bands. These are centered at 550 and 670 nm with 10 nm bandwidth and at 870 nm with 20 nm bandwidth. A field lens is applied to image the entrance pupil at infinite distance. This eliminates the need to adjust the focal length with varying distances of measurement.

The measurement configuraton is schematically represented in Fig. 3.3. The radiation source and the sensor system are mounted in the HSM head, which can be elevated above the ground by means of a tripod. The footprint of the sensor system is a curved surface around the centre view angle of 52°. The active radiation source illuminates a larger area surrounding the footprint. The maximum variation of the radiant intensity within the field of view relative to the average intensity remains within 15 %. The canopy reflectance attributed to the hot-spot reflectance due to the flashlight is measured by subtracting the estimated canopy reflectance caused by the solar and sky irradiance at the moment of maximum flashlight intensity. This estimation is obtained by means of linear interpolation between the measurements of the passive reflectance five milliseconds before and after the activation of the flashlamp.

Fig. 3.4 presents a simplified functional scheme of the HSM signal handling. The HSM control module is used to operate the sequence of measurements during the active mode. After the introduction of annotation by the user, the measurement is automatically performed after a start command. At the moment of maximum flaslight intensity the detector signals are measured. The analog signals of the three sensor detectors are simultaneously amplified by means of a low and high gain amplifier to obtain the required dynamic range. The analog signals are converted to 12-bits digital data. Auxiliary signals of the flashlight intensity are obtained in the same spectral bands for each measurement to correct for variations in the light source. Data are recorded on digital cassette tape, together with a time and day code and with annotation added by the operator. After conversion to computer compatible tape, the raw data are screened for measurement errors and preprocessed, calibrated and converted to reflectance data. The hot-spot reflectance ratio's infrared/red and green/red are calibrated relative to the reflectance ratio's for a standard white reflectance panel as determined in the laboratory. HSM calibration algorithms are given in Appendix II.

3.3.2 The CABO hand-held reflectance meter

The CABO reflectance meter was designed and developed by the Technical and Physical Engineering Research Service (TFDL) Wageningen. It consists of a sensor unit mounted at the end of a 2 m long rod and is linked with a processing unit in a portable bag. The processing unit is equiped with a direct read-out facility of the reflectance values by means of a connection to a programmable calculator.

The sensor unit is schematically represented in Fig. 3.5. The unit contains two silicon photo cells; one facing upward to measure the

hemispherical (= solar + diffuse sky) irradiance, and one facing downward to measure the radiation of all elements in the field of view. The effect of the elevation angle of the sun is corrected by an especially shaped diffusing glass at the upper side of the sensor unit. The field of view at the underside can be determined with changeable diaphragms.
Three band filters are used to measure the radiation in three spectral bands, centered at 654 nm and 823 nm with a bandwidth of 31 nm, and at 548 nm with a bandwidth of 80 nm. These filters are fixed onto a drum which rotates around the photo cells. In one rotation, 6 measurements are recorded, one in each band upward and downward, and sent to the processing unit. By dividing the signal value for reflected radiation per band by the corresponding value for incoming irradiance, output is available that is proportional to the coefficient of reflection.
The amount of time needed for one measurement is 0.5 seconds and for the processing of the signal 5 seconds. This is about the same time as required in the field to walk from one sampling place to another.

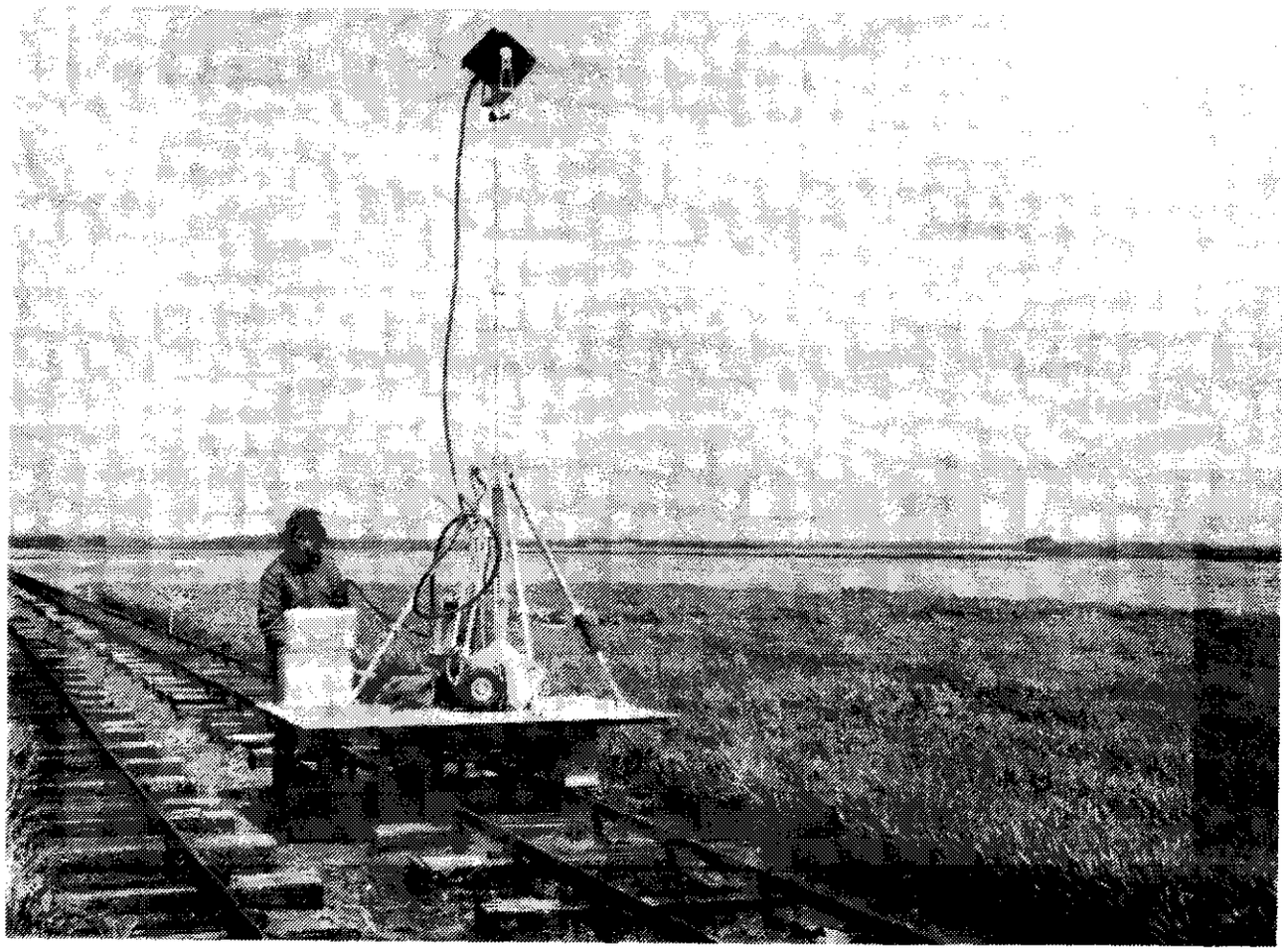

Fig. 3.1: the prototype HSM in use during the measurement programme at the test site in Eastern Flevoland in 1983.

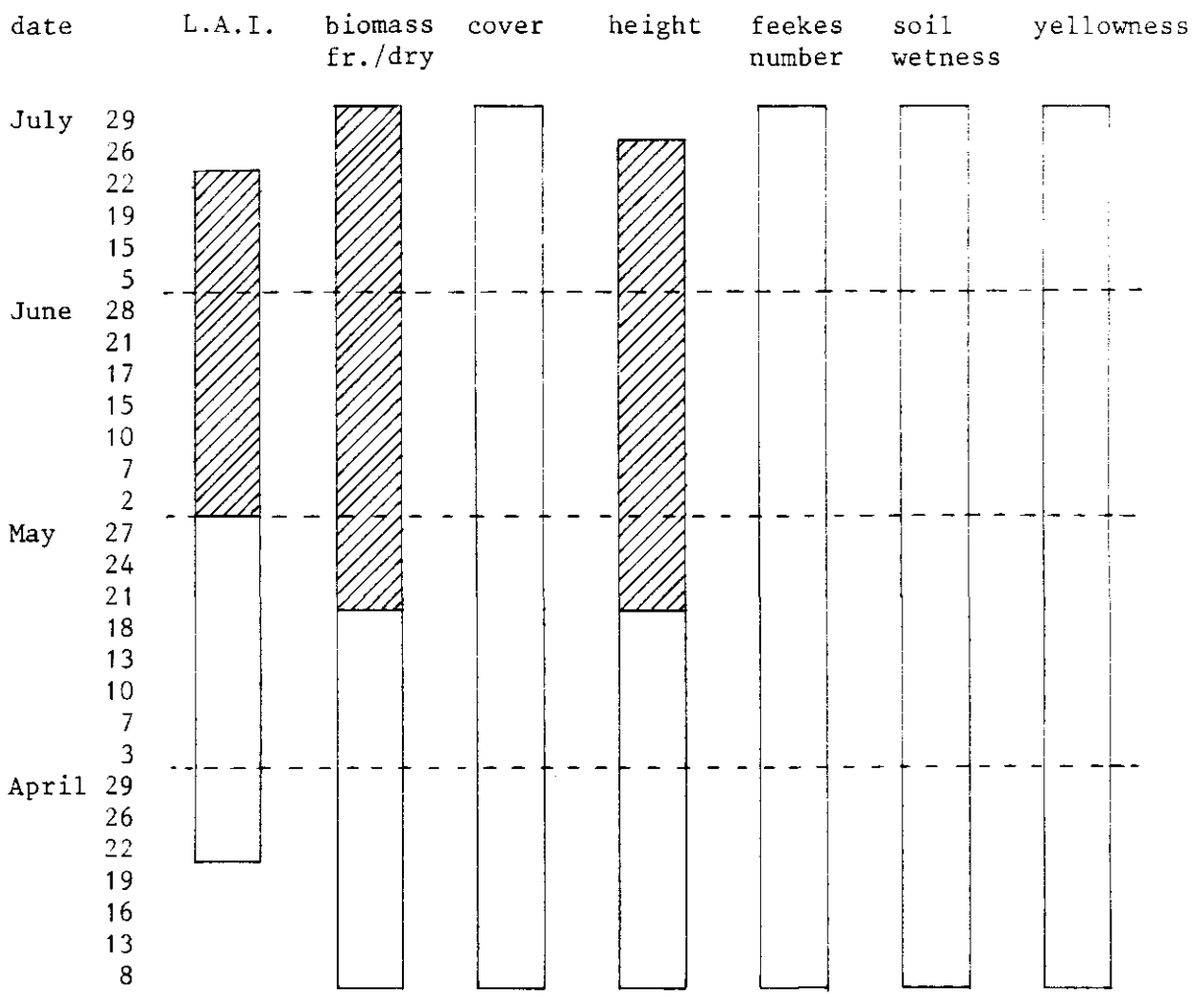

Fig. 3.2: Diagram of the collected ground truth at the fields of winter wheat during the measurement programme in 1982. The shaded bars represent ground truth collected on individual fields and the blank bars represent the ground truth collected as an average for all fields.

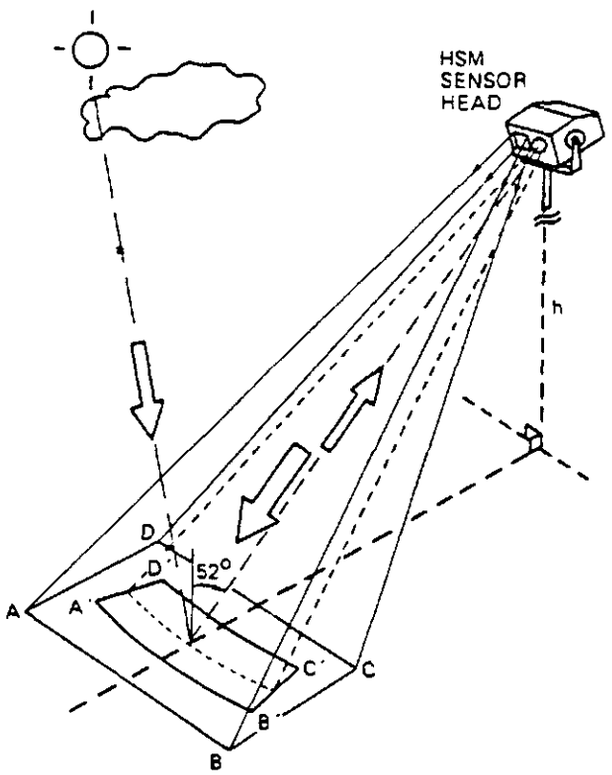

Fig. 3.3: HSM measurement configuration. The artificial radiant source and the sensor system are installed in the HSM sensor head. The curved footprint with a centre angle of view of 52 , A'B'C'D' lies within the area ABCD irradiated by the radiant source. The object is irradiated by the flash and the sun and the sky.

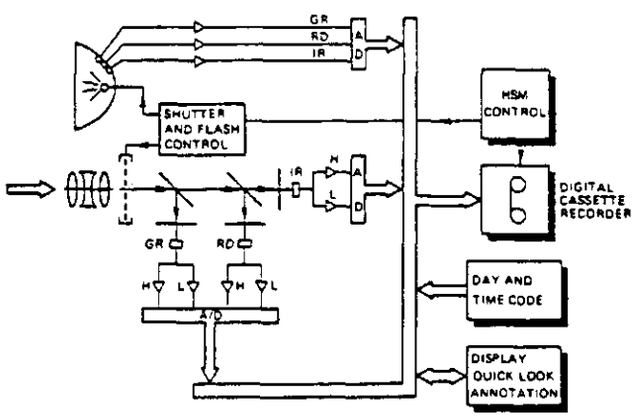

Fig. 3.4: functional scheme of the HSM.

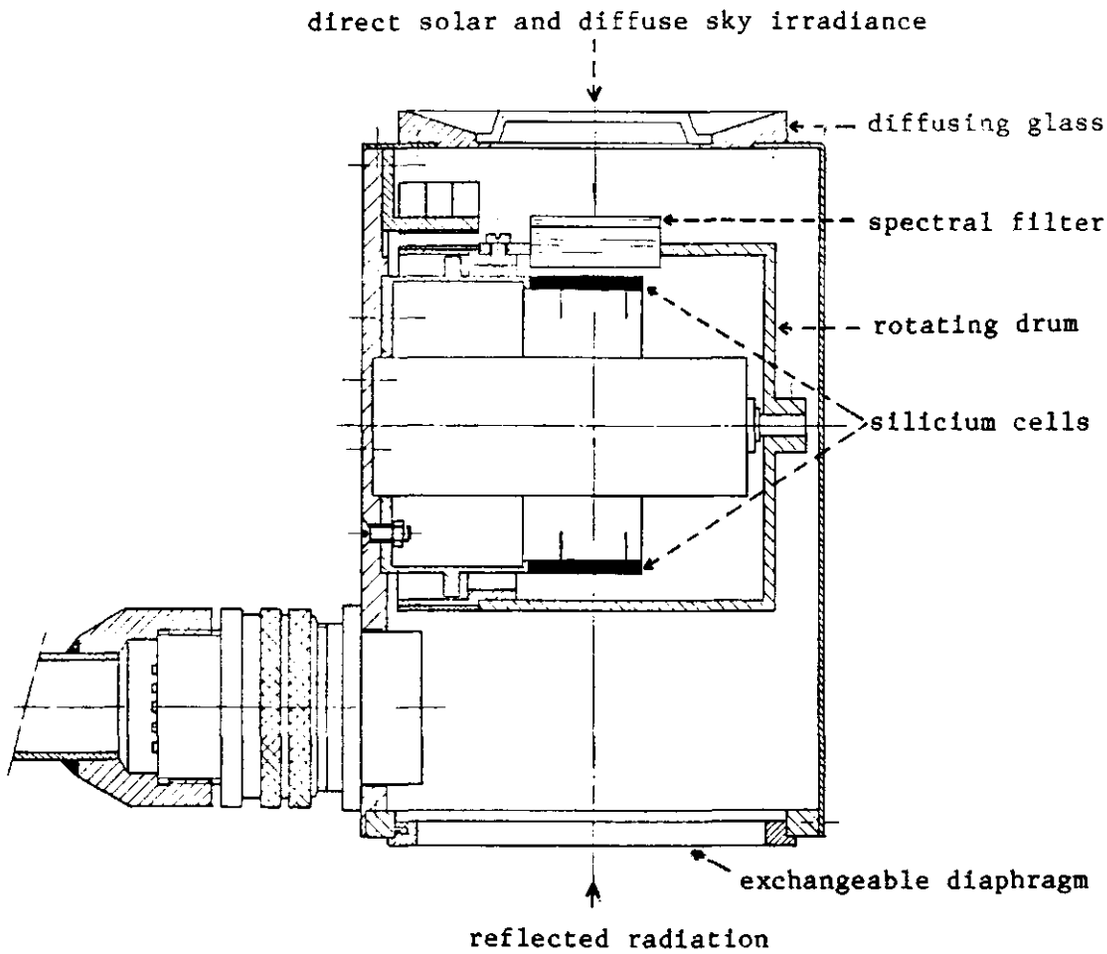

Fig. 3.5: schematic representation of the sensor unit of the CABO hand-held reflectance meter.

4 CROP GROWTH AND IR/R REFLECTANCE RATIOS

This chapter presents the IR/R reflectance curves of crop canopies for the HSM and the CABO reflectance meter. Because of the relative penetration capability of radiation in the near infrared part of the spectrum, ratios including IR reflectance seem most suitable for the determination of the amount of vegetative material, i.e. biomass and/or LAI. Therefore, the analysis is concentrated on the IR/R reflectance ratios during the growing season in relation to crop growth and development. Other reflectance ratios containing information about the colour of the vegetative material, e.g. green/red are not included in this study. Because of the HSM concept, the emphasis is on canopy structure and on the changes therein during the growing season. The discussion on crop reflectance and crop characteristics is therefore necessary limited and does not pretend a detailed analysis of all reflectance influencing factors.

4.1 Winter wheat

Smoothed values of dry canopy biomass and LAI of winter wheat in 1982 and 1983 are given in respectively Fig. 4.1 and 4.3. For 1982, average values are presented of the six plots of the winter wheat variety Tundra. For 1983, the biomass and LAI values of the varieties Arminda, Donjon, Durin and Okapi are averaged. The averaged HSM and CABO IR/R ratios are given in Figs. 4.2 and 4.4 for 1982 and 1983 respectively.

Winter wheat, like all cereals, is characterized by clearly defined phenological stages in its growth cycle. After germination, small seedlings appear above the ground which form small leaves and the first lateral stems. During the tillering stage in April, the observed IR/R ratio remains constant and is dominated by the soil reflectance. With further growth, biomass and LAI increase. From the moment that lateral stems are formed, the IR/R ratio increases sharply. This increase continues until a maximum is reached near the moment that the the flag leaf appears.
After flowering, the appearance of the crop canopy changes drastically with the formation of the ears. Reallocation of energy and nutrients takes place from the leaves and stems to the ears. Fresh biomass and LAI reach a maximum and then start decreasing with the ripening of the crop. The dry biomass increases until just before harvest. During the generative phase, the IR/R ratio is a monotone decreasing function in time. This is caused mainly by the increase in red reflectance due to yellowing of the crop and to some extend by the decrease in infrared reflectance due to decreasing leaf area and soil cover.

There is a positive correlation between the LAI and the IR/R ratio during most part of the growing season. Both parameters are increasing during vegetative growth and decreasing during the generative phase and ripening. The moment the maximum is reached is in general the same for both parameters, just before heading. The correlation between dry biomass and the IR/R ratio is positive in the vegetative phase of the growing season, and negative in the generative phase and during ripening.

In Fig. 4.2, the results of HSM measurements along-row and across-row are shown. The general shape in the curves is similar but

the level of IR/R reflectance is considerably lower at along-row view angle. This can be explained by the fact that at along-row view angle, more bare soil is visible than at across-row view angle.

In Fig. 4.4, the IR/R reflectance ratio of the HSM is compared with the IR/R ratio of the CABO meter. The shape of the curves is nearly identical but the level of the CABO reflectance ratio is higher. With the exception of only two dips in June, the CABO IR/R reflectance curve is as smooth as the HSM IR/R reflectance curve.

The different applications of nitrogen fertilizer and fungicide in 1982 on the Tundra plots did not result in the desired differentiation in growth and development. The within-field variations in crop parameters were larger than the variations between the average values of the six plots. Therefore, no relationships could be determined between the different treatments and growth and development of the crop, nor between the treatments and the IR/R reflectance curves.

4.2 Oats and barley

Oats and barley have a growth cycle that is comparable to that of winter wheat. Crop growth and development is illustrated in the Figs. 4.5/4.8 which give the smoothed values of LAI, dry biomass, and the HSM and CABO IR/R reflectance ratios with time.
During the vegetative phase, the LAI is increasing in time and during the generative phase and ripening, the LAI decreases again. Dry biomass is a continuously increasing function of time until the end of the growing season.
The HSM IR/R reflectance curve is for both crops similar in shape to that of winter wheat. However, no clear relationship exists between the IR/R ratio and the LAI. In general, the HSM IR/R ratio increases with LAI during the vegetative period. With oats, both the LAI and the IR/R ratio reach their peak value around June 10th. The LAI then decreases gradually within two months to a level of practically zero while the IR/R ratio decreases quickly within five weeks to the level of soil reflection. With barley, the LAI reaches its peak value already at the beginning of June and then gradually decreases within two months to a near zero level. The IR/R reflectance ratio reaches a peak value at the beginning of July and quickly decreases within 4 weeks to the level of soil reflection. The peak value of HSM IR/R reflectance is lowest for barley (maximum reflectance is 11), medium for oats (maximum reflectance is 14), and highest for winter wheat (maximum reflectance is 18).
The CABO IR/R reflectance curves of oats and barley differ from the HSM IR/R reflectance curves and are also different from those of winter wheat. During the period of vegetative growth, the CABO IR/R reflectance is not a smoothly increasing curve to a maximum value. For both crops, a plateau with relatively large fluctuations exists from the end of May to the end of June. After the end of June, the IR/R reflectance reaches a maximum value and then declines during the rest of the growing season.
Contrary to winter wheat, the CABO IR/R reflectance is of the same magnitude as the HSM IR/R reflectance for oats and barley. The HSM IR/R reflectance curves are smoother in appearance than the CABO IR/R reflectance curves.

4.3 Maize

Maize has a growth cycle with a distinct vegetative and generative phase. During the first two months of vegetative growth, LAI and biomass increase, as do the IR/R ratios, Figs. 4.9 and 4.10. The HSM IR/R ratio is presented for the whole growing season while the CABO IR/R reflectance is measured until the beginning of August only.
At the end of the vegetative phase, the crop has attained its maximum height together with soil cover. During heading, The visual appearance of the canopy changes due to structural changes, formation of cobs and panicles, and to changes in plant colour. The colour of the canopy top becomes more important. In the midst of August, the HSM IR/R reflectance ratio reaches its maximum value. Thereafter it decreases again to level off at a value of about 50% of the maximum value. The LAI and dry biomass reach their peak value simultaneously three weeks later towards the end of the growing season. In this respect, crop development of maize differs from that of the other cereals. The LAI is a monotone increasing function in time throughout most of the growing season. For wheat, barley and oats, the LAI reaches a maximum value at the end of the vegetative phase and then starts to decline again.

The IR/R ratio only correlates with the LAI and the dry biomass during the vegetative period. After flowering, the IR/R ratio decreases while the LAI and the dry biomass still increases for a while.

4.4 Beans

During the vegetative phase of the growth, i.e. the first five weeks after sowing, stem elongation takes place and green leaves increase in size and number. In the sixth week, the first flowers appear and pod formation starts. Crop parameters were only measured from the fourth week after sowing until the harvest. Figs. 4.11 and 4.12 give the growth in LAI, biomass and the HSM and CABO reflectance ratios IR/R in time.
From the beginning of July until the midst of August, the LAI gradually increases in time. In the second half of August the LAI decreases again. The IR/R ratios sharply increase from the beginning of July until a peak value is reached only one month later at the end of July. At that moment, the pods are clearly visible and maximum soil cover is attained. The IR/R ratios then start decreasing while the LAI and fresh biomass keep increasing for two more weeks. The decrease of the ratios during these two weeks might be explained by the fact that the crop appears to be more flattened and spread out, the maximum crop height being attained after about six weeks. The decrease in the IR/R ratios after these two weeks can be attributed to the gradual change in crop colour from green to yellow and the decreasing soil cover. The dry biomass increases until just before harvest when the plants have turned yellow and dry.

There is a positive correlation between the IR/R reflectance and the LAI and dry biomass only during the short period of the first month after emergence. Then again in the second half of August, the IR/R ratios decrease with decreasing LAI. The CABO IR/R reflectance curve is similar in shape to the HSM IR/R reflectance curve, but the level of the ratio is generally higher. There is no difference in smoothness of the curves.

4.5 Beets

This crop has a canopy morphology which does not change much in time when compared with the previous crops. After emergence, the leaves increase in size and number with the progress of the growing season. Contrary to the cereals and beans, no stem elongation, flowering, fruit setting or ripening takes place. Minor architectural changes may occur whith the drooping of leaves at periods of water stress.
Crop growth and development is given in Fig. 4.13 and the IR/R reflectance ratios are given in Fig. 4.14. Three weeks after sowing, the LAI, biomass and soil cover start to increase rapidly, until maximum soil cover is reached at the end of August. From there on, both LAI and dry biomass increase only relatively slowly. The IR/R reflectance ratios increase rapidly from three weeks after sowing until the end of August. From there on the IR/R ratios slowly start to decrease.
The general trend in CABO IR/R reflectance is similar to that in HSM IR/R reflectance, though the level of the ratio is higher. The HSM IR/R reflectance curve is slightly smoother in appearance than the CABO IR/R reflectance curve.
Until August, there is a positive correlation between LAI and dry biomass versus both IR/R reflectance ratios.

4.6 Potatoes

During the period of vegetative growth, stem elongation takes place and the leaves increase in size and number. The period of vegetative growth is followed by a period of flowers emerging at the top of the crop canopy. Furthermore, the following change in appearance during the growing season can be observed. After emergence, the plants first grow on the ridges and fill in the gaps between them. In this period they also grow upward and the LAI, soil cover and biomass increase steadily. At the end of this period, the plants grow sideways in the space between the ridges and decrease in height. The LAI and dry biomass reach a maximum and remain practically constant until the end of September. Maximum soil cover is reached in the last week of August. The growth of the crop is illustrated in Figs. 4.15, while the HSM and CABO IR/R reflectance ratios are given in Fig. 4.16. The HSM measurements are given for both view angles along and across the direction of the ridges.
During the first period, from June until September, the IR/R ratios correlate with the LAI and dry biomass. The HSM IR/R ratio for the field with view direction across the ridges is higher than the ratio for the field with view direction along the ridges. This can be explained by the larger fraction of bare soil that can be seen at view angles along the ridges. At the end of August, the ratios for both view angles become almost the same. After August, the correlation between the IR/R ratios versus LAI and biomass disappears. The IR/R reflectance ratios decrease while the LAI and biomass hardly change. This could be caused by the yellowing and lodging of the crop canopy which results in increasing values of the red reflectance.
The CABO IR/R reflectance curve is similar in form to the HSM IR/R reflectance curve, while the level of the ratios is higher. Both curves display fluctuations which might be caused by the influence of wind and rain. These weather influences change the visual appearance and the soil cover of the crop canopy almost daily.

4.7 Grass

Three cuttings took place in 1983, which resulted in three growth cycles. The growth in biomass and the IR/R reflectance ratios are given in Figs. 4.17 and 4.18 respectively. With the progress of the season, the observed IR/R ratios increase more slowly after each cutting. This can be explained by the decrease in growth rate of the grass. There is a clear relationship between biomass and the IR/R ratios from the moment the grass is cut back until an amount of dry biomass of about 0.25 kg/m2 (= 2.5 t/ha) is reached. At this moment, the biomass is still increasing while the IR/R ratios start to fluctuate. The CABO IR/R reflectance is higher than the HSM IR/R reflectance.

Because of the specific nature of grass as compared to the other crops, it is not considered for further analysis in this report.

4.8 Bare soil

In Fig. 4.19, the HSM and CABO IR/R reflectance is given for the bare soil plot, together with the estimated topsoil moisture classes. For both reflectance meters, almost total elimination of the influence of topsoil moisture is attained by taking the ratios of reflectance values in individual bands. The changes in soil surface structure from smooth and slaked, to cracked and crumbly, do not have a significant effect on the IR/R ratios. The average value for the HSM IR/R bare soil reflectance is 1.30, and for the CABO IR/R bare soil reflectance 1.16, both with a standard deviation of 0.07 (number of observations is 44).
Different types of tillage did not notably affect the level of the reflectance ratios.

4.9 Summary

The previous exercise confirms the complexity of the reflectance from crop canopies given in Chapter 2. With regard to possible relationships between the IR/R reflectance and the crop parameters LAI and biomass, the following is concluded:

During a part of the period of vegetative growth, the HSM IR/R reflectance ratio is positively correlated to dry biomass and LAI for all crops. The same is true for the CABO IR/R reflectance with the exception for oats and barley. However, the duration of the period for which this correlation exists differs for different crops. For some crops this period is limited to about four weeks (beans) while for other crops it lasts for about two months (potatoes). Also, the limits of the periods are not well defined. Sometimes the change from one phenological stage to another (wheat) marks the end of the period while other times the limits are less clear (beans, maize).
During the period after vegetative growth, both HSM and CABO IR/R reflectance ratios decrease in time for all cereals (wheat, oats, barley, maize), beans and potatoes. For cereals, the LAI also decreases in the period of generative growth and ripening. The decrease in IR/R reflectance, however, is also caused by changes in the colour of the crop canopy. Therefore, the relationships between IR/R reflectance and LAI are more complex during the generative stage of the growing season. For maize, the LAI keeps increasing while the

HSM IR/R reflectance decreases two weeks after cob appearance; for beans and potatoes, the LAI remains practically constant while both the HSM and CABO IR/R reflectance ratios decrease; for barley, both HSM and CABO IR/R reflectance ratios only start decreasing one month after the LAI starts decreasing; for wheat, the moment that the LAI starts decreasing coincides with the moment the IR/R ratios start to decrease.

From these observations, it is concluded that not only the LAI but especially the geometry of the canopy and the colour of the canopy components (leaves, stems, ears) affect the IR/R reflectance ratio. Therefore, the existence of a correlation between the LAI and the IR/R reflectance ratio only indicates a similar trend in both parameters during a certain time span.

For all crops except for oats and barley, the CABO IR/R reflectance is continuously higher than the HSM IR/R reflectance. The general shape of the IR/R reflectance curves is identical. In only a few cases, the CABO IR/R reflectance curves show more fluctuations than the HSM curves. For oats and barley, the shape of the CABO IR/R reflectance curves deviates from that of the HSM IR/R reflectance curves. The CABO curves for these two crops also show considerably more fluctuations.

For both reflectance meters the influence of soil surface roughness and moisture content is satisfactorily reduced by taking the ratios of the reflectance values in individual bands. The variety in weather conditions during CABO measurements in the growing season of 1983 ranged from very sunny to extremely cloudy (Noordman, 1984). This diversity in illumination conditions resulted a few times only in a more fluctuating IR/R reflectance curve with the CABO meter than with the HSM. Since the standard deviation in the average IR/R reflectance of bare soil is the same for both meters, it may be concluded that taking ratios of reflectance values might also be useful in reducing the influence of varying illumination conditions for the CABO meter.

In the next Chapter, HSM and CABO reflectance ratios are analysed in relation to the crop parameters LAI and biomass. For this analysis, periods of the vegetative stage of the growing season with a distinct correlation between the IR/R reflectance and the LAI or biomass are selected. Various crops are grouped together in order to evaluate the influence of canopy structure on the reflectance ratios obtained with the two instruments.

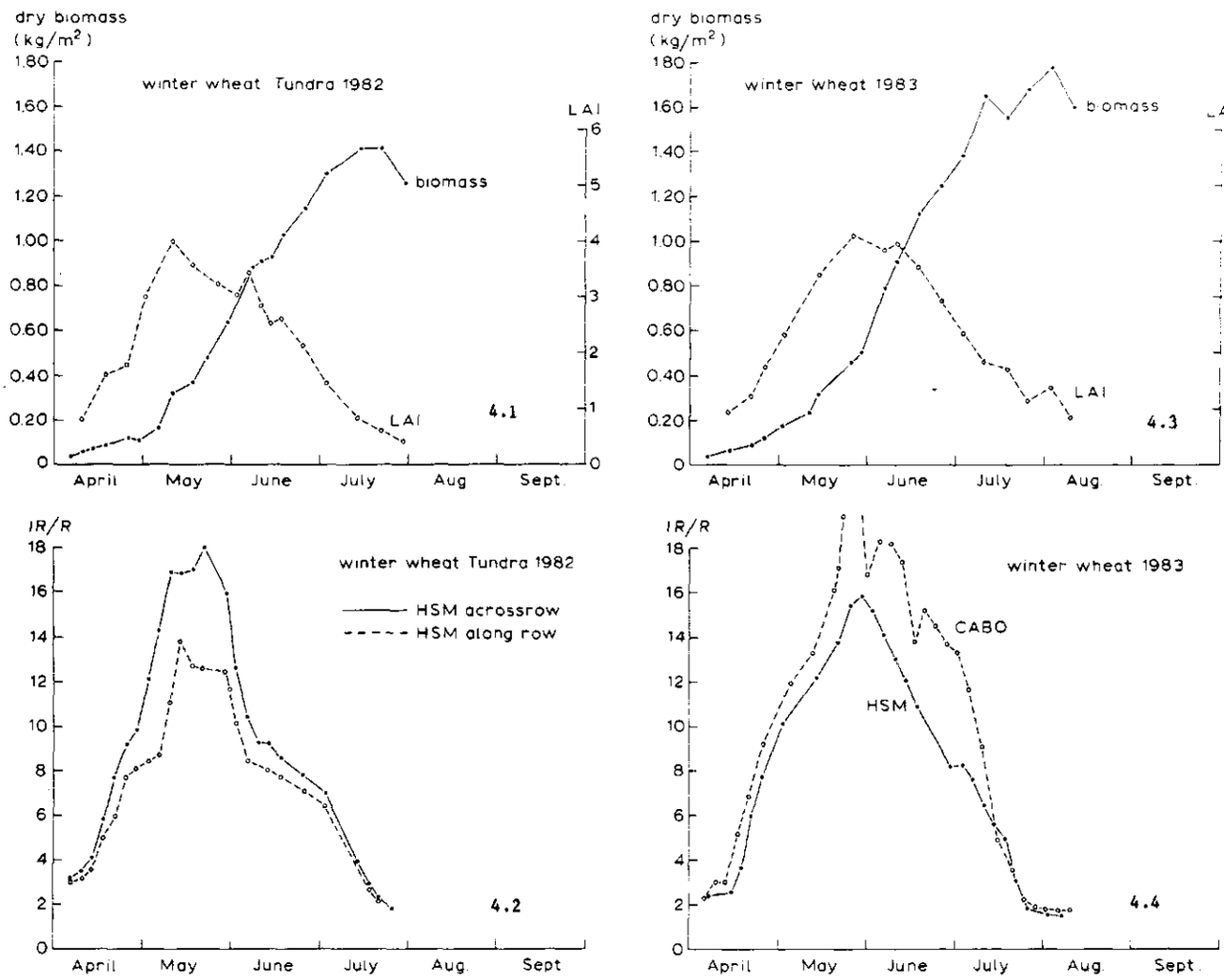

Fig. 4.1: smoothed values of the LAI and the dry biomass of the crop canopy during the growing season as an average of six fields of Tundra winter wheat, 1982.

Fig. 4.2: IR/R reflectance ratio during the growing season with the hot-spot reflectance meter (HSM) as an average of six fields of Tundra winter wheat, 1982. The HSM IR/R reflectance ratios are given for the measurements across the row direction of the crop and along the row direction.

Fig. 4.3: smoothed values of the LAI and the dry biomass of the crop canopy during the growing season as an average of the winter wheat varieties Arminda, Donjon, Durin, Okapi in 1983.

Fig. 4.4: IR/R reflectance ratio during the growing season with the HSM and the CABO reflectance meter as an average of the winter wheat varieties Arminda, Donjon, Durin, Okapi in 1983.

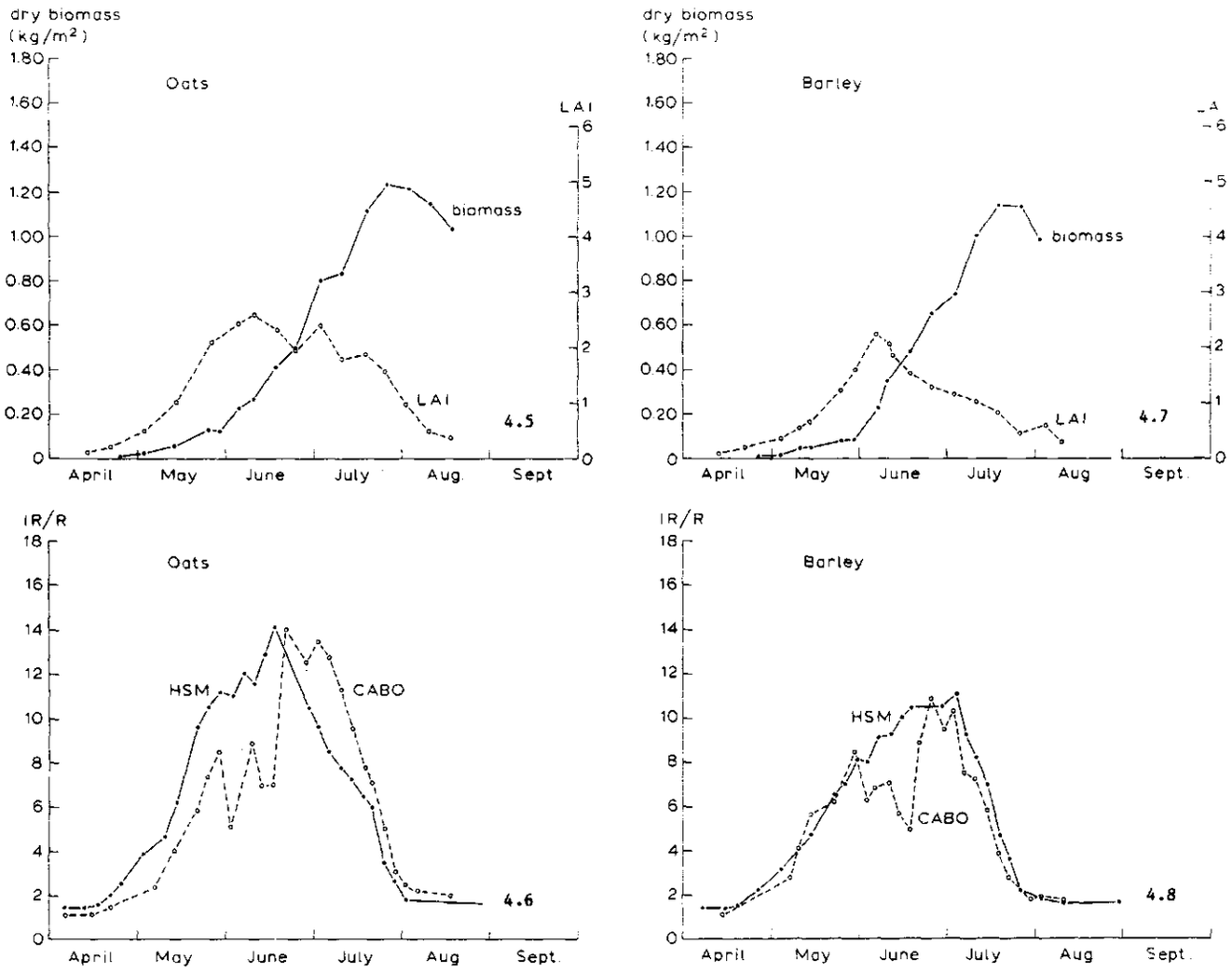

Fig. 4.5: smoothed values of the LAI and the dry biomass of the crop canopy of oats during the growing season, 1983.

Fig. 4.6: IR/R reflectance ratio of oats during the growing season with the HSM and the CABO reflectance meter, 1983.

Fig. 4.7: smoothed values of the LAI and the dry biomass of the crop canopy of barley during the growing season, 1983.

Fig. 4.8: IR/R reflectance ratio of barley during the growing season with the HSM and the CABO reflectance meter, 1983.

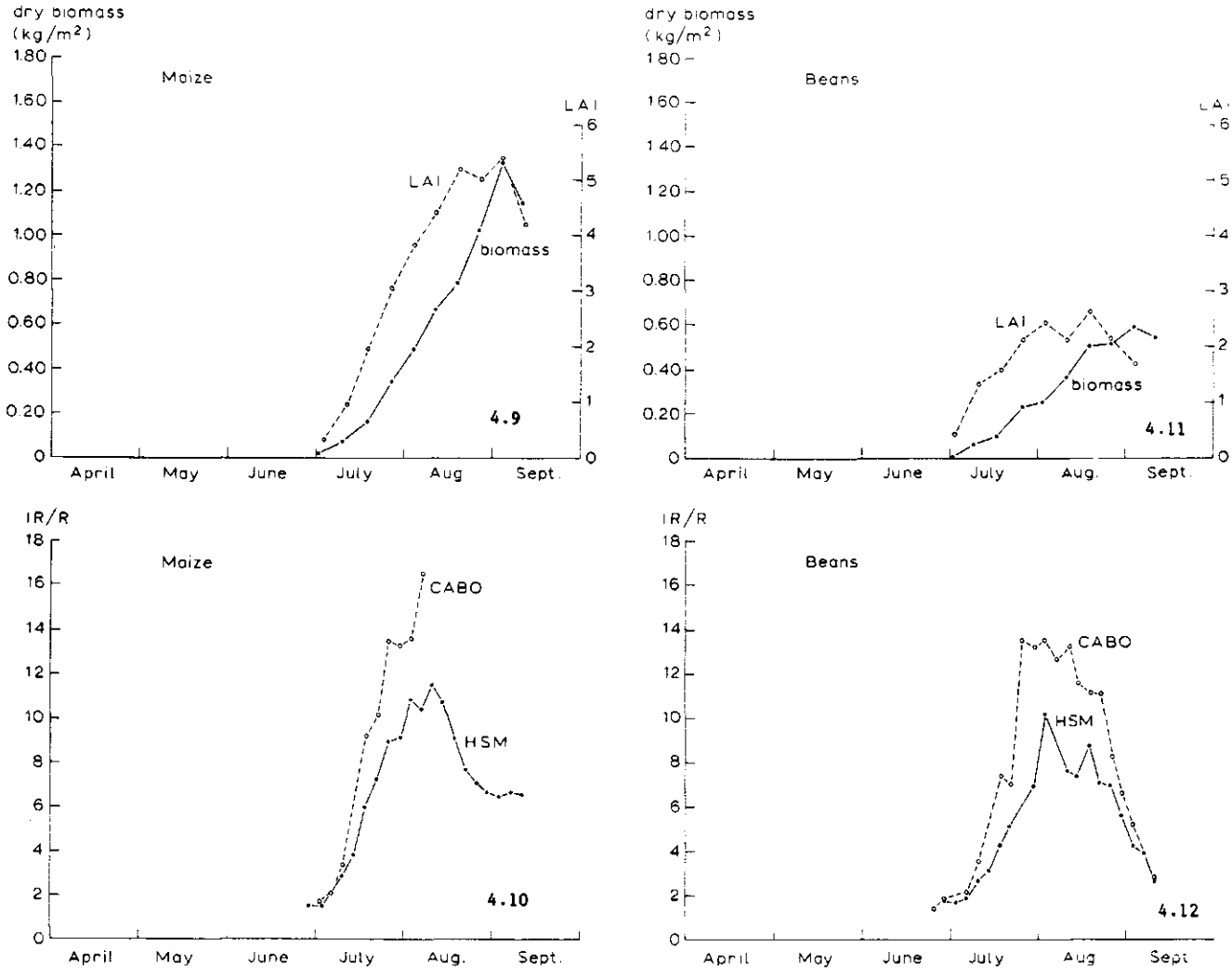

Fig. 4.9: smoothed values of the LAI and the dry biomass of the crop canopy of maize during the growing season, 1983.

Fig. 4.10: IR/R reflectance ratio of maize during the growing season with the HSM and the CABO reflectance meter, 1983.

Fig. 4.11: smoothed values of the LAI and the dry biomass of the crop canopy of beans during the growing season, 1983.

Fig. 4.12: IR/R reflectance ratio of beans during the growing season with the HSM and the CABO reflectance meter, 1983.

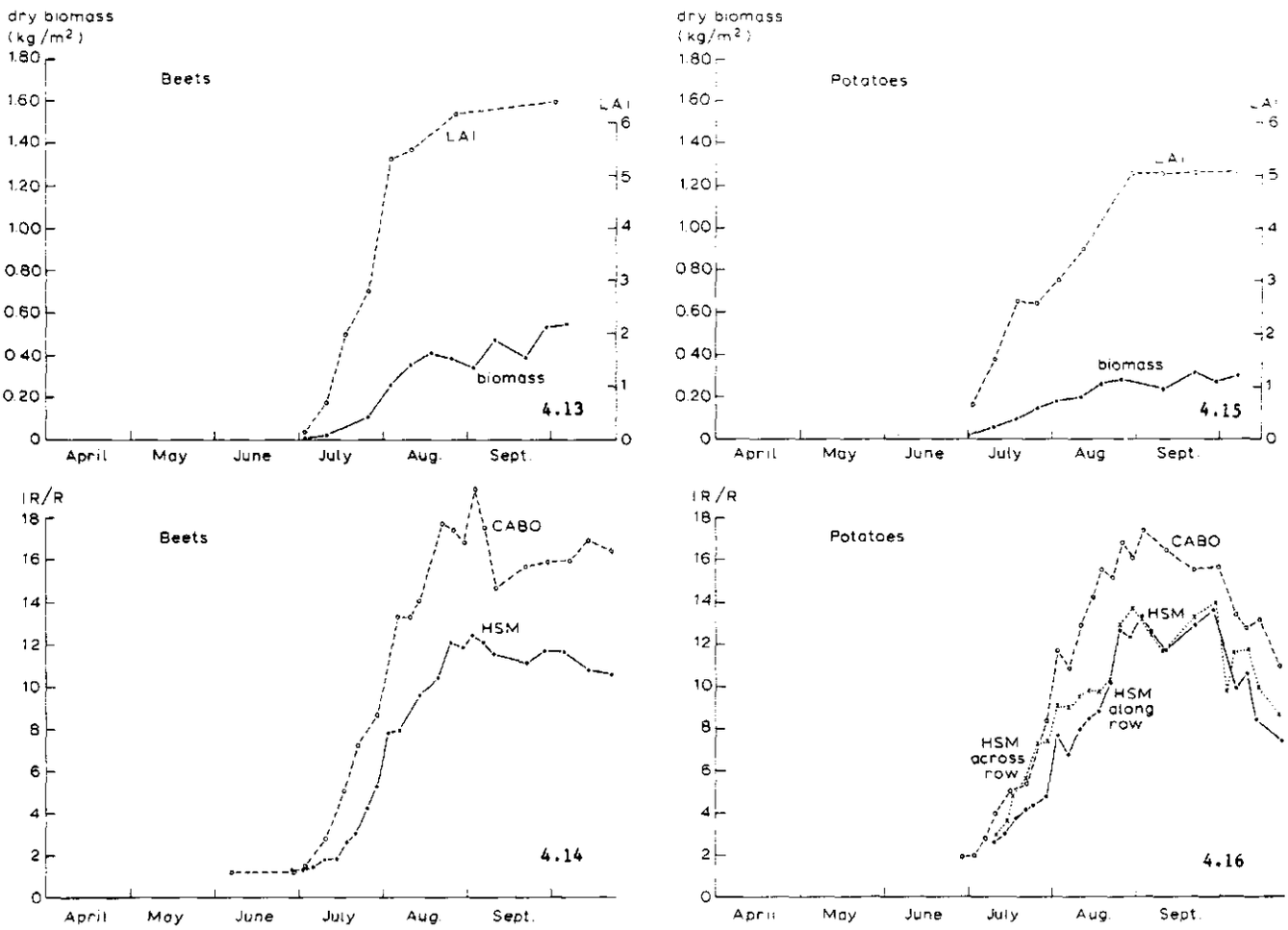

Fig. 4.13: smoothed values of the LAI and the dry biomass of the crop canopy of beets during the growing season, 1983.

Fig. 4.14: IR/R reflectance ratio of beets during the growing season with the HSM and the CABO reflectance meter, 1983.

Fig. 4.15: smoothed values of the LAI and the dry biomass of the crop canopy of potatoes during the growing season, 1983.

Fig. 4.16: IR/R reflectance ratio of potatoes during the growing season with the HSM and the CABO reflectance meter, 1983. For the HSM, IR/R reflectance ratios are presented measured across the row direction of the crop and along the row direction.

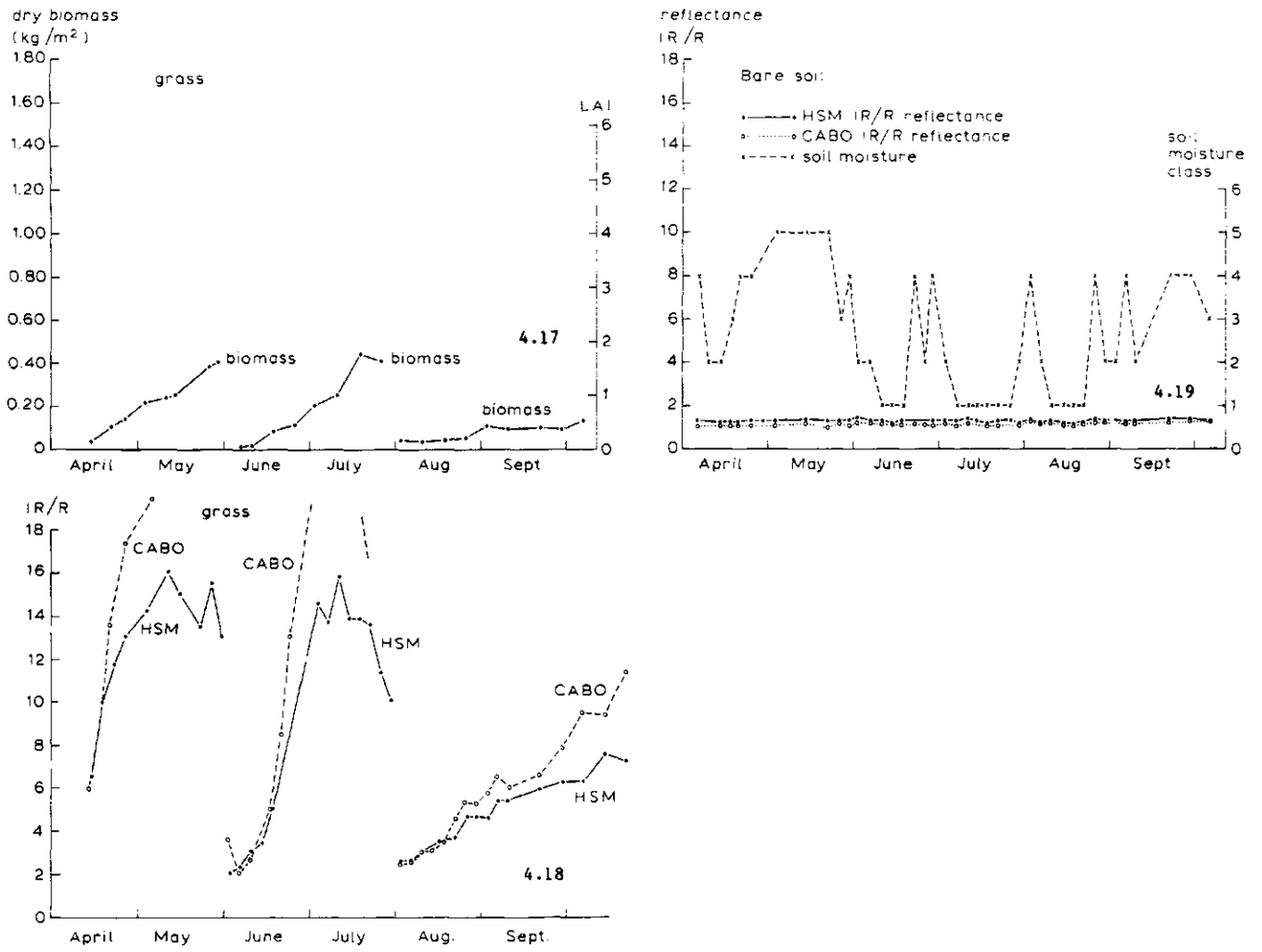

Fig. 4.17: smoothed values of the dry biomass of the crop canopy of grass during the growing season, 1983.

Fig. 4.18: IR/R reflectance ratio of grass during the growing season with the HSM and the CABO reflectance meter, 1983.

Fig. 4.19: Soil moisture class and the IR/R reflectance ratio of bare soil during the growing season with the HSM and the CABO reflectance meter, 1983. The soil moisture class is a scale from 1 (very dry) to 5 (very wet).

5 IR/R REFLECTANCE RATIOS VERSUS LAI AND BIOMASS

In this Chapter, the infrared/red reflectance ratios of the HSM and the CABO reflectance meter are studied in relation to the crop parameters LAI and biomass. The choice of these parameters is based on their usefulness in agricultural research and for practical monitoring possibilities.

5.1 Crops in 1982

In Figs. 5.1 and 5.2, the HSM IR/R reflectance ratio is plotted against LAI and dry biomass for all six fields of the winter wheat variety Tundra in 1982. Based on the development of the reflectance ratios in time (Chapter 4), only the vegetative period of the growing season is taken into account. During this period, the IR/R ratio is an ascending function of crop growth, i.e. biomass and LAI. In Fig. 5.1, the HSM measurements are plotted which were taken at view angle across the direction of the rows, and in Fig. 5.2, the measurements taken along the direction of the rows.
Up to an LAI value of 4, the relationship with the reflectance ratio appears to be linear. The relationship between the reflectance ratio and biomass is a bent curve and would be more adequately described by a (1-exp) function. The curves of HSM IR/R reflectance versus LAI or biomass for the different fields with HSM measurements across-row, are clustered more together than those along-row. No relationships could be established between the relevant position of the curves from the different wheat fields and the growth and development of the crop on those fields. On the one hand, this is caused by the failure to achieve significant differentiation in growth and development by means of nitrogen and fungicide applications. On the other hand, the irregularity in growth and development within the fields prevents comparative analysis between the fields. However, since the differences in average biomass and LAI development between the fields were relatively low, small differentation in the IR/R reflectance curves are only to be expected. The differentiation observed in the curves of IR/R reflectance versus LAI or biomass in Fig. 5.2 (HSM measurements along-row), could have been induced by differences in row structure. If a crop on two fields has the same amount of biomass but displays a developed difference in apparent row and inter-row width, this may result in a different canopy reflectance along the rows. Therefore, HSM measurements across-row would be more suitable for monitoring applications.

Plots of the HSM IR/R reflectance ratio versus fresh biomass are similar to those versus dry biomass. However, the data of the fresh biomass show a larger variation than the data of the dry biomass. This may be caused by differences in crop wetness at the field during sampling. For this reason, the use of dry biomass values should be preferred. Plots of the HSM IR/R ratio versus soil cover show a great similarity with plots of the HSM IR/R ratio versus LAI. Thus, the hypothesis of linearity between HSM reflectance and apparent soil cover is supported by the measurements in 1982.

5.2 Crops in 1983

For 1983, the crops are lumped into the category of 'small grain cereals' (winter wheat, oats, barley) and the 'other crops' (beet,

potato, maize, beans). Figs. 5.3 and 5.4 show the curves of the IR/R reflectance of respectively the HSM and the CABO meter versus LAI and dry biomass for the 'small grain cereals'. Again, only the period of vegetative growth is considered. The relationships between both the HSM and CABO reflectance ratios and LAI are quite linear, while the relations with biomass appear to be bent curves. The curves of IR/R reflectance versus LAI are grouped closer than the curves of IR/R reflectance versus biomass for both reflectance meters. In Fig. 5.4, the curves of the wheat varieties are clearly separated from those of oats and barley with the CABO reflectance meter. Furthermore, the CABO curves for oats and barley display many fluctuations, and no good relationship between the reflectance ratio and LAI or biomass exist. The CABO curves of the four wheat varieties are grouped together and shown as rather smooth curves. In Fig. 5.3, a different picture is presented for the HSM reflectance curves. For wheat, the curves of the HSM IR/R reflectance versus LAI or biomass are grouped together for only three of the four varieties. The variety Arminda has deviating curves. The curves for oats are similar to those of the three grouped wheat varieties in both the LAI and the biomass plots. In the LAI plot, the curve for oats has the same direction with an LAI offset of about 1. For barley, the relation between the HSM IR/R reflectance and LAI is linear up to a value of 2 only. With biomass, the relation for barley is different from those of the wheat varieties in that the level of saturation of the HSM IR/R reflectance is lower. For both barley and oats, the curves are smooth in appearance when compared with the curves of the CABO-meter reflectance.

Figs. 5.5 and 5.6 give the plots of the IR/R reflectance for respectively the HSM and the CABO reflectance meter versus LAI and biomass for all other crops combined (maize, beans, beets, potatoes). For maize, only the period of vegetative growth is considered while for the other crops the whole growing season is shown.
With both the HSM and the CABO reflectance meter, the relationship between IR/R reflectance and LAI is linear for all crops. The curves of IR/R reflectance versus LAI are grouped closer together than the curves of IR/R reflectance versus biomass. In both the HSM and CABO biomass plots, each crop is characterized by a specific shape of the curve. Only during the early growing season up to a biomass value of about 200 g/m2, the curves are linear and are grouped together relatively close. For beets, the relationship remains linear up to a biomass value of about 450 g/m2 for both reflectance meters. Potatoes have a linear curve up to 250 g/m2 for the CABO reflectance meter while the curve for the HSM reflectance is irregular in shape. For both beets and potatoes, CABO and HSM reflectance ratios decrease at the end of the growing season (at maximum biomass values). The curves for beans level off after a biomass value of 250 g/m2 and a level of saturation in both reflectance ratios is reached. Maize has curves of HSM IR/R reflectance versus biomass which are similar in shape to those of the small cereals. The level of saturation of the HSM reflectance however, is lower.

5.3 Summary

The results of this comparative analysis can be summarized as follows:
- In general, the plots of the IR/R reflectance versus LAI and biomass are similar for the CABO and the HSM reflectance meter. For oats and

barley, the curves of HSM IR/R reflectance versus LAI can be grouped together with the curves of the other small grain cereals. For the CABO meter, these crops have deviating curves which can not be grouped with any other crop. With the HSM, the curves for oats and barley are also smoother in appearance than with the CABO meter. The curves of the winter wheat varieties can all be grouped together in the LAI and biomass plots for the CABO meter. For the HSM, the curve of the variety Arminda deviates from the curves of the other varieties in both LAI and biomass plots. For all other crops and varieties (maize, beans, potatoes, beets, okapi, durin, donjon), only small differences exist between the performances of the two reflectance meters.
- For all crops, the curves of the IR/R reflectance versus LAI are grouped closer together than the curves of the IR/R reflectance versus biomass for both the HSM and the CABO meter. In general, the relationship between IR/R reflectance and LAI is linear during the vegetative part of the growing season for the cereals (except for oats and barly with the CABO meter) and during the whole growing season for the other crops. The relationship between IR/R reflectance and biomass is linear only during the first part of the vegetative growing season up to a value of 200 g/m2. During this limited period, the curves are also grouped together relatively close.

The best prospect for monitoring crop growth (the amount of vegetative material) seems to be the relationship between the IR/R reflectance and LAI. For most crops, the curves are closely grouped together and can be described by a linear relationship. Based on the visual interpretation of the presented figures, the HSM offers advantages over the CABO reflectance meter for oats and barley only.

In the following Chapters, regression analysis is applied to derive the coefficients which describe the linear relations between the IR/R reflectance ratio and LAI. This is done first for each crop and treatment (nitrogen, fungicide 1982) individually. Then, various crops are lumped together and average coefficients of regression are determined. The coefficients of regression are applied to estimate the LAI of the original data set. The coefficients of correlation and standard errors of estimate (SEE) are used to evaluate and compare the results for the different steps of lumping. This is done for both the HSM and the CABO IR/R measurements to enable a quantitative comparison of the two reflectance meters.

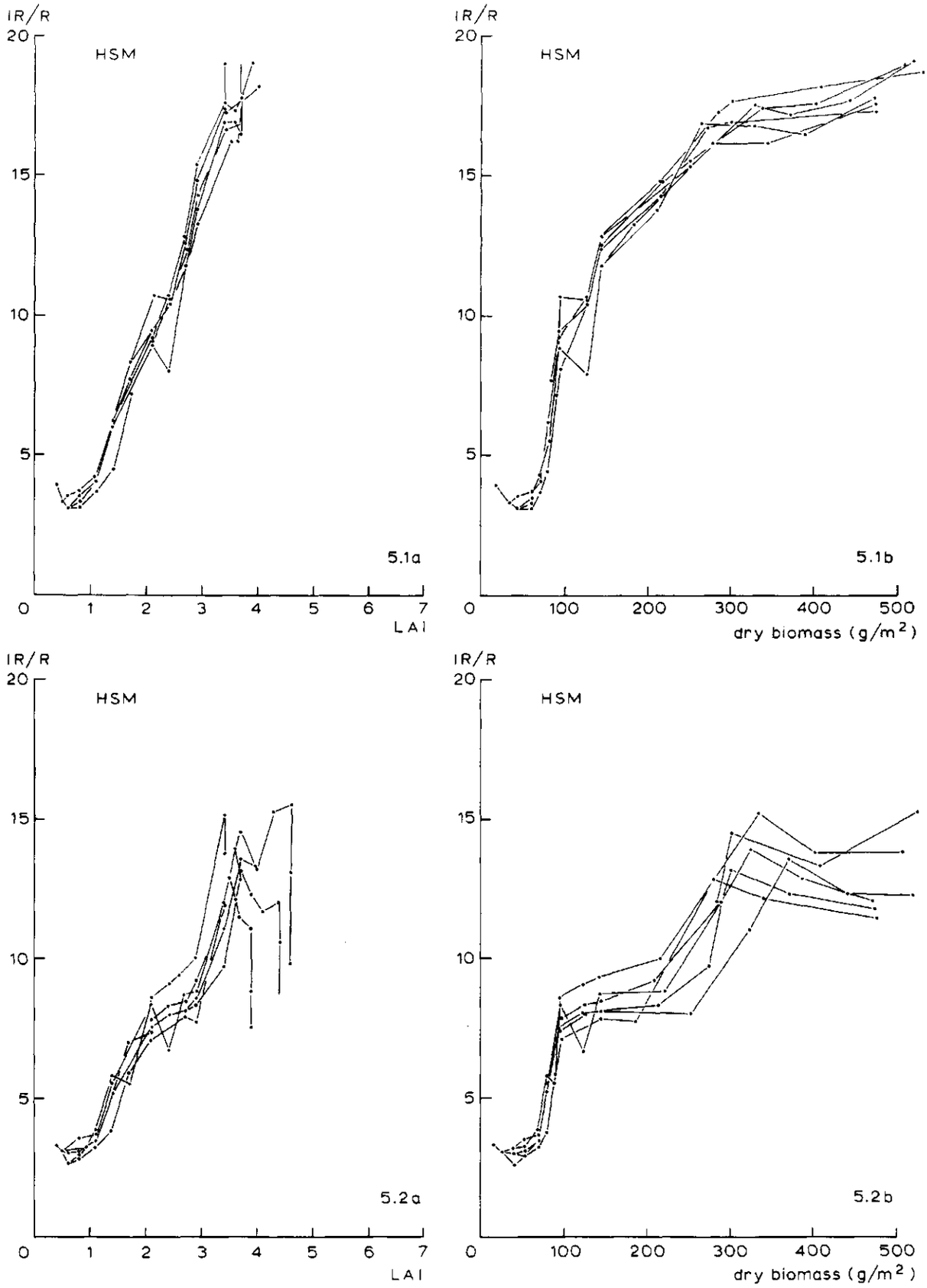

Fig 5.1: HSM IR/R reflectance ratio versus LAI (5.1a) and dry biomass of the crop canopy (5.1b) of six fields of Tundra winter wheat, 1982. The HSM measurements are made across the row direction of the crop.
Fig 5.2: the same as Fig. 5.1 but with HSM measurements made along the row direction of the crop.

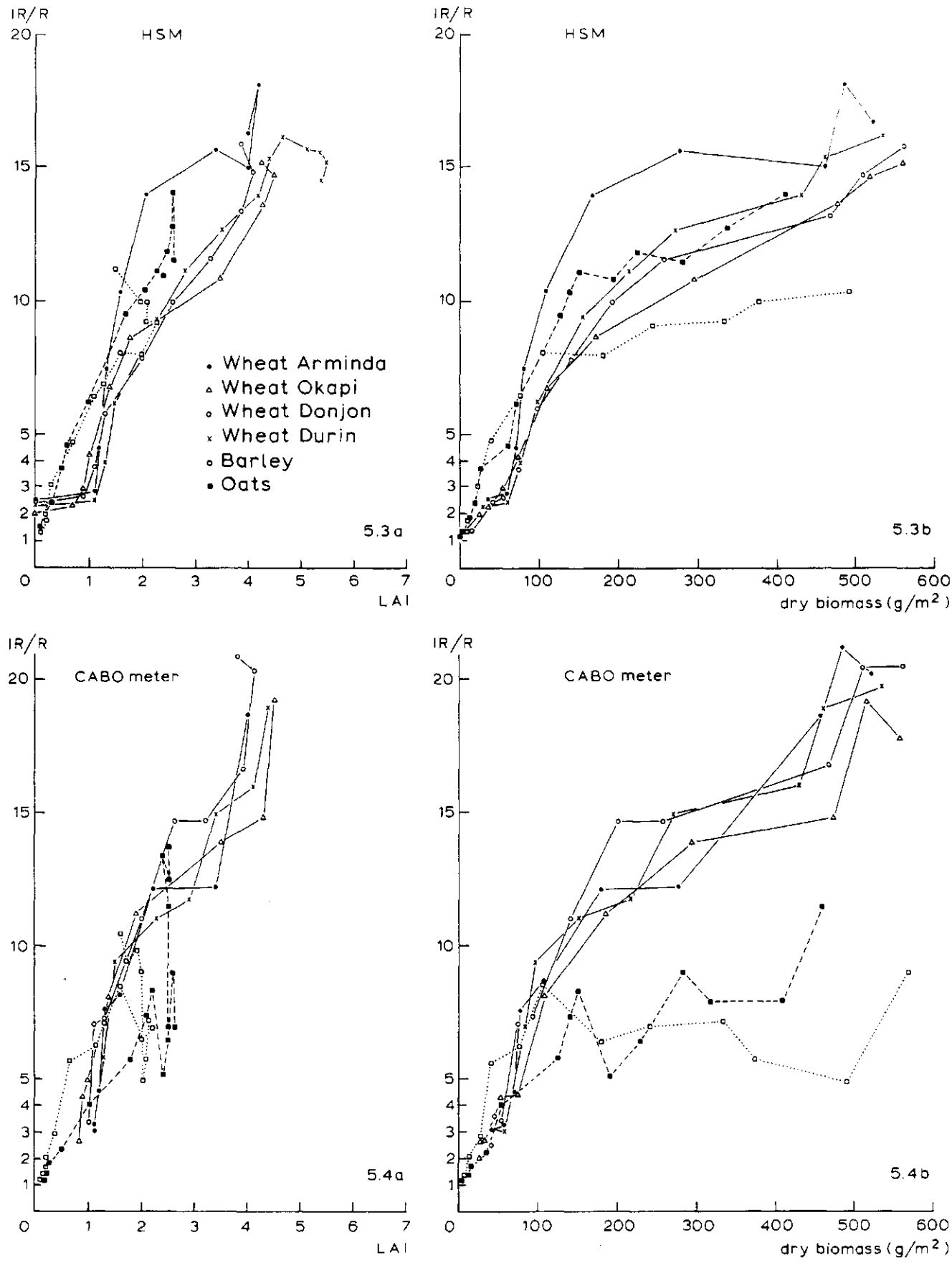

Fig 5.3: HSM IR/R reflectance ratio versus LAI (5.3a) and dry biomass of the crop canopy (5.3b) of the winter wheat varieties Arminda, Okapi, Donjon, Durin, and of oats and barley, 1983.
Fig. 5.4: the same as Fig. 5.3 but with reflectance measurements of the CABO reflectance meter.

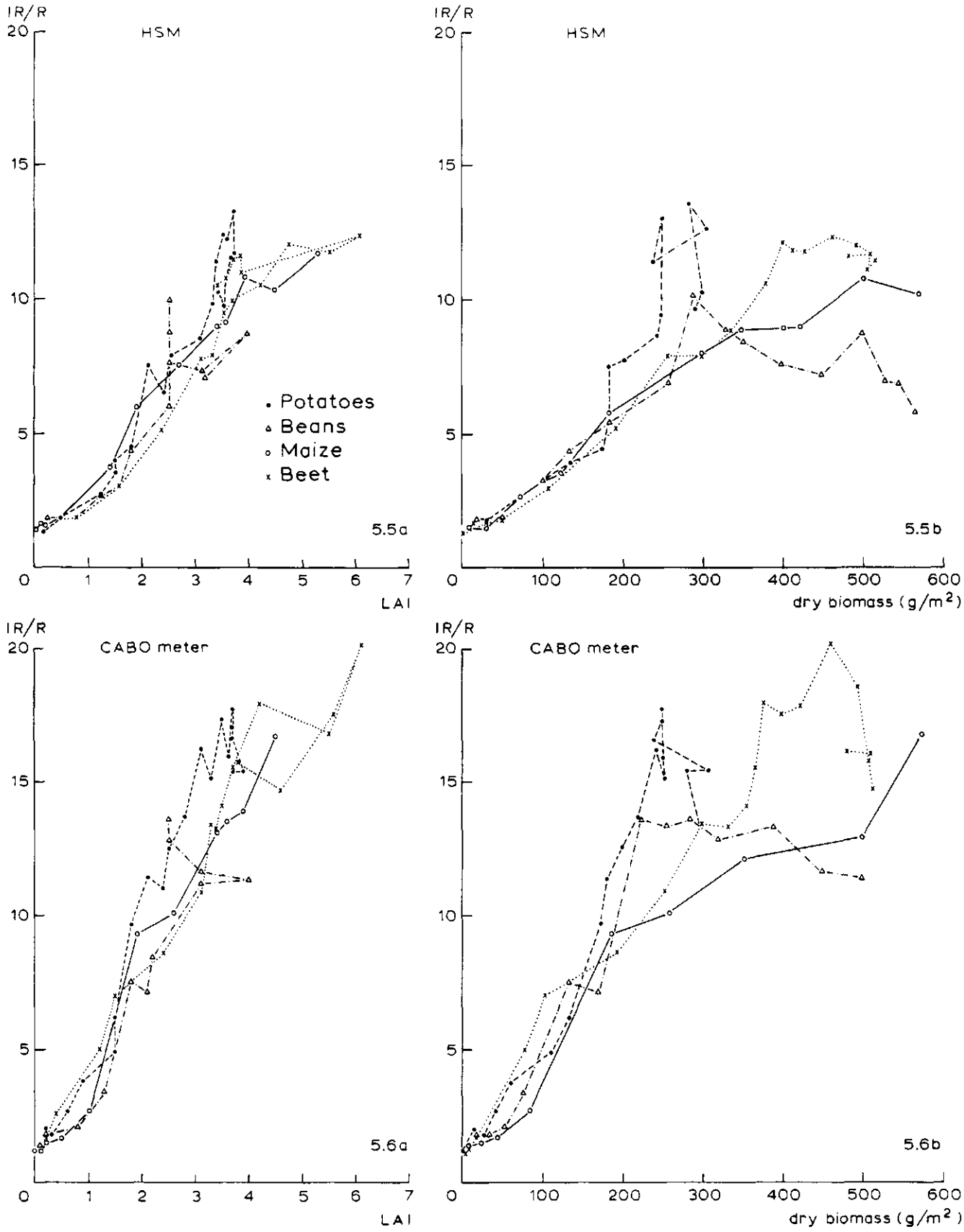

Fig 5.5: HSM IR/R reflectance ratio versus LAI (5.5a) and dry biomass of the crop canopy (5.5b) of potatoes, beets, beans and maize, 1983.
Fig. 5.6: the same as Fig. 5.5 but with reflectance measurements of the CABO reflectance meter.

6 LINEAR REGRESSION BETWEEN HSM IR/R REFLECTANCE AND LAI

Regression analysis and calculation of the standard error of estimate (SEE $=\sqrt{(\Sigma(y-\hat{y})^2/n)}$) are used to determine the correlation between the observed HSM IR/R reflectance ratio and the crop parameter LAI.

To study the correlation between HSM IR/R reflectance and the LAI, and to compare the correlation for different crops and fields, linear regression analysis was applied to the HSM IR/R ratio - LAI data pairs for each crop and each field. This was done first for the specific part of the growing season in which the relation between the IR/R reflectance ratio and the LAI appears linear. For most crops (wheat, oats, barley, beans, maize) this is the vegetative period of the growing season (Chapter 5). Secondly, linear regression analysis was applied to the complete data set for the whole growing season for selected crops.

In order to test the hypothetical insensitivity of the HSM to differences in crop structure, this was also done for the data pairs formed by combining the data sets of more crops and fields into larger groups. In theory, the combination of data of crops which differ only in leaf angle distribution into larger groups, should have a minimal effect on the correlation. In reality, crops differ in more aspects than leaf angle distribution only, and clustering will have a negative effect on the coefficient of correlation and the SEE.

The results of this exercise are summarized in Tables 6.1 and 6.2. In Table 6.1, the coefficients of regression are given for individual crops and fields, and for crops and fields clustered into groups of increasing magnitude. Table 6.2 gives the coefficients of correlation and the SEE's. The period of the growing season for which the regression analysis is performed, is also indicated. Because of the large influence of the view direction of the HSM with respect to the direction of sowing (Chapter 4), crops with comparable measurement configuration are grouped together. The Tables 6.1.a and 6.2.a give the results for HSM measurements along the rows, and the Tables 6.1.b and 6.2.b for HSM measurements across the rows.

6.1 Crops in 1982

For he period of six weeks during vegetative growth (half April to the end of May), high coefficients of correlation are obtained for the individual fields of Tundra winter wheat (Table 6.2). When all six fields are grouped together, the coefficients of correlation are nearly unaffected and the SEE's do not increase significantly.

In Figs. 6.1 and 6.2, the plots are given of all the HSM IR/R reflectance ratios versus LAI for HSM measurements along-row and across-row respectively. The slope of the regression line is steeper at measurements across-row than along-row. The highest correlation between the LAI and the HSM IR/R reflectance ratio exists at measurements across the row; r2 = 0.97 across-row versus 0.94 along-row. The coefficients of regression for the group of six fields combined are used to estimate the LAI from the HSM IR/R measurements for the individual fields. In Figs. 6.3 and 6.4, the results are visualized for plot number 1, using HSM measurements along-row and

Table 6.1a: HSM regression LAI and IR/R ratio along the rows, selected data, regression coefficients.

year + plotnr.	crop and variety	individual rc	individual y(x=0)	individual range	grouped: level 1 grp	grouped: level 1 rc	grouped: level 1 y(x=0)	grouped: level 2 grp	grouped: level 2 rc	grouped: level 2 y(x=0)
1982-1	Tundra winter wheat	3.14	0.91	13/4-27/5	1	3.08	0.77	1	3.17	0.66
1982-2	Tundra winter wheat	2.90	1.00	13/4-27/5	1	"	"	1	"	"
1982-3	Tundra winter wheat	3.26	0.59	13/4-27/5	1	"	"	1	"	"
1982-4	Tundra winter wheat	2.75	1.24	13/4-27/5	1	"	"	1	"	"
1982-5	Tundra winter wheat	3.34	0.49	13/4-27/5	1	"	"	1	"	"
1982-6	Tundra winter wheat	3.09	0.35	13/4-27/5	1	"	"	1	"	"
1983-10	Arminda winter wheat	3.89	-0.13	16/3- 3/6				1	"	"
1983-5	L6 11 Maize	2.17	0.89	1/7- 9/8	2	2.87	-0.28			
1983-8	Bintje Potatoes	3.84	-1.97	15/7-16/9	2	"	"			
1983-9	Prelude Beans	3.05	-1.18	12/7- 6/9	2	"	"			

Table 6.1b: HSM regression LAI and IR/R ratio across the rows, selected data, regression coefficients.

year + plotnr.	crop and variety	individual rc	individual y(x=0)	individual range	grouped: level 1 grp	grouped: level 1 rc	grouped: level 1 y(x=0)	grouped: level 2 grp	grouped: level 2 rc	grouped: level 2 y(x=0)	grouped: level 3 grp	grouped: level 3 rc	grouped: level 3 y(x=0)	grouped: level 4 grp	grouped: level 4 rc	grouped: level 4 y(x=0)	grouped: level 5 grp	grouped: level 5 rc	grouped: level 5 y(x=0)
1982-1	Tundra winter wheat	4.61	-0.15	13/4-27/5	1	4.72	-0.18	1	4.15	0.34				1	4.04	0.76	1	3.53	1.19
1982-2	Tundra winter wheat	4.75	-0.06	13/4-27/5	1	"	"	1	"	"				1	"	"	1	"	"
1982-3	Tundra winter wheat	5.31	-0.86	13/4-27/5	1	"	"	1	"	"				1	"	"	1	"	"
1982-4	Tundra winter wheat	4.41	0.48	13/4-27/5	1	"	"	1	"	"				1	"	"	1	"	"
1982-5	Tundra winter wheat	4.68	-0.01	13/4-27/5	1	"	"	1	"	"				1	"	"	1	"	"
1982-6	Tundra winter wheat	4.80	-0.96	13/4-27/5	1	"	"	1	"	"				1	"	"	1	"	"
1983-11	Okapi winter wheat	3.01	1.29	16/3- 3/6	2	3.45	0.48	1	"	"	1	3.34	1.41	1	"	"	1	"	"
1983-12	Donjon winter wheat	3.67	0.14	16/3- 3/6	2	"	"	1	"	"	1	"	"	1	"	"	1	"	"
1983-13	Arminda winter wheat	3.89	-0.13	16/3- 3/6	2	"	"	1	"	"	1	"	"	1	"	"	1	"	"
1983-14	Durin winter wheat	3.53	0.06	16/3- 3/6	2	"	"	1	"	"	1	"	"	1	"	"	1	"	"
1983-6	Leanda Oats	4.39	1.23	13/4-21/6	3	4.24	1.27				1	"	"	1	"	"	1	"	"
1983-7	Audley Barley	3.63	1.57	21/4-10/6	3	"	"				1	"	"	1	"	"	1	"	"
1983-2	Monohil Beets	3.10	1.13	19/7- 6/9	4	2.63	1.18										1	"	"
1983-4	Bintje Potatoes	3.01	-1.69	5/7-23/9	4	"	"												

Table 6.2a: HSM regression LAI and IR/R ratio along the rows, selected data, correlation.

year + plotnr.	crop and variety	individual r^2	individual SEE	max. LAI	range	growing season	grouped: level 1 grp	level 1 r^2	level 1 SEE	grouped: level 2 grp	level 2 r^2	level 2 SEE
1982-1	Tundra winter wheat	0.95	0.28	3.8	13/4-27/5	1/4-29/7	1	0.94	0.30	1	0.93	-
1982-2	Tundra winter wheat	0.96	0.26	4.4	13/4-27/5	1/4-29/7	1	"	0.27	1	"	0.27
1982-3	Tundra winter wheat	0.93	0.30	3.4	13/4-27/5	1/4-29/7	1	"	0.33	1	"	-
1982-4	Tundra winter wheat	0.94	0.28	4.4	13/4-27/5	1/4-29/7	1	"	0.30	1	"	-
1982-5	Tundra winter wheat	0.97	0.21	4.7	13/4-27/5	1/4-29/7	1	"	0.27	1	"	-
1982-6	Tundra winter wheat	0.93	0.30	3.9	13/4-27/5	1/4-29/7	1	"	0.33	1	"	0.33
							-----total:		0.30			
1983-10	Arminda winter wheat	0.95	0.27	3.6	16/3- 3/6	1/3- 5/8				1	"	0.47
										-----total:		0.32
1983-5	LG 11 Maize	0.99	0.19	6.4	1/7- 9/8	7/6-23/9	2	0.85	0.49			
1983-8	Bintje Potatoes	0.96	0.18	3.9	15/7-16/9	10/6-14/10	2	"	0.50			
1983-9	Prelude Beans	0.94	0.14	3.1	12/7- 6/9	7/6- 6/9	2	"	0.23			
							-----total:		0.43			

Table 6.2b: HSM regression LAI and IR/R ratio across the rows, selected data, correlation.

year + plotnr.	crop and variety	individual r^2	individual SEE	max. LAI	range	growing season	grouped: level 1 grp	level 1 r^2	level 1 SEE	grouped: level 2 grp	level 2 r^2	level 2 SEE	grouped: level 3 grp	level 3 r^2	level 3 SEE	grouped: level 4 grp	level 4 r^2	level 4 SEE	grouped: level 5 grp	level 5 r^2	level 5 SEE
1982-1	Tundra winter wheat	0.96	0.23	3.8	13/4-27/5	1/4-29/7	1	0.97	0.23	1	0.90	0.32				1	0.91	0.33	1	0.82	0.56
1982-2	Tundra winter wheat	0.98	0.17	4.4	13/4-27/5	1/4-29/7	1	"	0.18	1	"	0.35				1	"	0.36	1	"	0.66
1982-3	Tundra winter wheat	0.97	0.17	3.4	13/4-27/5	1/4-29/7	1	"	0.26	1	"	0.46				1	"	0.47	1	"	0.74
1982-4	Tundra winter wheat	0.98	0.17	4.4	13/4-27/5	1/4-29/7	1	"	0.17	1	"	0.26				1	"	0.25	1	"	0.51
1982-5	Tundra winter wheat	0.98	0.18	4.7	13/4-27/5	1/4-29/7	1	"	0.17	1	"	0.33				1	"	0.33	1	"	0.63
1982-6	Tundra winter wheat	0.98	0.17	3.9	13/4-27/5	1/4-29/7	1	"	0.22	1	"	0.27				1	"	0.29	1	"	0.50
							-----total:		0.21												
1983-11	Okapi winter wheat	0.95	0.34	4.5	16/3- 3/6	1/3- 5/8	2	0.95	0.37	1	"	0.67	1	0.92	0.44	1	"	0.69	1	"	0.50
1983-12	Donjon winter wheat	0.96	0.24	4.3	16/3- 3/6	1/3- 5/8	2	"	0.27	1	"	0.42	1	"	0.31	1	"	0.46	1	"	0.32
1983-13	Arminda winter wheat	0.95	0.27	4.2	16/3- 3/6	1/3- 5/8	2	"	0.34	1	"	0.35	1	"	0.40	1	"	0.39	1	"	0.37
1983-14	Durin winter wheat	0.96	0.25	5.5	16/3- 3/6	1/3- 5/8	2	"	0.26	1	"	0.57	1	"	0.36	1	"	0.60	1	"	0.40
							-----total:		0.32	-----total:		0.40									
1983-6	Leanda Oats	0.98	0.14	2.6	13/4-21/6	14/3-12/8	3	0.97	0.16				1	"	0.52	1	"	0.29	1	"	0.45
1983-7	Audley Barley	0.95	0.18	2.2	21/4-10/6	14/3- 9/8	3	"	0.20				1	"	0.24	1	"	0.21	1	"	0.23
							-----total:		0.17				-----total:		0.41	-----total:		0.39			
1983-2	Monohil Beets	0.99	0.12	4.6	19/7- 6/9	10/6-14/10	4	0.83	0.61										1	"	1.30
1983-4	Bintje Potatoes	0.95	0.27	3.9	5/7-23/9	10/6-14/10	4	"	0.56										1	"	0.42
							-----total:		0.58										-- total:		0.61

across-row respectively. In both figures, the estimated LAI fits the observed LAI during the period of vegetative growth. The figures also confirm the better performance for the HSM measurements across-row than along-row. There is no correlation between estimated and observed LAI during the period of generative growth and ripening neither for the measurements along- nor across-row. From the moment of flowering until the beginning of ripening (begin June-half July), the LAI is underestimated by about 25 %.

6.2 Crops in 1983

Cereals

In 1983, only one variety of winter wheat (Arminda) was measured both along- and across-row, while the other three varieties and oats and barley were measured across-row only. Therefore, the analysis for cereals was concentrated on HSM measurements across the row. The selected period for the regression analysis is generally six weeks from half April to the beginning/midst of June. Only for oats, the selected period is nine weeks, Table 6.1.b.

For the winter wheat varieties, the coefficients of correlation for the individual fields are 0.95/0.96 and the SEE averages 0.28. When all four varieties are combined, the coefficients of correlation remain the same, but the SEE increases to 0.32.
The combination of oats with barley results in a coefficient of correlation and a SEE which does not deviate much from the values for the individual crops; r2 = 0.97 and SEE = 0.17.

For oats, the results of the regression analysis are visualized in Figs. 6.5 and 6.6. In Fig. 6.5, the observed LAI is given together with the estimated LAI from the HSM IR/R measurements using the coefficients of regression for oats only. In Fig. 6.6, the estimated LAI is derived from the coefficients of regression from oats and barley combined. In both figures, the LAI is fairly well estimated during the period of vegetative growth, while the LAI is again largely underestimated during generative growth and ripening. There is hardly any difference between the two estimators of LAI.

For the cereals the linear regression analysis is also applied to the IR/R reflectance-LAI data set of the whole growing season. The results for the combination of oats and barley are illustrated for oats in Figs. 6.7 and 6.8. When the analysis is based on the whole growing season, the SEE for the period of vegetative growth increases from 0.17 to 0.32, and the coefficient of correlation decreases from from 0.97 to 0.88. If the data for the whole growing season are used in the calculation, the estimation of the LAI becomes slightly better with a SEE of 0.33, Fig. 6.8. For the regression based on the vegetative period only, the total SEE is 0.37, Fig. 6.6. These differences are only minimal.
For winter wheat, the results of the comparison are visualized in Figs. 6.9/6.11. Fig. 6.9 gives a plot of measured HSM IR/R ratio versus LAI for all four varieties and for the whole growing season. The slope of the regression line through the data set of the vegetative period only is about the same as that for the regression line through all data points. The difference is the relative position of the regression lines; the measurements taken after the period of

vegetative growth pull the line of regression through all data points downward. In Fig. 6.10, the estimated LAI is given based on the regression through the data from the vegetative period only, and in Fig. 6.11, the estimated LAI is based on the regression through all data points. In general, the estimation of the LAI for the entire season is better for the regression through all data points, though the discrepancy between estimated and observed LAI is still large, SEE = 0.43.

Beets and potatoes across-row

For beets and potatoes, the data points are selected from about 1 month after sowing until 1 month before harvest, Table 6.2.b. The slopes of the regression lines through the IR/R reflectance ratios and the observed LAI from the individual crops are quite similar, Table 6.1.b. However, the abcisses are different, which is markedly illustrated in Fig 6.12. Therefore, when the data for the two crops are combined, the coefficients of correlation decrease from 0.95/0.99 for the individual crops to 0.83 for the crops combined. The SEE increases from an average 0.39 to 0.58. The results of the regression analysis are given for beets in Figs. 6.13 and 6.14. Fig 6.13 shows the good fit between the observed LAI and the LAI estimated from the regression through the data points of beets only. In this figure, no selection in data points is made and the regression is based on the measurements for the whole growing season. In Fig. 6.14, the decrease in accuracy in estimated LAI is illustrated when the estimation of LAI is based on the regression through the data points of beets and potatoes combined. The SEE increases from 0.28 in Fig. 6.13 to 0.50 in Fig. 6.14.

Maize, beans and potatoes along-row

When analysed individually, these crops show a high to very high coefficient of correlation (r2 = 0.94/0.99) for the linear regression between HSM IR/R reflectance and the LAI. The regression coefficients, however, are markedly different for the three crops, Table 6.1.a. Therefore, clustering of the crops reduces the coefficients of corelation to 0.85 and increases the SEE from an average 0.17 per crop, to 0.43, Table 6.2.a. In Figs. 6.15/6.17, some of the results of the regression analysis are shown. Fig. 6.15 gives the IR/R reflectance ratios versus observed LAI together with the regression lines per crop and the regression line through all data combined. For maize, only 1 month of the vegetative part of the growing season was analysed. For beans and potatoes, two months of the vegetative period are selected. In Fig. 6.16, the observed LAI for maize is plotted with the estimated LAI derived from the coefficients of regression for the data set of maize only. Up to the midst of August, the fit between estimated and observed LAI is very good, SEE = 0.19. Then the estimated LAI starts to decline while the observed LAI still increases until a maximum value at the beginning of September. The SEE for the whole growing season is 1.91. Fig. 6.17 gives the estimated LAI which is derived from the coefficients of regression for the data set of maize, beans and potatoes combined. A good fit between estimated and observed LAI is only present for the two weeks from the midst to the end of July. Already before the beginning of August, the LAI is seriously underestimated. The SEE during the vegetative period of the growing season is increased to 0.43, and for the whole growing season to 2.12.

Since the HSM IR/R reflectance of potatoes was measured both across and along the direction of the rows, a comparison between the view angles could be made. At both view angles, the coefficient of correlation is the same (r2 = 0.95/0.96), but at a view angle along the row the SEE is considerably smaller than at a view angle across the rows; SEE = 0.18 versus 0.27.

6.3 Cereals in 1982 and 1983

An attempt is also made to lump all the 'small grain cereals' (across-row HSM measurements) of 1982 and 1983. In Table 6.2.b, it is seen that grouping of the varieties of winter wheat results in decreasing coefficients of correlation from 0.95/0.98 for the individual varieties to 0.90 for all varieties together. If oats and barley 1983 are included, the coefficient of correlation increases to 0.91 because of the increased number of observations along the line of regression. The SEE increases from an average value of 0.21 for the individual crops, to 0.39 for all crops combined.
Fig. 6.18 gives the plot of the datapoints of HSM (across-row) IR/R reflectance versus LAI for all 'small grain cereals' during the selected period of vegetative growth. The data points are closely dispersed around the line of linear regression. In Fig. 6.19, the observed LAI for Tundra plot number 1 1982, is plotted together with the estimated LAI derived from the coefficients of regression for the whole group of small grain cereals. In Fig. 6.20, the same is given for the Okapi winter wheat plot 1983, and in Fig. 6.21 for the oats plot 1983. When these figures are compared with the Figs 6.4 and 6.5, the loss in accuracy in estimating LAI due to the lumping of the crops is apparent. For Tundra plot 1, the SEE for the vegetative part of the growing season increases from 0.23 to 0.33, and for oats from 0.14 to 0.29. For Okapi winter wheat it increases even more, from 0.34 to 0.69.

6.4 Summary

For the regression applied to the selected period of the growing season, high to very high coefficients of correlation are found for the individual crops, r2 = 0.94/0.99. The SEE's range from 0.12 to 0.30. When the small grain cereals wheat, oats and barley in 1983 are combined, the coefficient of correlation decreases to 0.92 and the SEE's increase to 0.24/0.52. When the small grain cereals of 1982 and 1983 are combined, the coefficient of correlation decreases only to 0.91 and the SEE becomes 0.39. Lumping of the crops beets and potatoes, or maize, beans and potatoes results in higher losses in correlation. The coefficients of correlation decrease to 0.83/0.85 and the SEE's increase to 0.43/0.50. When all the crops of 1983 (HSM measurements across-row) are lumped, the coefficient of correlation becomes 0.82 and the SEE 0.61.

For wheat, HSM measurements across-row results in lower values for the SEE than HSM measurements along-row. For potatoes, the opposite is true; HSM measurements along-row give a lower SEE than HSM measurements across-row.

For the regression applied to the whole growing season, the

correlation between HSM IR/R reflectance and LAI is lower for the period of vegetative growth. When the whole growing season is considered, the correlation is a little higher than when the regression is based on the vegetative part of the growing season only. For a single crop, the coefficient of correlation then ranges from 0.85 to 0.97. The decrease of the correlation with the clustering in groups is less than for the regression based on the selected data discussed above.

For interpretation of the results, the calculated coefficients of correlation and SEE's should be compared with those for the CABO reflectance meter. In the next Chapter, the correlations between CABO IR/R reflectance and LAI are calculated for the various levels of lumping. Based on the results, a comparison is made between the HSM and the CABO reflectance meter in Chapter 8.

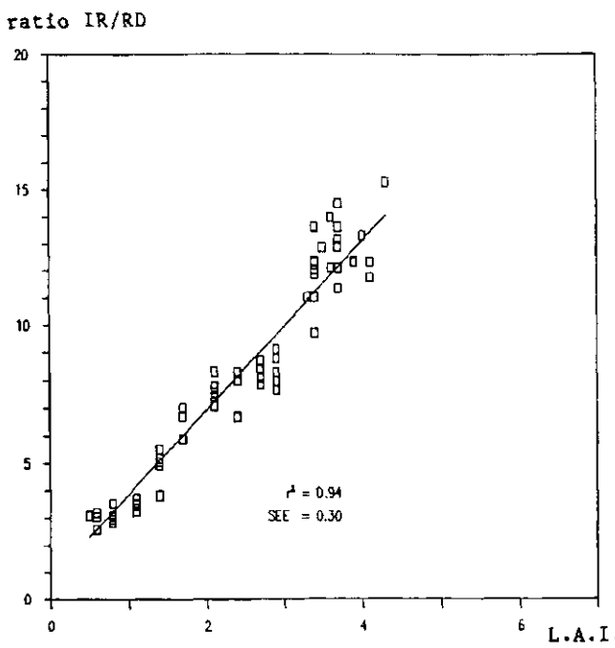

Fig. 6.1: HSM IR/R ratio versus LAI; Tundra winter wheat, along row, 4/13-5/27 1982.

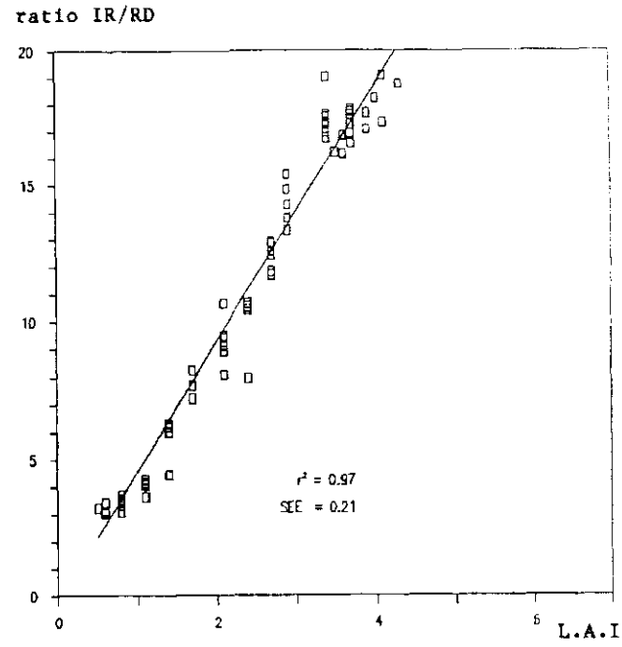

Fig. 6.2: HSM IR/R ratio versus LAI; Tundra winter wheat, across row, 4/13-5/27 1982.

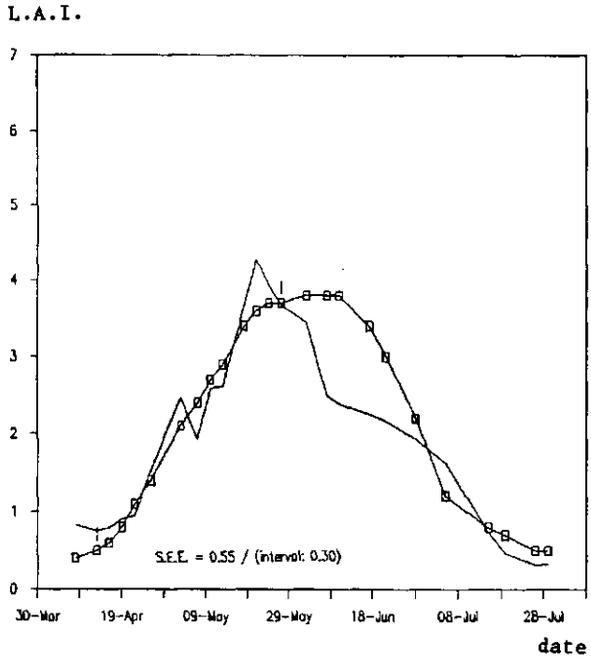

Fig. 6.3: measured and calculated LAI in time; Tundra winter wheat plot 1, along row, 4/13-5/27 1982.

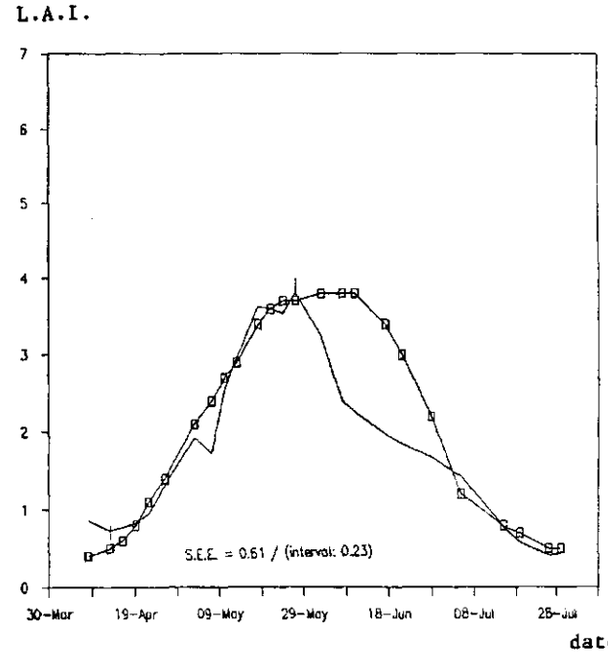

Fig. 6.4: measured and calculated LAI in time; Tundra winter wheat plot 1, across row, 4/13-5/27 1982.

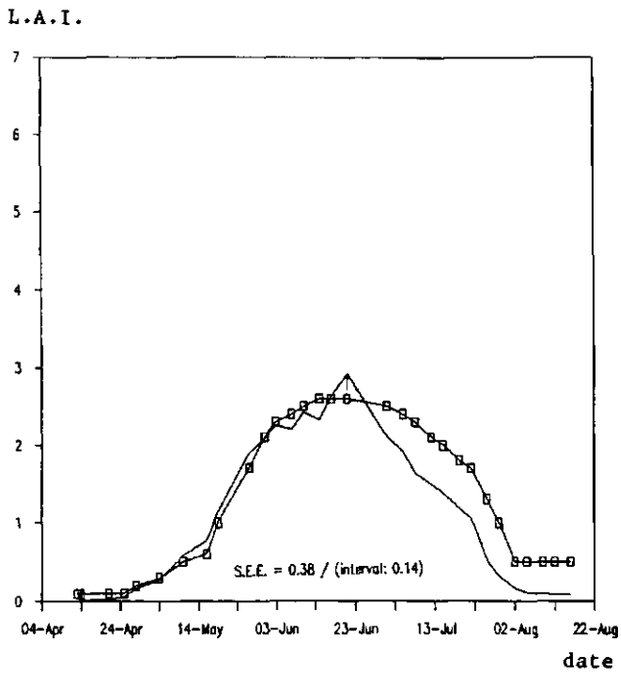

Fig. 6.5: measured and calculated LAI in time; Oats, across row, 3/14-6/21 1983.

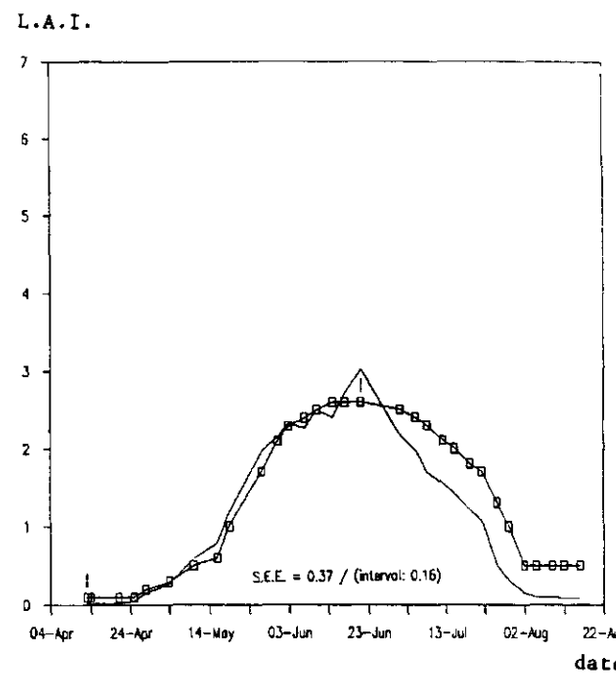

Fig. 6.6: measured and calculated LAI in time; Oats, across row, 4/13-6/21 1983.

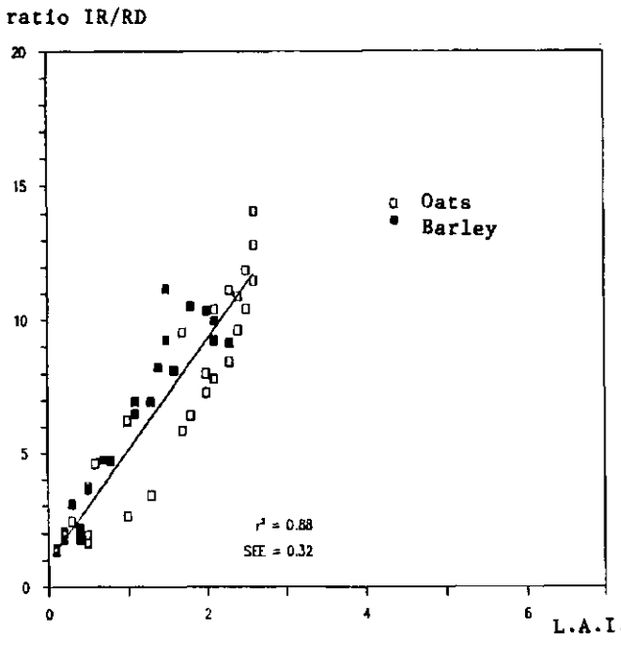

Fig. 6.7: HSM IR/R ratio versus LAI; Oats and Barley, across row, all data 1983.

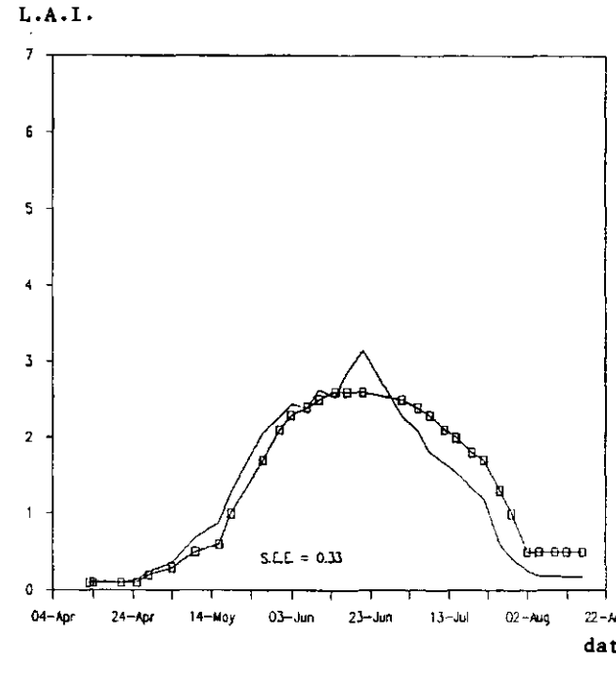

Fig. 6.8: measured and calculated LAI in time; Oats, across row, all data 1983.

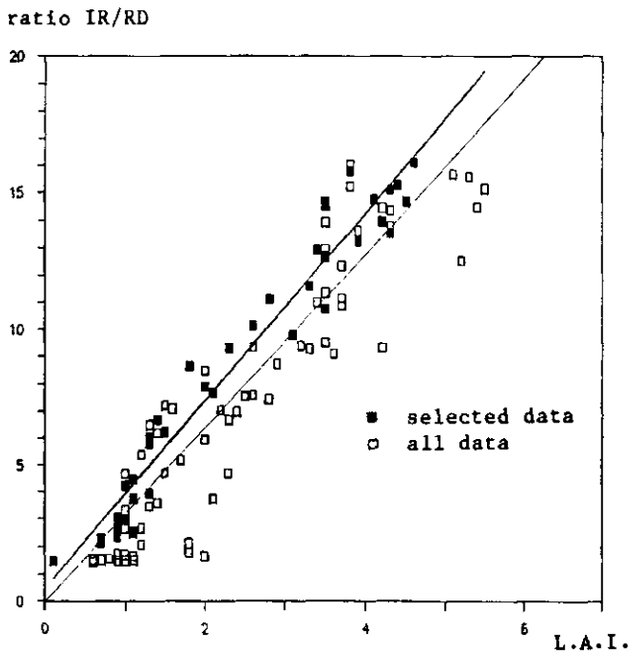

Fig. 6.9: HSM IR/R ratio versus LAI; All winter wheat varieties, across row, 3/16-6/3 1983.

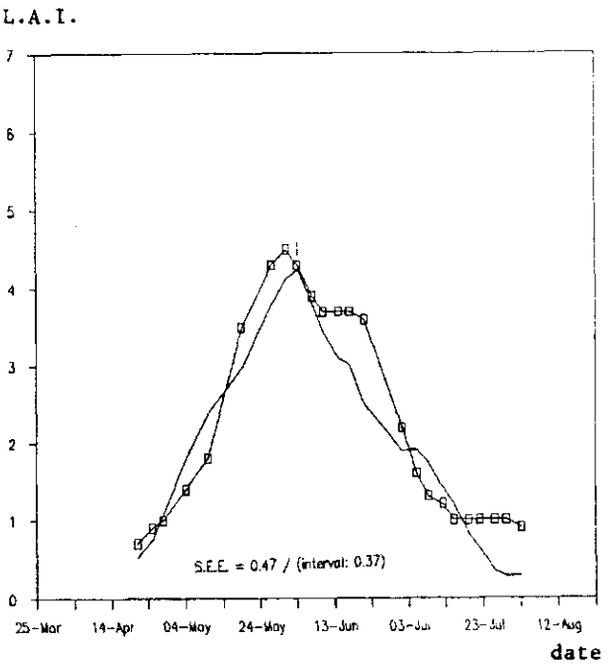

Fig. 6.10: measured and calculated LAI in time; Winter wheat Okapi, across row, 3/16-6/3 1983.

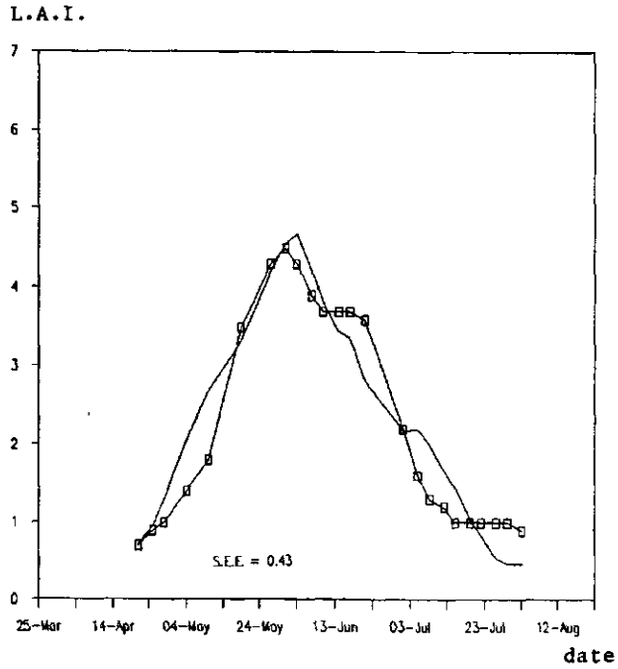

Fig. 6.11: measured and calculated LAI in time; Winter wheat Okapi, across row, all data 1983.

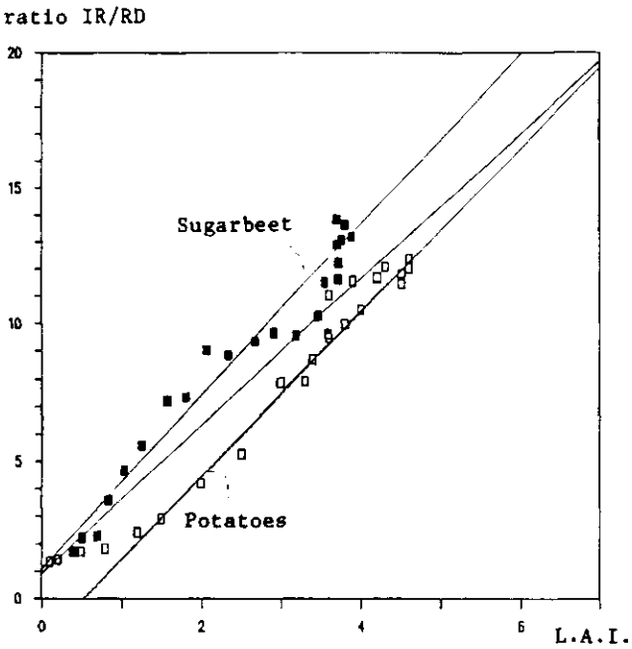

Fig. 6.12: HSM IR/R ratio versus LAI; Sugarbeet and Potatoes, across row, selected data 1983.

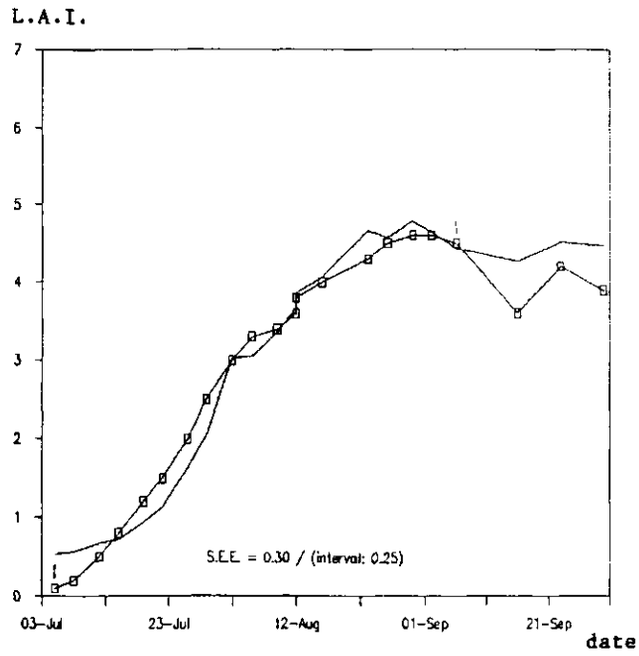

Fig. 6.13: measured and calculated LAI in time; Sugarbeet, across row, selected data 1983.

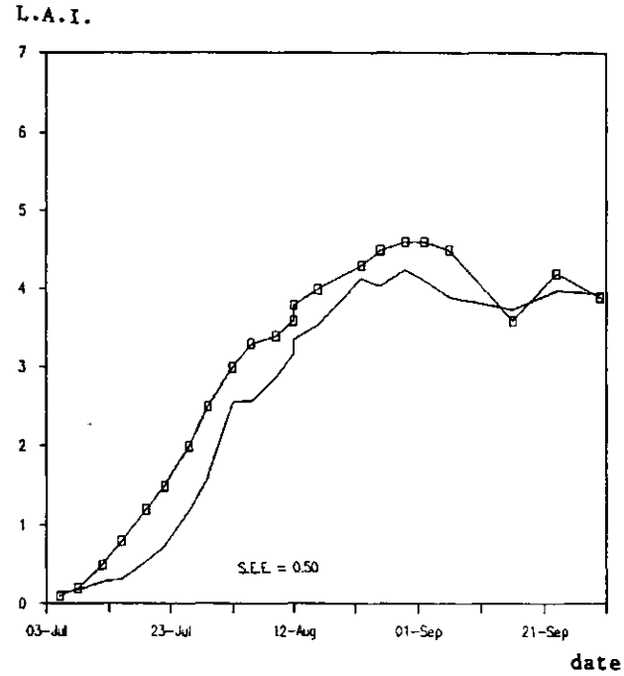

Fig. 6.14: measured and calculated LAI in time; Sugarbeet, across row, all data 1983.

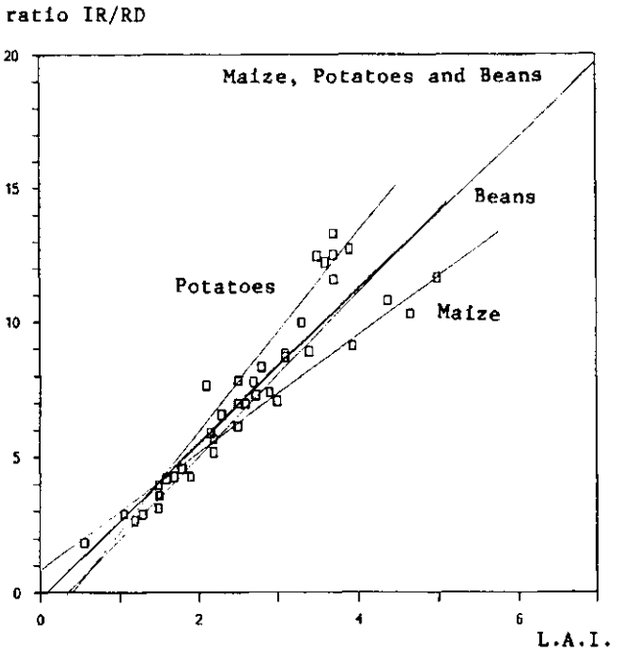

Fig. 6.15: HSM IR/R ratio versus LAI; Maize, Potatoes and Beans, along row, selected data 1983.

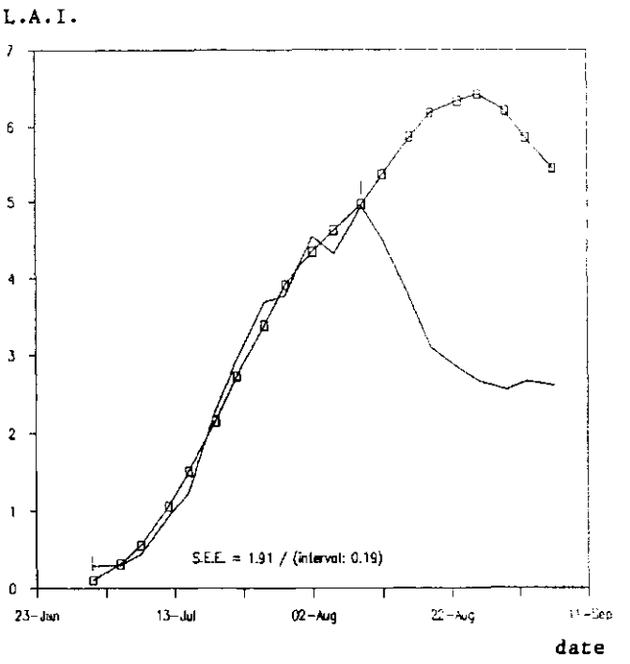

Fig. 6.16: measured and calculated LAI in time; Maize, along row 7/1-8/9 '83.

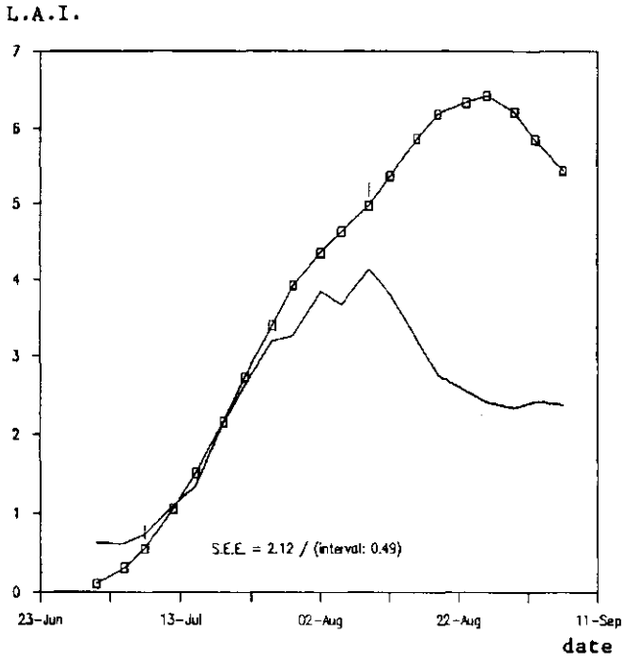

Fig. 6.17: measured and calculated LAI in time; Maize Potatoes and Beans, along row, selected data 1983: Maize.

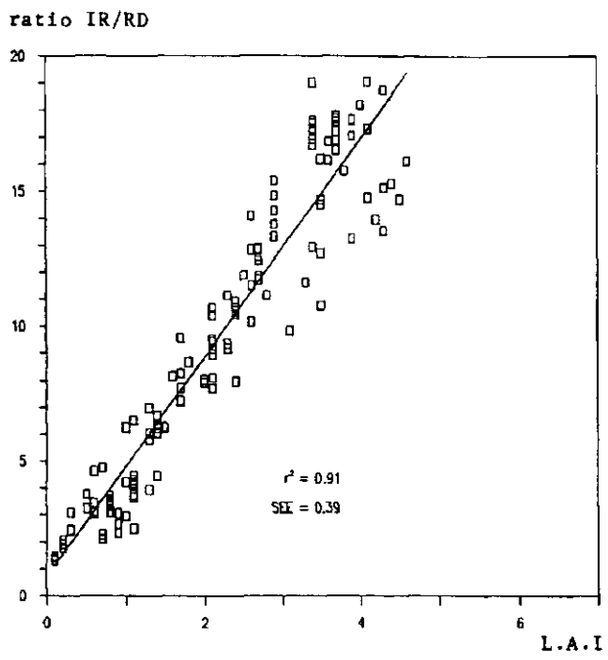

Fig. 6.18: HSM IR/R ratio versus LAI; Winter wheat, Oats and Barley, across row, selected data both 1982 and 1983.

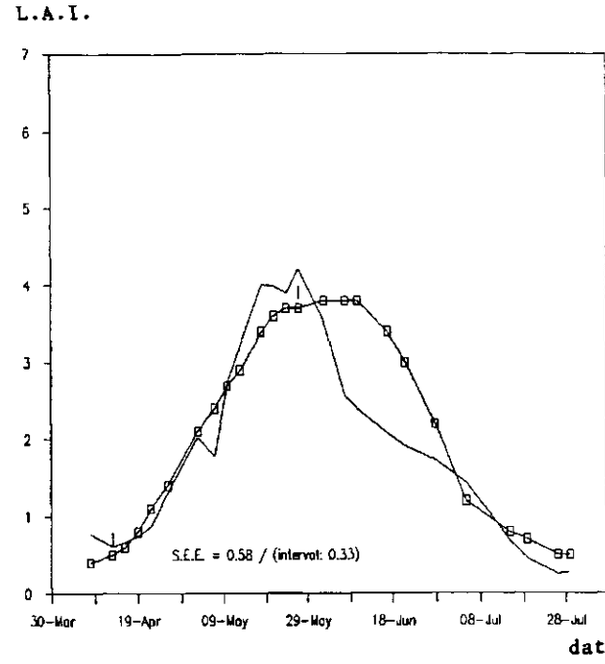

Fig. 6.19: measured and calculated LAI in time; Winter wheat, Oats and Barley across row, selected data of 1982 and 1983: Winter wheat Tundra, 1982.

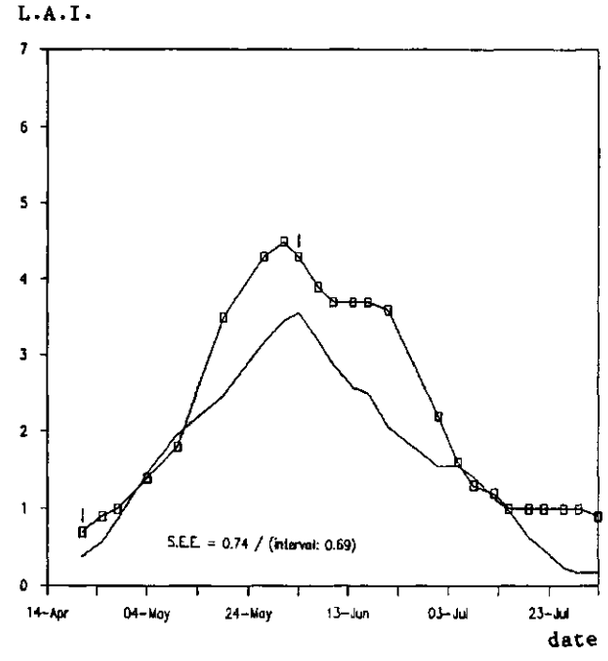

Fig. 6.20: measured and calculated LAI in time; Winter wheat, Oats and Barley across row, selected data of 1982 and 1983: Winter wheat Okapi, 1983.

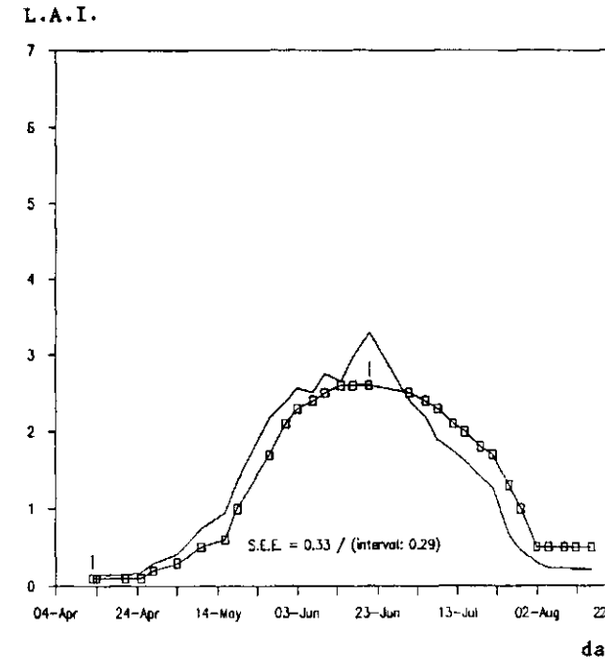

Fig. 6.21: measured and calculated LAI in time; Winter wheat, Oats and Barley across row, selected data of 1982 and 1983: Oats, 1983.

7 LINEAR REGRESSION BETWEEN CABO IR/R REFLECTANCE AND LAI

The method described in the previous Chapter is also applied to the data collected with the CABO reflectance meter. The same routine of calculation and lumping is followed.

The results of this exercise are summarized in Tables 7.1 and 7.2. In Table 7.1, the coefficients of regression are given for individual crops and fields, and for crops and fields clustered in groups of increasing magnitude. Table 7.2 gives the coefficients of correlation and the SEE's. The part of the growing season for which the regression analysis is performed is also indicated. Since the CABO reflectance measurements are taken vertically, there is no differentiation in across-row and along-row data.

7.1 Small grain cereals

Tundra winter wheat in 1982

In 1982 CABO reflectance measurements were taken at field 1 only. As with the HSM data, only the data pairs of the vegetative period (half April until the end of May) are used. This results in a very high coefficient of correlation of 0.97 and a low SEE of 0.21 (Table 7.2). There is almost no difference with the values calculated for the across-row HSM measurements for this field ($r2=0.96$, SEE = 0.23). During the period of generative growth and ripening the "fit" of the regression curve remains fairly good, unlike the regression curve obtained with the HSM data.

Small grain cereals in 1983

The selected periods for the regression analysis are the same as for the HSM regression, about six weeks from half April until the beginning or midst of June. For oats, this period lasts three weeks longer (Table 7.1).
For the individual fields of winter wheat varieties, the coefficients of correlation range from 0.90 to 0.93, and the SEE's from 0.37 to 0.41. If the four varieties are combined, the coefficient of correlation drops to a relatively low 0.87, and the SEE increases to an average of 0.54. This is worse than for the HSM, where the decrease was only minimal (Chapter 6.2).
In Fig. 7.1 the plot of the CABO IR/R reflectance ratios versus the LAI is shown for the lumped 1983 wheat varieties. It shows a rather large dispersion of the data points around the regression line. This is even better illustrated in Fig. 7.2, in which the estimated LAI is compared with the measured LAI for the Donjon plot. The estimated LAI is derived from the CABO IR/R measurements by means of inversion of the regression equation from the group of the four winter wheat varieties. Especially in the middle of the season, the estimated LAI fluctuates considerably. The SEE for the estimated LAI is 0.56 for the whole growing season and 0.47 at the period of vegetative growth.

For the 1983 winter wheat varieties, regression analysis is also applied to the data of the entire growing season. This results in lower values for the coefficient of correlation (0.78-0.92) and a higher SEE of 0.36-0.76 for the individual varieties. Lumping of the varieties results in a coefficient of correlation of 0.79 and an

Table 7.1: regression LAI and IR/R ratio, selected data CABO-meter, regression coefficients.

year + plotnr.	crop and variety	individual rc	individual y(x=0)	individual range	grouped: level 1 grp	grouped: level 1 rc	grouped: level 1 y(x=0)	grouped: level 2 grp	grouped: level 2 rc	grouped: level 2 y(x=0)	grouped: level 3 grp	grouped: level 3 rc	grouped: level 3 y(x=0)	grouped: level 4 grp	grouped: level 4 rc	grouped: level 4 y(x=0)
1982-1	Tundra winter wheat	4.19	0.67	13/4-27/5				1	3.77	0.77				1	4.19	0.45
1983-10	Arminda winter wheat	5.00	-0.79	16/3- 3/6				1	"	"				1	"	"
1983-11	Okapi winter wheat	3.74	1.58	16/3- 3/6	1	4.49	0.73	1	"	"	1	4.32	0.55	1	"	"
1983-12	Donjon winter wheat	4.78	0.87	16/3- 3/6	1	"	"	1	"	"	1	"	"	1	"	"
1983-13	Arminda winter wheat	5.97	-1.02	16/3- 3/6	1	"	"	1	"	"	1	"	"	1	"	"
1983-14	Durin winter wheat	4.17	0.55	16/3- 3/6	1	"	"	1	"	"	1	"	"	1	"	"
1983-6	Leanda Oats	2.45	1.18	13/4-21/6	2	2.44	1.70				1	"	"	1	"	"
1983-7	Audley Barley	4.77	1.09	21/4-10/6	2	"	"				1	"	"	1	"	"
1983-2	Monohil Beets	3.83	0.58	5/7-23/8	3	4.05	0.66				2	4.05	0.47	1	"	"
1983-4	Bintje Potatoes	4.19	0.64	5/7-30/9	3	"	"				2	"	"	1	"	"
1983-5	LG 11 Maize	3.39	0.40	1/7- 5/8	4	4.03	0.35				2	"	"	1	"	"
1983-8	Bintje Potatoes	4.36	0.45	5/7-30/9	4	"	"				2	"	"	1	"	"
1983-9	Prelude Beans	3.02	0.57	28/6-22/7	4	"	"				2	"	"	1	"	"
data of the entire growing season																
1983-11	Okapi winter wheat	3.87	0.96	1/3- 5/8	5	4.10	0.46									
1983-12	Donjon winter wheat	4.88	-0.55	1/3- 5/8	5	"	"									
1983-13	Arminda winter wheat	5.69	-1.38	1/3- 5/8	5	"	"									
1983-14	Durin winter wheat	3.76	-0.98	1/3- 5/8	5	"	"									

Table 7.2: regression LAI and IR/R ratio, selected data CABO-meter, correlation.

year + plotnr.	crop and variety	individual r^2	individual SEE	max. LAI	range	growing season	grouped: level 1 grp	grouped: level 1 r^2	grouped: level 1 SEE	grouped: level 2 grp	grouped: level 2 r^2	grouped: level 2 SEE	grouped: level 3 grp	grouped: level 3 r^2	grouped: level 3 SEE	grouped: level 4 grp	grouped: level 4 r^2	grouped: level 4 SEE
1982-1	Tundra winter wheat	0.97	0.21	3.8	13/4-27/5	1/4-29/7				1	0.88	0.32				1	0.88	0.22
1983-10	Arminda winter wheat	0.89	0.41	3.6	16/3- 3/6	1/3- 5/8				1	"	0.60				1	"	0.55
1983-11	Okapi winter wheat	0.93	0.41	4.5	16/3- 3/6	1/3- 5/8	1	0.87	0.49	1	"	0.50	1	0.85	0.43	1	"	0.42
1983-12	Donjon winter wheat	0.90	0.39	4.3	16/3- 3/6	1/3- 5/8	1	"	0.47	1	"	-	1	"	0.57	1	"	0.66
1983-13	Arminda winter wheat	0.91	0.38	4.2	16/3- 3/6	1/3- 5/8	1	"	0.67	1	"	-	1	"	0.76	1	"	0.84
1983-14	Durin winter wheat	0.93	0.37	5.5	16/3- 3/6	1/3- 5/8	1	"	0.43	1	"	-	1	"	0.37	1	"	0.37
							-----total:		0.54	-----total:		0.47						
1983-6	Leanda Oats	0.87	0.33	2.6	13/4-21/6	14/3-12/8	2	0.77	0.43				1	"	0.70	1	"	0.65
1983-7	Audley Barley	0.97	0.10	2.2	21/4-10/6	14/3- 9/8	2	"	0.65				1	"	0.23	1	"	0.27
							-----total:		0.52				-----total:		0.57			
1983-2	Monohil Beets	0.98	0.22	4.6	5/7-23/8	10/6-14/10	3	0.96	0.26				2	0.94	0.24	1	"	0.29
1983-4	Bintje Potatoes	0.96	0.26	3.9	5/7-30/9	10/6-14/10	3	"	0.28				2	"	0.30	1	"	0.26
							-----total:		0.27									
1983-5	L6 11 Maize	0.97	0.26	6.4	1/7- 5/8	7/6-23/9	4	0.92	0.47				2	"	0.52	1	"	0.59
1983-8	Bintje Potatoes	0.94	0.29	3.9	5/7-30/9	10/6-14/10	4	"	0.41				2	"	0.38	1	"	0.32
1983-9	Prelude Beans	0.91	0.23	3.1	28/6-22/7	7/6- 6/9	4	"	0.32				2	"	0.34	1	"	0.46
							-----total:		0.42				-----total:		0.36	-----total:		0.48

data of the entire growing season

1983-11	Okapi winter wheat	0.89	0.48	1/3- 5/8	5	0.79	0.46
1983-12	Donjon winter wheat	0.86	0.50	1/3- 5/8	5	"	0.69
1983-13	Arminda winter wheat	0.92	0.36	1/3- 5/8	5	"	0.74
1983-14	Durin winter wheat	0.78	0.76	1/3- 5/8	5	"	0.95
					-----total:		0.73

average SEE of 0.73. The mentioned coefficients of correlation and SEE's apply to the whole growing season.
The SEE for the entire season, using the regression for the selected periods, however, is slightly better with 0.70. In Fig. 7.3, the regression through the data of the entire season for all varieties combined, is shown. Comparison of Fig 7.4, which shows the LAI estimated from the regression for the entire season, and Fig 7.2, in which the same is presented for the selected periods, shows clearly that there is almost no difference. The regression lines are almost identical, though it should be noted that the lower coefficient of correlation for the line representing the entire season means that this relation is less reliable.

The lumping of oats and barley gives the poorest results of all groups, a coefficient of correlation of 0.77, and a SEE of 0.52. The coefficients of correlation for the individual crops are 0.87 and 0.97, and the SEE's are 0.33 and 0.10. Figs. 7.5 and 7.6 show clearly that the results of this regression analysis are only valid for a restricted period.
Regression through the data of the entire season is not practical, because of the typical "bulb-shape" of the LAI versus the CABO IR/R reflectance curves (Figs. 7.7 and 7.8).

Wheat, oats and barley

The regression coefficients of oats differ from the coefficients of wheat and barley. This causes the low correlation of the oats-barley group, and is the main reason for the rather low (0.85) coefficient of correlation for the total group of small cereals of 1983. This is only slightly lower than the coefficient of correlation for the wheat plots taken together (0.87) and much higher than that of the oats-barley group (0.77). The average SEE for the small cereals of 1983 is 0.57.

Clustering of all wheat fields in both 1982 and 1983 results in a coefficient of correlation of 0.88, almost the same as the coefficient of correlation of the clustered 1983 wheats. For the CABO meter, there is no difference between the 1982 and 1983 winter wheat fields. When the data from the selected parts of the growing season are thrown together for all the small grain cereals wheat, oats and barley, the coefficient of correlation is still 0.88.

7.2 Non-cereal crops and maize

The lumping of the non-cereal crops is done with the same groups as with the HSM regression. Additionally, these groups are combined to form one large 'non-cereal' group.

Sugar beets and potatoes

For potatoes, all data are used in the regression analysis. This results in a high coefficient of corelation of 0.96, with a SEE of 0.26. Fig. 7.10 shows the comparison between measured and estimated LAI. In Fig. 7.11, the same is presented for sugarbeets. For this crop, the data from the first week of July until the third week of August are selected. The calculated coefficient of correlation is even higher than that for potatoes with 0.98, and a SEE of only 0.22.

While the lumping of these two crops results in a large decrease in correlation for the HSM, the CABO regression shows a high coefficient of correlation of 0.96 for the grouped data with a SEE of 0.27. In Fig. 7.9, the regression lines of potatoes and sugarbeets are very much alike.

Maize, beans and potatoes

For maize and beans, only one month of the vegetative part of the growing season is analysed. For potatoes, the data of the entire growing season are used. The individual coefficients of correlation are respectively 0.97, 0.91 and 0.94. This is lower than the values obtained with the HSM. The SEE values are 0.26, 0.23 and 0.29 (Table 7.2).

In Figs 7.12, 7.13 and 7.14 the estimated LAI values, derived from the inversion of the regression equations, are compared with the measured values. While the estimated curves and the actual curves for maize and potatoes show a good fit for all data (maize was only monitored until the first week of August), the curves for beans show a large differentiation after the selected part of the growing season. Clustering of these three crops results in a drop of the coefficient of correlation, but only to a relative high 0.92. The average SEE increases to 0.42. Fig. 7.15 shows the different regression lines.

Potato fields 4 and 8

Comparison of the CABO data from both fields of potatoes gives an impression on the variation due to local differences in plant growth conditions and all types of sampling, measuring and calculation errors. The two regression lines are very similar, as are the calculated coefficients of correlation and SEE's.

All non-cereal crops combined

Combination of the two fields of potatoes with maize, beets and beans results in a high coefficient of correlation of 0.94. This is probably caused by the relatively smaller influence of the data of the beans, and the fact that all five regression lines are grouped very closely together. The combined SEE is 0.36. Fig 7.16 shows the regression line of the grouped non-cereals. Only the selected parts of the growing season are used in the calculation.

7.3 Summary.

Regression analysis applied to selected parts of the growing season results in high to very high coefficients of correlation for the individual crops, ranging from 0.87 to 0.98. The SEE's range form 0.10 to 0.41. Combination of the data of the 1983 wheat fields results in a drop of the correlation from an average of 0.92 per crop to 0.87. Further lumping with the 1982 wheat field (Tundra) does not affect this correlation. Lumping with oats and barley gives a slightly lower correlation, due to the different nature of the regression coefficients for oats.
The lumping of maize and the non-cereal crops potatoes, beets and beans can be done without much loss in correlation. Lumping of all these crops still gives a coefficient of correlation of 0.94. The

average SEE for the group is only 0.36.

For the regression applied to the entire growing season, the correlation between CABO IR/R reflectance and LAI is lower for the period of vegetative growth. If the total growing season is considered, the correlation is a little higher than if the regression is based on the vegetative part of the growing season only. For single crops, the coefficient of correlation for the entire growing season ranges from 0.78 to 0.92. Clustering of the all-season data of the across-row winter wheat plots results in a decrease to 0.79, which is more than the decrease for clustering of the selected data (Table 7.1 and 7.2).

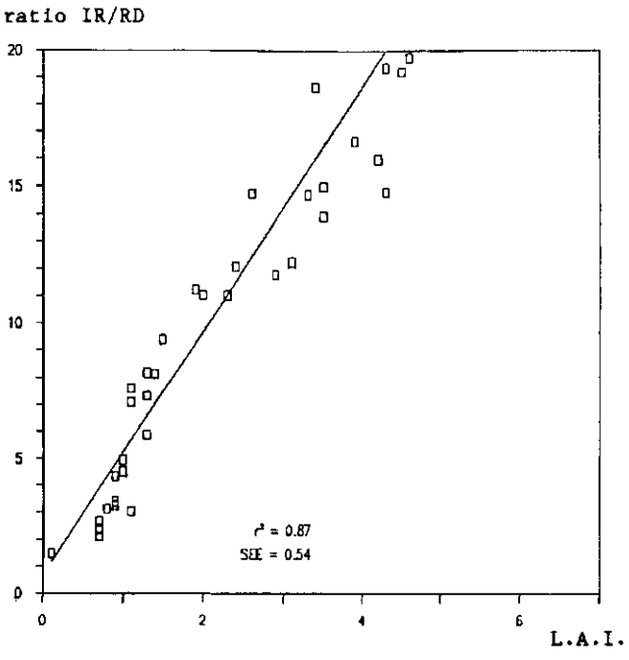

Fig. 7.1: CABO IR/R ratio versus LAI; all winter wheat varieties, 4/16-6/3 1983.

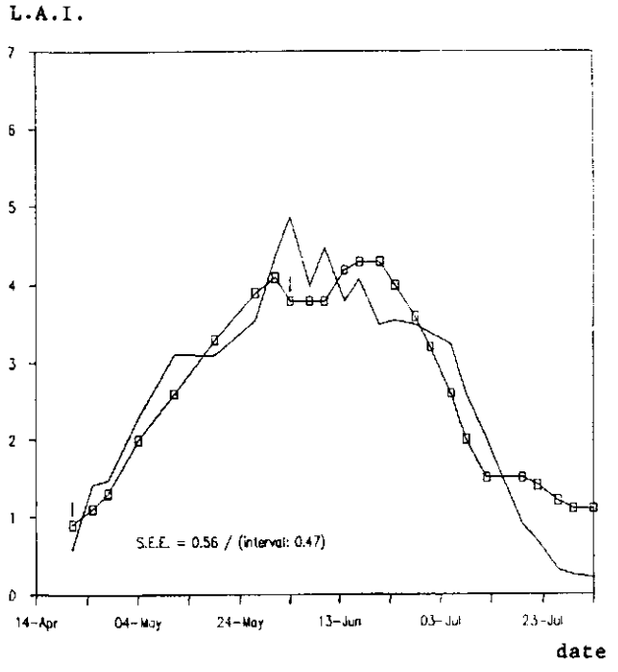

Fig. 7.2: measured and calculated LAI in time; all winter wheat varieties: Winter wheat Okapi, 4/21-6/3 1983.

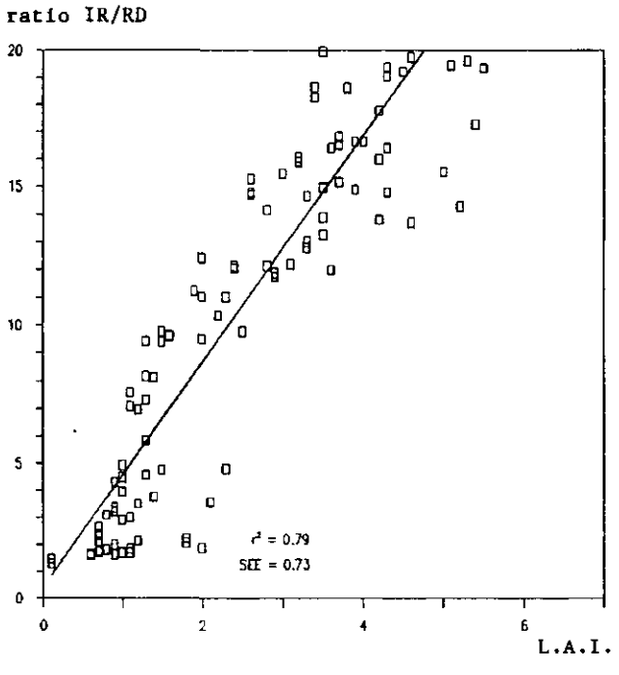

Fig. 7.3: CABO IR/R ratio versus LAI; all winter wheat varieties, all data of 1983.

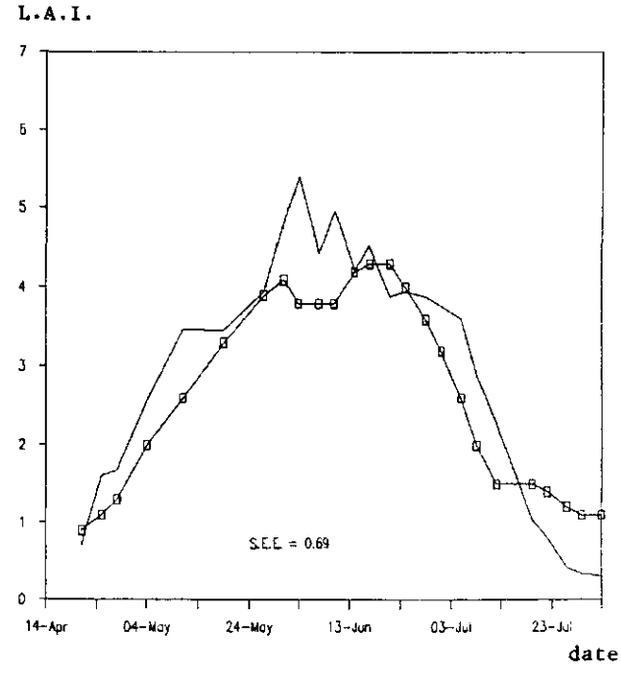

Fig. 7.4: measured and calculated LAI in time; all winter wheat varieties: Winter wheat Okapi, all data of 1983.

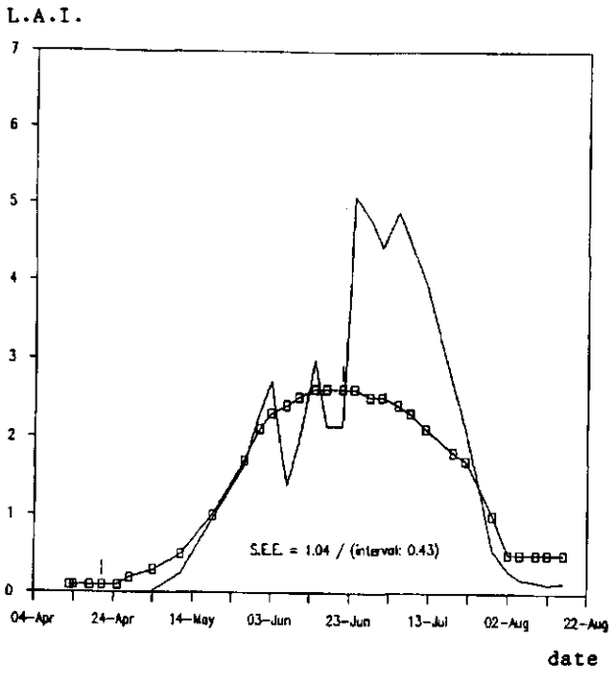

Fig. 7.5: measured and calculated LAI in time; Oats, 4/13-6/21 1983.

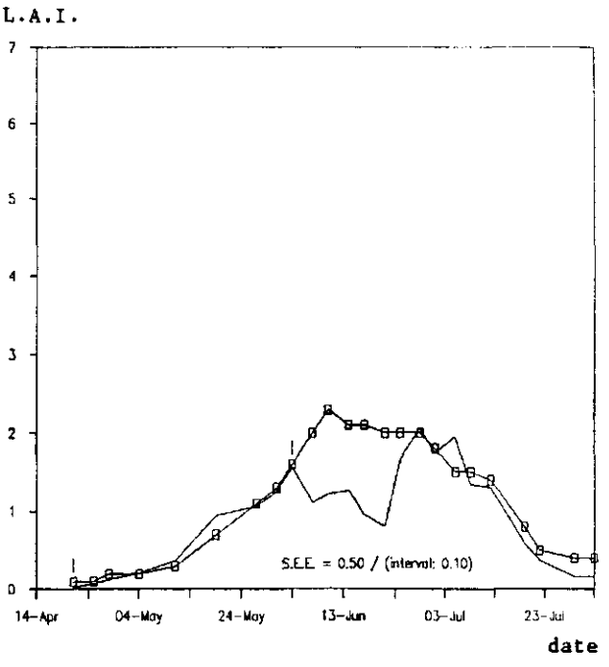

Fig. 7.6: measured and calculated LAI in time; Barley, 4/21-6/3 1983.

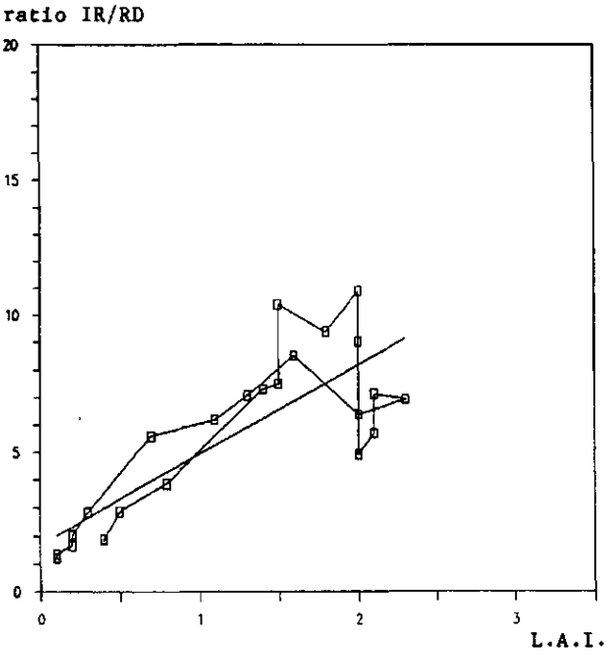

Fig. 7.7: CABO IR/R ratio versus LAI; Barley, all data 1983.

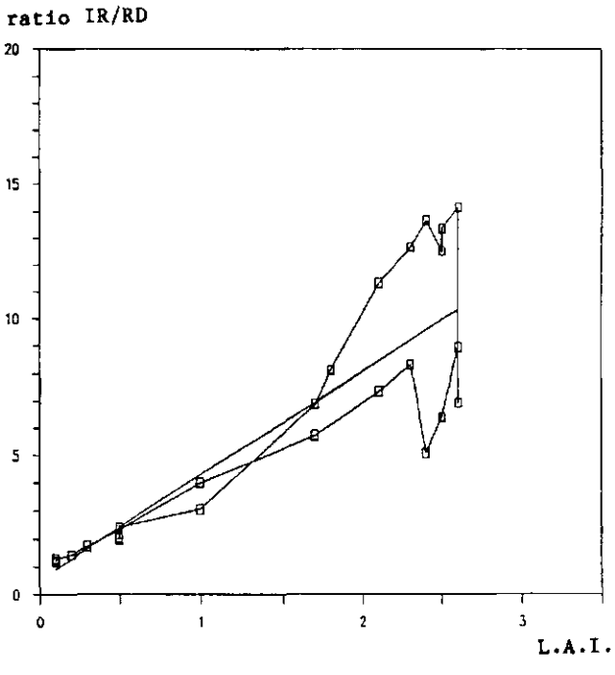

Fig. 7.8: CABO IR/R ratio versus LAI; Oats, all data 1983.

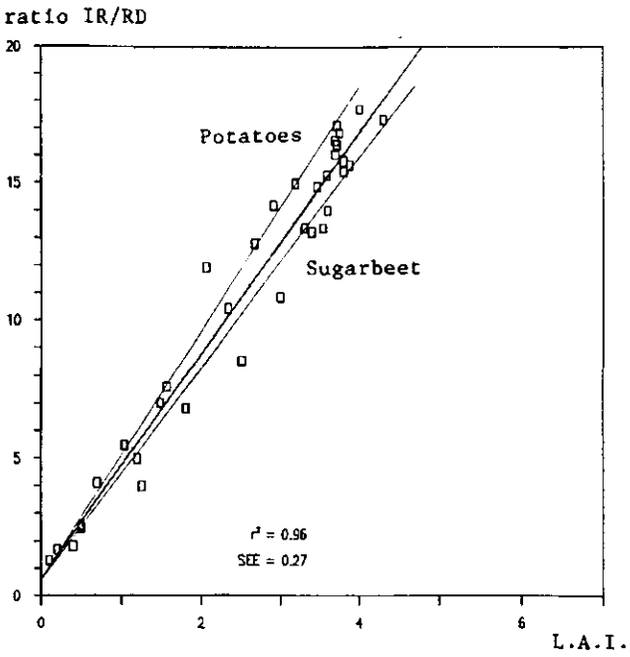

Fig. 7.9: CABO IR/R ratio versus LAI; Sugarbeet and Potatoes, selected data 1983.

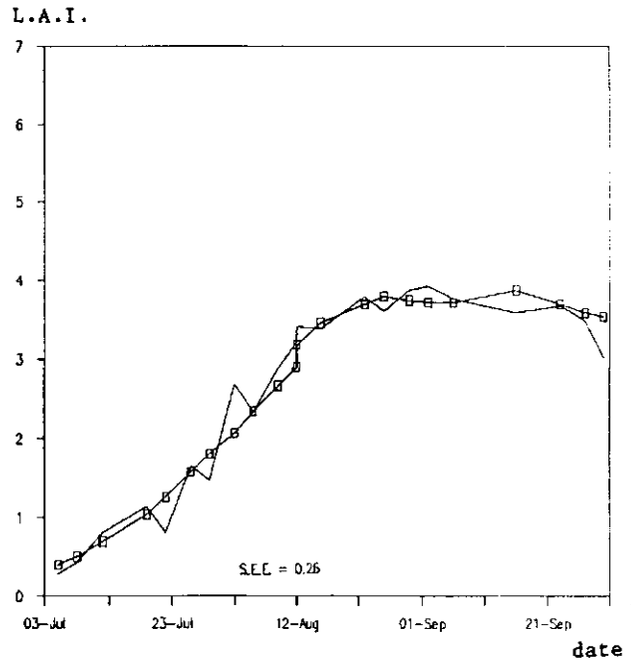

Fig. 7.10: measured and calculated LAI in time; Potatoes, 6/10-10/14 1983.

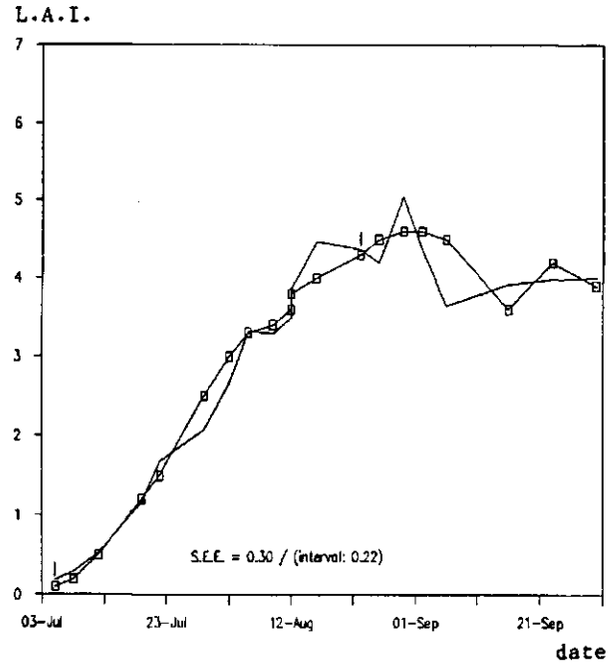

Fig. 7.11: measured and calculated LAI in time; Sugarbeet, 7/5-9/23 1983.

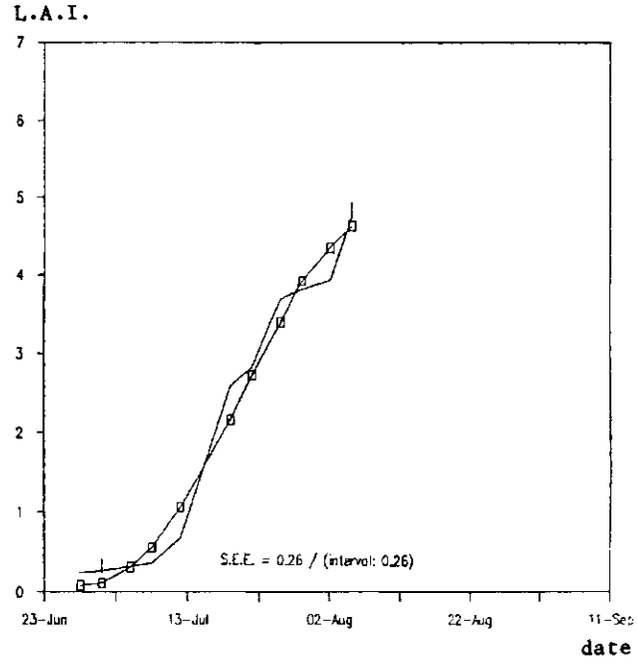

Fig. 7.12: measured and calculated LAI in time; Maize, 7/1-8/5 1983.

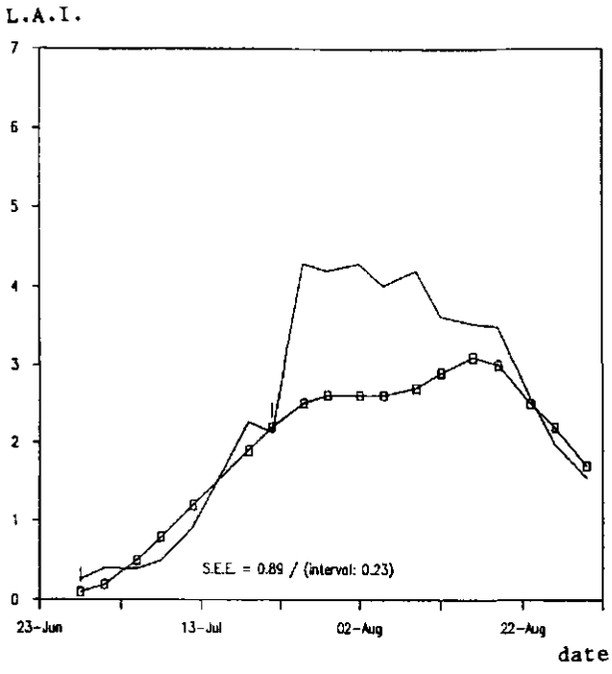

Fig. 7.13: measured and calculated LAI in time; Beans, 6/28-7/22 1983.

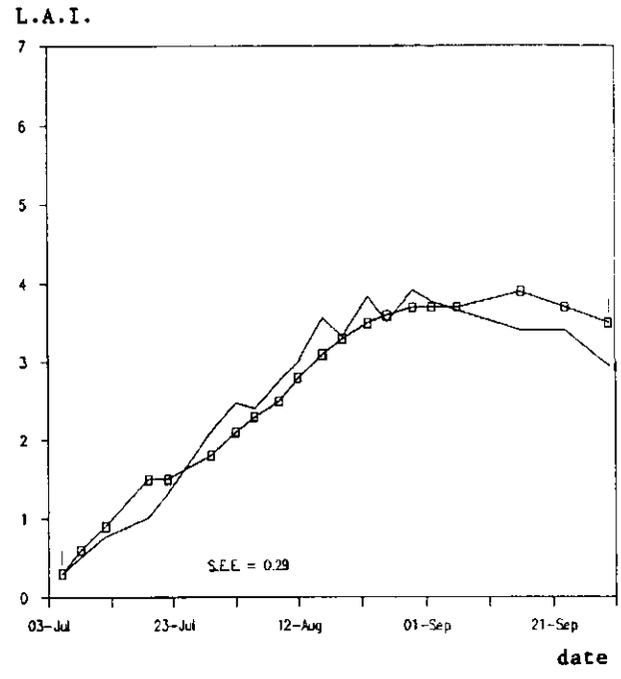

Fig. 7.14: measured and calculated LAI in time; Potatoes, 7/5-9/30 1983.

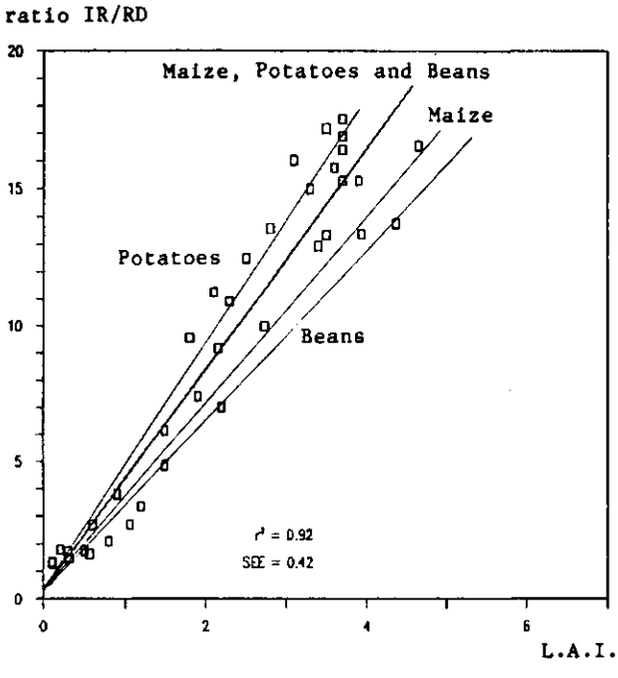

Fig. 7.15: CABO IR/R ratio versus LAI; Maize, Potatoes and Beans. selected data 1983.

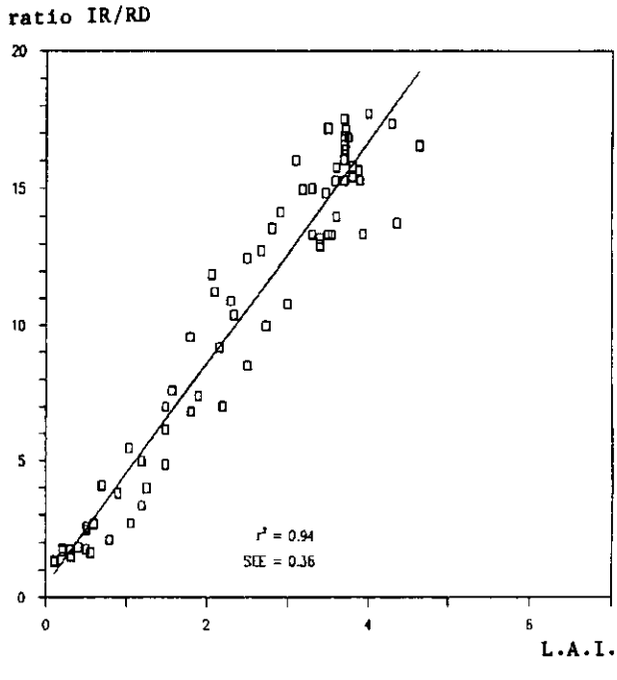

Fig. 7.16: CABO IR/R ratio versus LAI; Maize, Potatoes, Beets and Beans. selected data 1983.

8 SUMMARY AND DISCUSSION

8.1 IR/R reflectance and crop parameters

8.1.1 Leaf Area Index

For all investigated crops, the IR/R reflectance is a monotone ascending function of the Leaf Area Index LAI during the vegetative part of the growing season. The relationship between the IR/R reflectance and LAI is linear and can be described with linear regression equations. For the HSM, the coefficients of correlation range from 0.94 to 0.99 for the regression for individual crops and varieties. For the CABO meter, the correlations are slightly lower and range from 0.87 to 0.98. Because there are no replicates of the experiments (in 1983 other crops and varieties were measured at a different location than in 1982), the validity of the calculated coefficients of regression can not be tested. Also, a statistical analysis indicating the reliability could not be executed. Therefore, the calculated coefficients of regression should not be considered for predictions of the LAI. They are only computed to enable comparison between the HSM and the CABO reflectance meter, see Chapter 8.2.

After the canopy has closed the crops can be divided into two categories based on the further development of the crop canopy.
For beets and potatoes, the canopy architecture does not change very drastically and the LAI only increases a little more until the end of the growing season. General trends in the reflectance ratios are related to changes in spectral colour and/or to collapse of the canopy at the end of the growing season (more bare soil becomes visible). The IR/R reflectance ratio decreases and shows more fluctuations.
For the other crops, the canopy architecture changes relatively drastically after the period of vegetative growth. New organs like ears (small grain cereals), panicles and cobs (maize), or pods (beans) are formed in the canopy at the expense of the green leaves. With the formation of these organs and the loss of green leaves, the canopy spectral colour changes accordingly. The changes in IR/R reflectance are therefore the combined result of the changes in canopy structure, LAI and spectral colour of the canopy components. For the crops in this category, the IR/R reflectance is a monotone decreasing function during most of the generative phase of growth and ripening of the crop.

8.1.2 Canopy biomass

The relationship between canopy biomass and the IR/R reflectance is not adequately described by linear equations during the whole growing season for all crops.
For beets and potatoes, the IR/R reflectance is a monotone increasing function with canopy biomass. At the end of the growing season, the IR/R reflectance may decrease because of yellowing and/or lodging of the crop canopy. During the first two months of the growing season, the relation between the IR/R reflectance and the canopy biomass can be described with linear equations until a value of 2.5 t/ha canopy biomass is reached for potatoes, and 4.0 t/ha for beets. The overall IR/R reflectance curve may be described better by a (1-exp) growth function.
For all other crops (wheat, oats, barley, maize, beans) the

relationship between the IR/R reflectance and the canopy biomass is twofold. During most of the vegetative period of the growing season, the IR/R reflectance is a monotone increasing function of canopy biomass. During generative growth and ripening, the IR/R reflectance decreases with canopy biomass. At neither the vegetative nor the generative stage, the relationship is truly linear. In Fig. 8.1, the HSM IR/R reflectance ratio is plotted against canopy biomass for all six fields of Tundra wheat in 1982. Separate linear regression analysis on the rising and falling limbs of the plot results in coefficients of correlation of 0.89 for HSM measurements across the row, and of 0.71/0.79 for HSM measurements along the row. The data are more dispersed around the line of regression for the falling limb than for the rising limb. This again points to the complexity of the reasons for the decrease in the IR/R reflectance during generative growth and ripening of the crop. In Fig. 8.2, the biomass calculated from the inversion of the two regression equations (HSM across-row) is given together with the measured biomass. Despite the relative low coefficients of correlation, the growth in canopy biomass is reasonably well calculated.

8.2 The HSM and the CABO reflectance meter

Based on visual analysis of the curves of the IR/R reflectance ratio during the growing season (Chapter 4), there is hardly any preference for the CABO reflectance meters or for the HSM. The level of the IR/R reflectance ratio is higher with the CABO meter, but the shape of the curves is generally the same. Only for oats and barley, the HSM IR/R reflectance curves deviate from the CABO IR/R reflectance curves. In general, the CABO curves display only slightly more fluctuations than the HSM reflectance curves, while for oats and barley the fluctuations are much more evident.

For individual crops, the quantitative relation between IR/R reflectance and LAI is slightly better for the HSM. The coefficients of correlation for the linear regression between the IR/R reflectance and the LAI for the HSM range from 0.94 to 0.99, with SEE values from 0.15 to 0.30. For the CABO meter the coefficients of correlation range from 0.87 to 0.98, the SEE from 0.20 to 0.50.
When various crops and varieties are grouped together to determine the average coefficients of regression, the CABO meter performs generally better than the HSM (Table 8.1). Only for the small grain cereals (wheat, barley, oats) clustered together, the correlation between IR/R reflectance and LAI is higher with the HSM.

Table 8.1: Coefficients of regression and standard errors of estimate with the HSM and CABO meter for various crops and varieties grouped together.

	CABO		HSM	
	r2	SEE	r2	SEE
wheat, barley, oats	0.85	0.57	0.92	0.41
maize, potatoes, beans	0.92	0.42	0.85	0.43
beets, potatoes	0.96	0.27	0.83	0.58
maize, potatoes, beans, beets	0.94	0.42	-	-
all crops together	0.88	0.48	0.82	0.61

In the cluster of all crops, the measurements of the wheat crops in 1982 are included for the HSM measurements, but not included for the CABO measurements. However, this is not the reason for the relative low correlation obtained with the HSM. It is rather the deviating slope of the regression line for the crops beets, potatoes, maize and beans that results in the low correlation.

From the regression exercises, it is concluded that the HSM performs better than the CABO reflectance meter when a) only individual crops and varieties are considered, and b) only the small grain cereals are clustered. A significant advantage over the CABO meter is reached for the crops oats and barley. For all other clusters of crops, including the large group of all crops, the CABO meter performs better. Therefore, it is concluded that, using the HSM concept, the expected increase in correlation between the IR/R reflectance and LAI for groups of crops with different canopy structure, is not demonstrated.

Two explanations are suggested for this lack in difference between the performances of the CABO reflectance meter and the HSM.
First, the canopy structure of agricultural crops in the field differs too much from the theoretical model used as basis for the HSM concept. Notably the row structure of the crops has a large influence on the HSM reflectance at 52^{o} view angle off nadir (Chapter 4). If measurements are taken at vertical view angle, as with the CABO meter, the direction of the rows has less influence on the reflectance, and no influence when an active source of radiation is used. Therefore, the theoretical advantages of independence of HSM reflectance of the leaf angle distribution might be offset by the influence from the canopy row structure at 52^{o} view angle.
Second, the differences in reflectance from the various crops might be attributed more to the differences in spectral colour of the canopy components than to differences in the leaf angle distribution. Both the HSM and the CABO reflectance meter would therefore detect differences between crops based on the spectral leaf colour.
To investigate both suggested explanations, regular reflectance measurements during the growing season of several single canopy components, and of HSM measurements at vertical view angle are needed.

The HSM and CABO reflectance meter are also compared on their practical workability in the field. Since the CABO meter was especially designed for this purpose, it offers many advantages. It is light-weight, easily portable and produces instantaneous output. The

prototype of the HSM is heavy-weight and not easily portable. Single band reflectances can not be considered separately because of the divergent nature of the irradiant flux. These handicaps should be overcome before the HSM can be operationaly used as a field instrument. When the HSM is used for crop monitoring, measurements should always be made at the same view angle either along or across the direction of the rows. With the CABO meter, the view angle is vertical and problems may only arise with the choice of position relative to the sun.

8.3 Recommandations

In this report, no answers are given to the question of the suitability of reflectance measurements, either with HSM or CABO meter, for the determination of plant parameters like LAI, soil cover or biomass. This is partly caused by the failure to achieve differences in crop growth and development in the 1982 experiments, and partly because the experiments were not reproduced in a sufficiently large number to allow statistical analysis. Based on the analyses presented in this report, some recommandations are given for further research on the subject.

- Study of reflectance in individual spectral bands in the visible and near infrared part of the spectrum.
In this report, only reflectance ratios are used because of the requirements of the HSM concept. This leads to a loss in potentially useful information and to an increased difficulty in measurement analysis. Reflectance ratios of crops, combining the reflectance in the near infrared and in the visible part of the spectrum, are influenced by both the amount of vegetative material as by the colour of the vegetative material. If reflectance measurements are to be useful for crop growth monitoring, a method must be developed for distinguishing between these two qualities of the crop. Radiation in the near infrared part of the spectrum penetrates relatively deeply in crop canopies and is potentially suitable for monitoring quantities of vegetative material, i.e. biomass, LAI or soil cover. Radiation in the visible part of the spectrum does not penetrate the canopy as deeply and responds to changes in canopy colour at relatively low levels of biomass. Since the colour of a crop relates to its photosynthetic activity, reflectance measurements in the green and red part of the spectrum are potentially useful for determining the 'quality' of the vegetative material (i.e. crop colour, photosynthetic capability). Measuring reflectance during senescence gives probably an easier method to asses photosynthetic activity then measurement of LAI in the conventional way.

- Study of canopy reflectance in relation to crop development. It is necessary to study the physiological meaning of peaks and dips in the reflectance curves. A redefinition of development stage on the basis of changes in canopy reflectance is needed. For instance, the peak in infrared/red red reflectance of the cereals appears related with the change from vegetative to generative phase but it does not coincide with the phenomenon of flowering.

- Adaption of the prototype HSM:
1) Automatic correction for the divergent nature of the radiant flux, based on the distance between the sensor head and the canopy surface.

This allows the analysis of reflectance in the individual passbands.
2) Combination of the vertical view angle of the CABO meter with the active source of radiation of the HSM. The vertical view angle makes the measurements less dependent on the row direction of the crops. The active source of radiation is needed to be independent of varying solar illumination conditions for the analysis of reflectance in individual passbands.
3) Light weight and easily portable.

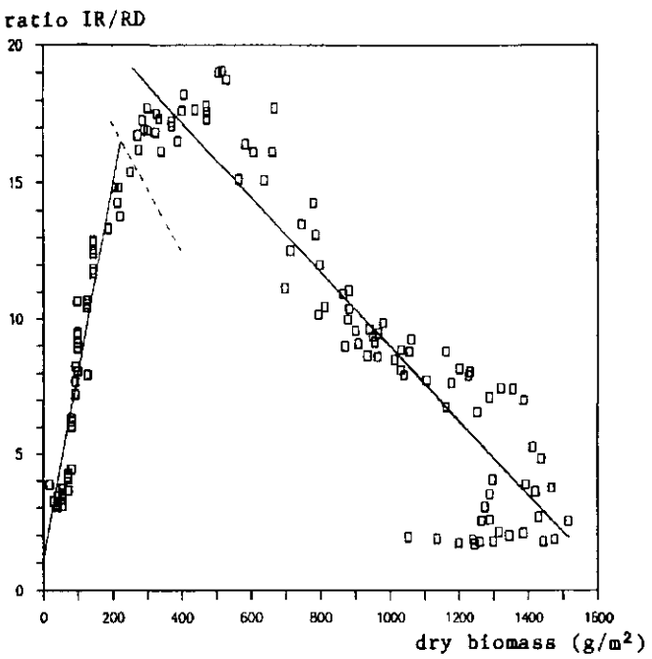

Fig. 8.1a: HSM IR/R ratio versus dry biomass; Winter wheat Tundra, across row, all data 1982.

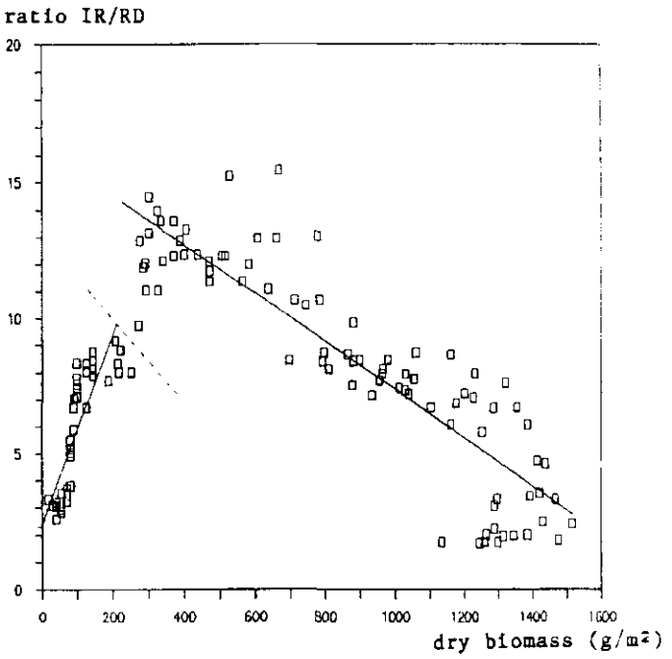

Fig. 8.1b: HSM IR/R ratio versus dry biomass; Winter wheat Tundra, along row, all data 1982.

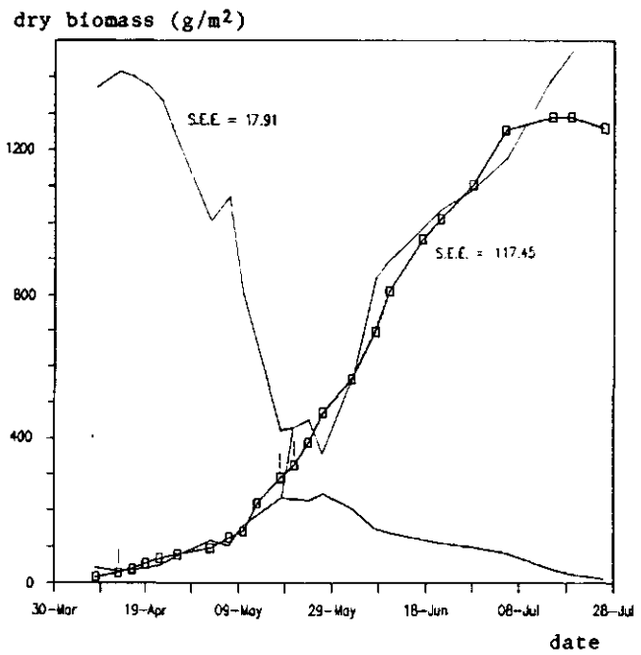

Fig. 8.2: measured and calculated dry biomass in time; Winter wheat Tundra, across row, combined regressions.

REFERENCES

Bunnik, N.N.J, 1978. The multispectral reflectance of shortwave radiation by agricultural crops in relation with their morphological and optical properties. Thesis, Communications Agricultural University Wageningen, the Netherlands.

Bunnik, N.N.J. et al., 1983. Hot-spot reflectance measurements applied to green biomass estimation and crop growth monitoring. IInd International Colloquium on Spectral Signatures in Remote Sensing (ISP-INRA). Proceedings pp. 111-121.

Bunnik, N.N.J. et al., 1984. Evaluation of ground based hot-spot reflectance measurements for biomass determination of agricultural crops. Eighteenth International Symposium on Remote Sensing of Environment, 1-5 october 1984. Proceedings pp 1033-1041

Clevers, J.G.P.W., 1986. Application of remote sensing to agricultural field trials. Thesis, Agricultural University Wageningen Papers 86-4, The Netherlands.

Geerts, R., 1982. HSM op Proefboerderij "Droevendaal". Internal report CABO.

van Kasteren, H.W.J., 1981. A spectrometer to determine soil coverage and biomass in situ. Ist International Colloquium on Spectral Signatures in Remote Sensing (ISP-INRA). Proceedings pp. 125-132

Noordman, H., 1982. HSM 1983 op Proefboerderij "de Schreef". Internal report CABO.

Suits, G.H., 1972. The calculation of the directional reflectance of a vegetative canopy. Remote Sensing of Environment, 2.

Uenk, D., 1982. Bepaling van grondbedekking en biomassa met behulp van een reflectiemeter (Dutch). CABO-verslag 41, Centrum voor Agrobiologisch Onderzoek, Wageningen, the Netherlands.

Verhoef, W., 1984. Light scattering by leaf layers with application to canopy reflectance modelling: the SAIL model. Remote Sensing of Environment, 16.

Warren Wilson, J., 1965. Stand structure and light penetration I. Analysis by point quadrats. Journal of applied ecology, 2 (2).

APPENDIX I

Deriviation of the canopy hot-spot reflectance properties

I.1. Directional reflectance of a uniform leaf canopy

For reasons of simplicity an infinitively horizontally extended uniform leaf canopy is considered. The canopy is assumed to be a homogeneous diffuse scattering medium.
For the (passive) bidirectional geometry the directional reflectance, r, is defined as:

$$r\ (\theta_o,\theta_s,\psi;\lambda) = \frac{\pi L(\theta_o,\theta_s,\Psi;\lambda)}{E_i(\lambda)}$$

The spectral radiance L (W/m^2 sr nm) is dependent of the zenith observation angle θ_o, the zenith solar angle θ_s, and their azimuthal difference angle ψ. The total irradiance E_i (W/m^2 nm), is equal to the sum of the incident direct solar flux E_s, and the incoming diffuse sky irradiance E_-.

$$E_i\ (\lambda) = E_s\ (\theta_s;\lambda) + E_-\ (\lambda)$$

The radiance leaving the top of the canopy into the direction of observation can be described by means of a two-stream radiative transfer model. The incident radiation is transferred in upward (+) and downward (-) diffuse fluxes. The direct solar flux is attenuated to $E_s(x)$ at depth x.
For the case of an isotropic (Lambertian) approximation of the internal diffuse flux, the upwelling diffuse flux at depth x equals:

$$E_+(x) = \pi L_+(x),$$

where L_+ is the scattered radiance in upward direction (integrated for a total hemispere).
The same approximation holds for the downwelling diffuse flux $E_-(x) = \pi L_-\ (x)$.

The radiative transfer equations for the three fluxes within the canopy are described by linear first order differential equations with constant coefficients for extinction (a) and backscattering (σ) of diffuse fluxes, and extinction (k) forward scattering (s) and backscattering (s') of the direct solar flux.

$$\frac{d}{dx} E_+(x) = -aE_+(x) + \sigma E_-(x) + s'E_s(x)$$

$$\frac{d}{dx} E_-(x) = -\sigma E_+(x) + aE_-(x) - sE_s(x)$$

$$\frac{d}{dx} E_s(x) = kE_s(x)$$

The solution of this set of simultaneous equations is:

$$E_+(x) = A\, e^{mx} + B\, e^{-mx} + C\, E_s(0)\, e^{kx}$$

$$E_-(x) = hA\, e^{mx} + h^{-1}B\, e^{-mx} + D\, E_s(0)\, e^{kx}$$

$$E_s(x) = E_s(0)\, e^{kx}$$

$E_s(0)$ is the solar flux at the top of the canopy.
The constants A and B are found by substitution of the boundary conditions:
1) At the top of the canopy (x=0), E_- equals the diffuse sky irradiance.
2) The downwelling radiation is reflected by the soil at depht $x = -x_1$
$E_+(-x_1) = \rho_s \{E_-(-x_1) + E_s(-x_1)\}$ where ρ_s is the hemispherical soil reflectance.
The other constants in equations (6) are:

$$m = \sqrt{a^2 - \sigma^2} \qquad h = (a + m)/\sigma$$

$$C = \frac{s\sigma - s'(k-a)}{m^2 - k^2} \qquad D = \frac{s'\sigma + s(k+a)}{m^2 - k^2}$$

The fluxes illuminate the randomly distributed canopy components present in the canopy layer, dx.
The resulting directional radiance, dL(x), is equal to the sum of the scattered proportions of the direct solar flux and both diffuse fluxes.

$$\pi dL(x) = \{uE_+(x) + vE_-(x) + wE_s(x)\}dx$$

The weighting factors u, v, w are depending from observation direction.

The radiance contribution which leaves the canopy top is attenuated by a factor corresponding with the probability of gap: $p(x) = \exp(-Kx)$,
in which K is the extinction coefficient into the direction of observation.

The contribution of the total canopy to the directional radiance is found by integration of the product of dL(x) and p(x) over the canopy height.
The contribution of the soil radiance, attenuated by the total canopy layer, equals $\exp(-Kx_1).E_+(-x_1)$.
The total directional radiance of the crop L, is found by addition of canopy and soil contributions.

For a homogenous canopy of thickness x_1, the following equation holds:

$$\pi L(\Theta_o,\Theta_s,\psi) =$$

$$(uC + vD + w).E_s(0).\{1-\exp(-x_1(K+k))\}/(K+k)$$

$$+ \rho_s\ (D+1).E_s(0).\exp(-x_1(K+k))$$

$$+ A\ (u+vh).\{1-\exp(-x_1(K+m))\}/(K+m)$$

$$+ B\ (u+vh^{-1}).\{1-\exp(-x_1(K-m))\}/(K-m)$$

$$+ \rho_s\ \{hA.\exp(-x_1(K+m)) + h^{-1}B.\exp(-x_1(K-m))\}$$

The single scattering contribution to the radiance is expressed by the term:

$$w.E_s(0).\{1-\exp(-x_1(K+k))\}/(K+k)$$

$$+ \rho_s.E_s(0).\exp(-x_1(K+k))$$

The terms including the constants C and D present the single scattering of diffuse flux generated by scattering of direct flux. The multiple scattering contribution is described by the terms including the constants A and B.
Instead of expressing all scattering and extinction coefficients proportional to the leaf area density, all these coefficients may be multiplied by the canopy height. In this case, all scattering and extinction coefficients become proportional to the leaf area index.

I.2. Canopy reflectance in the hot-spot

The hot-spot geometry is defined by the following simplifications:

a) the angles of observation and illumination coincide; $\Theta_o = \Theta_s$ and $\Psi = o$

b) all directly illuminated canopy elements are also observed directly; $p(x) = 1$ for single scattering

c) absence of sky irradiance; $E_{-}(0) = 0$

For the hot-spot condition at least in the visible part of the spectrum, it is assumed that the single scattering of direct flux will be the dominant contribution to the total canopy reflectance. This term is:

$r_b = \frac{w}{K}(1 - e^{-K}) + \rho_s e^{-K}$ where $1-e^{-K}$ equals the apparent soil cover.

After substitution of Suits' coefficients, the ratio between the single scattering coefficient, w, and the extinction coefficient, K, can be written as:

$$\frac{w}{K} = \rho \cdot \frac{1 + \frac{1}{2}tg\Theta_o tg\Theta_o.X}{1 + 2/\pi.tg\Theta_o.X}$$

where X is the ratio of the area index for the vertical and the horizontal elements of a Suits canopy.
For an observation angle of 52° (when $\frac{1}{2}tg\Theta_o = 2/\pi$), w/K equals ρ; the hemisperical reflectance of the leaves.

It is concluded that for the single scattering approach and for dense canopies (exp(-K)=0), the hot-spot reflectance r_b, becomes equal to ρ.
For dense canopies ($r_b = w/K$) and the special view angle of 52°, the single scattering reflectance is independent of X, the parameter for leaf inclination angle in the model of Suits.
The other solution $\Theta_o = 0^o$ should be excluded since for nadir view only the horizontal components will contribute to the single scattering reflectance in the hot-spot.

The particular oblique observation angle indentified earlier by Warren Wilson is also found by assuming that the sum of the horizontal and vertical leaf area indices is constant. In this case K cos Θ_o, describing the total projected leaf area into the direction of observation is constant for $tg\Theta_o = \pi/2$ ($\Theta_o = 57.5°$). The difference between the two angles 52° and 57.5° is small.
This means that the canopy hot-spot reflectance also for the condition of uncompleted soil cover is not sensitive to changes of the leaf inclination distribution function. When it is assumed that the soil reflectance and the leaf reflectance do not change, the hot-spot reflectance will only vary with the leaf area index. Since for leaf canopies, the green leaf biomass per unit of soil area is proportional to the LAI, the measurement of the hot-spot reflectance could be considered as an estimator of biomass.

I2.1. The hot-spot reflectance of an infinitely thick canopy

A uniform canopy with large LAI can be approximated by an infinitely thick canopy, because more than 10 leaf layers do no longer effect change of reflectance due to multiple scattering.
Because of the boundery condition for $x = -\infty$ and the corresponding extinction of internal fluxes it is concluded that $B = 0$.
For the condition $E_-(0) = 0$ follows: $A = -D/h.E_s(0)$.

The irradiant fluxes for this case are given by:

$$E_+(x) = \{- D/h\ e^{mx} + C\ e^{Kx}\}E_s(0)$$

$$E_-(x) = \{ - e^{mx} + e^{Kx}\}\ D\ E_s(0)$$

$$E_s(x) = E_s(0)\ e^{Kx}$$

The expression for the radiance contribution of layer dx is:

$$\pi dL(x) = \{-(u/h+v)D\ e^{mx} + (uC+vD+w)e^{Kx}\}E_s(0).dx$$

The hot-spot reflectance, r_∞, is found after integration of dL(x):

$$r_\infty = -D(u+hv)/hm + (uC+vD)/K + w/K$$

The terms added to the single scattering reflectance are corresponding with single and multiple diffuse scattering. In particular in the near infrared the multiple scattering will attribute substantially to the total reflectance.

I2.2. Hot-spot reflectance of multiple layer canopies

As the simplest case a two-layer canopy is considered.
The single scattering reflectance term is given by:

$$r_b = w1/K1.(1-e^{-K1}) + w2/K2.(1-e^{-K2}).e^{-K1} + \rho_s e^{-(K1+K2)}$$

For the view angle with $tg\Theta_o = 4/\pi$ Suits' model is equal to:
$r_b = \rho_s + (\rho_2 - \rho_s)\, B_t + (\rho_1 - \rho_2)\, B_1$
with B_1 and B_t being the apparent cover of layer 1 and the total canopy.
For dense canopies the single scattering reflectance is equal to ρ_1.

I2.3. Hot-spot reflectance of a thick uniform layer with different optical properties

Consider a Suits' canopy with a large LAI composed by scattering components with different optical properties. The average values of the single scattering and extinction coefficients are equal to the respective sums of the contributions of the individual fractions.

$$W = W_1 + W_2 + W_3 + \ldots \qquad K = K_1 + K_2 + K_3 + \ldots$$

The total horizontally and vertically projected leaf area indices are:

$$H = H_1 + H_2 + H_3 + \ldots \qquad V = V_1 + V_2 + V_3 + \ldots$$

The single scattering reflectance in the hot-spot for $\Theta_o = 52°$ can be written as:

$$r_b = \frac{\rho_1(H_1 + 0.81V_1) + \rho_2(H_2 + 0.81V_2) + \ldots}{H + 0.81V}$$

For the chosen oblique view angle this term can be approximated by:

$$r_b = f_1\rho_1 + f_2\rho_2 + \ldots$$

in which f_1, f_2, ... are the fraction of the total leaf area index, with a hemispherical reflectance of the corresponding components ρ_1, ρ_2, ...

I3. Hot-spot reflectance for a ground-based configuration

The principles described in the previous sections have lead to the development of a ground-based instrument. The main difference between the characteristics of such an instrument and the principles derived is dealing with the use of a diverging radiant flux instead of a collimated flux. In this section equations are derived which describe the interaction of a diverging flux with the scattering components distributed within a homogeneous canopy layer. From these equations the need to apply reflectance ratios in different spectral bands will be demonstrated. Thereafter it will be shown how the hot-spot reflectance from the artificial radiant source can be found by substraction of the directional (passive) solar reflectance.

I3.1.

The configuration of a ground-based hot-spot reflectance meter (HSM) is shown in figure 3.3. The radiant source and the sensor system are co-positioned at distance a above the canopy top. The radiant flux of the artifical source, $\emptyset(t)$, changes in time and is directed towards the canopy within a solid angle, Ω. This angle is a conical sector with a centre off-nadir axis under angle Θ. The average irradiance at a horizontal plane at distance x, is given by:

$$E(x,t) = \frac{\emptyset(t)}{\Omega} .(a-x)^{-2}.\cos^3\Theta$$

The irradiance at the canopy top is:

$$E(0,t) = \frac{\emptyset(t)}{\Omega} .a^{-2}.\cos^3\Theta$$

The direct irradiance within the canopy at distance x (x>a) is attenuated:

$$E(x,t) = E(0,t).a^2(a-x)^{-2}.e^{Kx}$$

The canopy radiance into the direction of the sensor due to single scattering by an infinitesimal layer is described by:

$$\pi dL_c(t) = w.E(x,t).dx$$

The total radiance caused by single scattering of all elements is calculated by integration over the canopy depth (x=0 to x=-xl).

The exact solution is:

$$\pi L_c = w.a.E(0,t).F(a,x1) \text{ with } F(a,x1) = 1 - \frac{a}{x1+a}.e^{-Kx1} - Ka\ e^{Ka}.I$$

where I is defined by $\int e^{-t}.t^{-1}.dt$ over Ka to K(a + x1).

The single scattering radiance contribution of the soil is described by:

$$\pi L_s(t) = \rho_s.E(0,t).a^2.(a+x1)^{-2}.e^{-Kx1}$$

For the case that x1<<a, the contributions of canopy and soil to the single scattering reflectance are approximated by:

$$\pi L_c(t)/E(0,t) = (1-e^{-Kx1}).w/K$$

$$\pi L_s(t)/E(0,t) = \rho_s.e^{-Kx1}$$

I3.2.

The irradiance at the canopy top is inversely proportional to the square of the distance between the radiant source and the canopy top. A measurement in a single spectral band will therefore be dependent on the distance. In order to eliminate as much as possible this distance effect, two solutions are applied:
a. Rationing of radiance values measured in different spectral bands.
b. Satisfying the condition x1<<a.
Rationing in two spectral bands gives as result for the exact solution:

$$\frac{L(\lambda1,t)}{L(\lambda2,t)} = A.\ \frac{w(\lambda1).\int e^{Kx}a^2(a-x)^{-2}dx + \rho_s(\lambda1)e^{-Kx1}.a^2(a+x1)^{-2}}{w(\lambda2).\int e^{Kx}a^2(a-x)^{-2}dx + \rho_s(\lambda2)e^{-Kx1}.a^2(a+x1)^{-2}}$$

where $A = \emptyset(\lambda1,t).\Omega(\lambda2)/\emptyset(\lambda2,t).\Omega(\lambda1)$

By using a relatively large distance between the radiant source and by reduction of the solid angle by means of a mirror, the virtual radiant source will be present at large distance, fullfilling the condition x1<<a.
In this case the reflectance ratio can be written as:

$$\frac{r_b(\lambda1)}{r_b(\lambda2)} = \frac{w(\lambda1).(1-e^{-K})/K + \rho_s(\lambda1)e^{-K}}{w(\lambda2).(1-e^{-K})/K + \rho_s(\lambda2)e^{-K}}$$

When a Suits' canopy is assumed and $\Theta = 52°$, the ratio can be written as:

$$\frac{r1}{r2} = \frac{\rho 1.B + \rho 1_s(1-B)}{\rho 2.B + \rho 2_s(1-B)} \qquad \text{with } B = 1-\exp(-H-0.81V)$$

I3.3.

The spectral radiance of a plant canopy is equal to the sum of the radiances attributed to the radiative transfer of power from different sources. When an active radiant source is applies, the total radiance is equal to the radiance in the hot-spot added to the (passive) radiance caused by solar and sky irradiance. The hot-spot radiance itself is found by substraction of the radiance measured at time t_m during illumination by the active radiant source and the passive radiance assessed at time t_m.

APPENDIX II.

HSM calibration algorithms

The analog detector signal in each spectral band is proportional to the radiance of the object observed at the entrance pupil of the sensor.

$$S_o(\lambda_i) = H_o(\lambda_i)\, L_o(\lambda_i)$$

The transfer function $H(\lambda)$ is given by:

$$H(\lambda) = A.\Omega.T(\lambda).Q(\lambda).G(\lambda)$$

A : area of entrance pupil
Ω : field of view
$T(\lambda)$: optical transmittance in wavelength interval, λ_i
$Q(\lambda)$: quantum efficiency of the detector
$G(\lambda)$: gain factor (low and high).

For each sensor detector a low and high gain amplifier is applied. The values measured in the high gain mode are applied for the range of low radiant intensity values.

The sensor signals can show variation as a function of time during the sequence of an active HSM measurement.
The contribution Sp due to the presence of solar irradiance should be assessed at time t1 which corresponds with the moment of maximum flash light intensity. The signals Sp are measured 5 msec prior and after the active measurement at respectively t0 and t2. The assessment of the passive contribution is performed by linear interpolation.

$$Sp(t1) = (Sp(t0) + Sp(t2)/2$$

The signal value attributed to the hot-spot radiance Sh, is obtained by substraction of the signals for the active and the passive measurements at time t1:

$$Sh = Sa - Sp = H(La-Lp) = H.L$$

The hot-spot radiance value L is described by:

$$\pi L(t1).\Omega_a = r.\cos^3\Theta.a^{-2}.\phi(t1)$$

where r is the hot-spot reflectance and a is the distance of the flash to the canopy top.

The hot spot signal value can be written as:

$Sh(t1) = J.r.a^{-2}.\phi(t1)$, with J as a constant.

The reference signal value measured from the radiant source is proportional to the flux $\phi(t1)$. The irradiance at the fiber entrance during the flash is equal to the sum of the irradiance caused by the flash itself and the passive (solar) irradiance.

$$Sr(t1) = Sf(t1) + Sp(t1) = H'\{Ef(t1) + Ep(t1)\}$$

The passive contribution is estimated from linear interpolation of the signals at t0 and t2.

When the fiber entrance irradiance due to the flash is expressed by: $Ef = \beta.\phi(t1)$
Sf becomes: $Sf = H'.\beta.\phi(t1)$

By taking the ratio between the hot-spot signal value and the irradiance at the fiber entrance, the flux value ϕ is eliminated.

$$R(t1) = \frac{Sh}{Sf} = r.a^{-2}.J/(H'.\beta)$$

The dependance of the vertical distance between the virtual source and the canopy top is eliminated by calculation of the ratio between $R(t_1)$ for two different spectral bands (i and j).

$$V_{ij} = A_{ij}.r_i/r_j$$

The constants A_{ij} have been determined by the measurement of the ratios V_{ij} of an extended white object. The reflectance ratios of this white object have been measured relative to the reflectance ratios for the same spectral bands of a standard reflectance panel. This panel has been coated with Kodak White Reflectance Paint.

By means of a monochromator and a radiometer, the reflectance ratios of the white object and the standard panel have been determined.
The radiometer ratio values for both calibration objects can be expressed by:

$$R_{w,ij} = (\rho_{w,i}/\rho_{w,j}).(E_i/E_j)$$

$$R_{r,ij} = (\rho_{r,i}/\rho_{r,j}).(E_i/E_j)$$

The reflectance of the white object is given by ρ_w. The reflectance of the standard reference panel is given by ρ_r. The irradiance due to the monochromatic radiant source is given by E.
The measurement of ratio V for the standard white object is equal to:

$$V_{w,ij} = A_{ij}.\rho_{w,i}/\rho_{w,j}$$

The reflectance ratio of the standard white object is found from the ratio between R_w and R_r, which results in the equations for the calibration factors C_{ij}.

$$C_{ij} = A_{ij}(\rho_{r,i}/\rho_{r,j}) = V_w/(R_w/R_r)$$

The following values of the calibration factors have been measured by TPD in April 1984.

λ_i	λ_j	C_{ij}
870	670	2.4814
870	550	3.4722
550	670	0.7179

The calibrated hot-spot reflectance ratio values of an object relative to the reflectance ratios of the standard reference are found by dividing the measured V_{ij} by C_{ij}. When the reflectance of the reference panel for both wavelengths i and j are supposed to be equal: $V_{ij}/C_{ij} = r_i/r_j$

The ratios between the high and low gain analog amplification values for the three spectral bands are:

λ	G(h)/G(L)
550	9.948
670	10.015
870	10.052

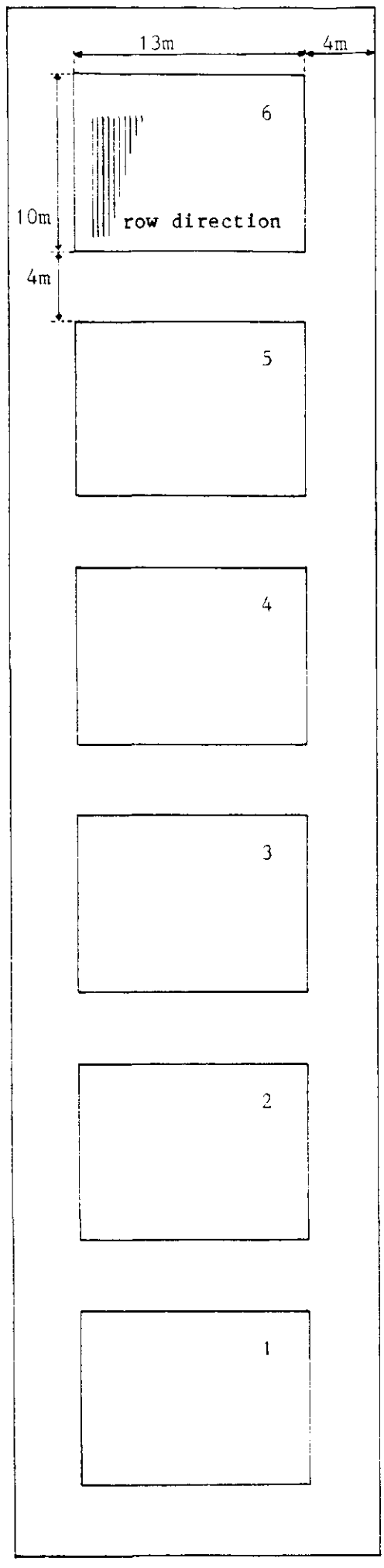

N

Appendix III

Test site Wageningen 1982.

Kavel 7

Testfarm "Droevendaal"

All fields are sown in with winter wheat (Tundra). The row direction is the same for all fields.

field no.	fungicide	fertilizer (kg. N.)
1	no	50
2	no	50 + 50 + 50
3	no	50 + 150
4	yes	50
5	yes	50 + 50 + 50
6	yes	50 + 150

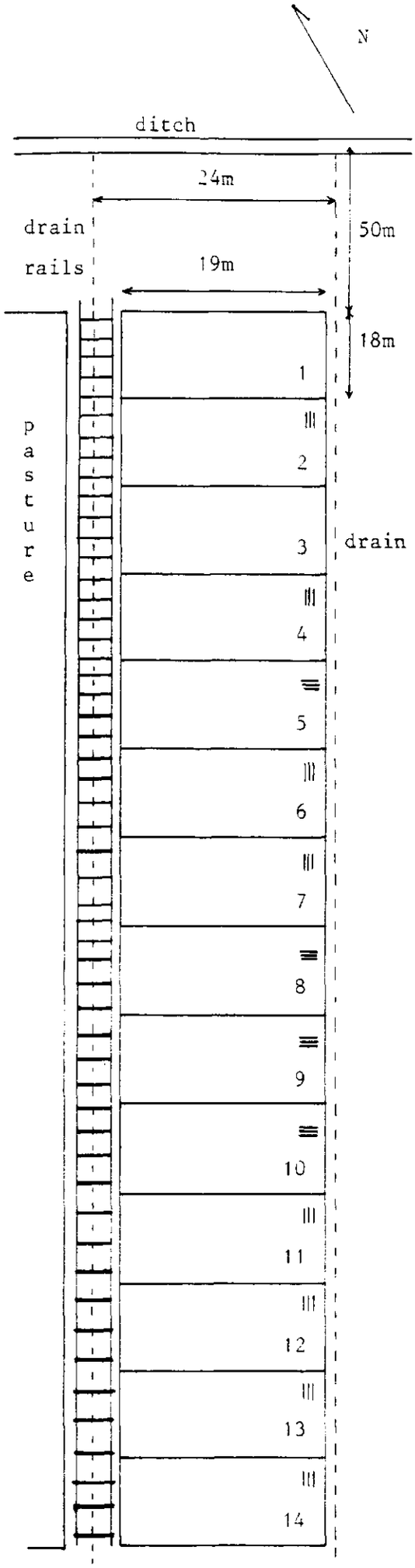

Appendix III

Test site Flevoland 1983.

Kavel 26, fields 6 and 7

Testfarm "De Schreef"
Roodbeenweg 9
Dronten

≡ row direction

field no.	crop
1	Grass, mixture.
2	Sugarbeet, monohil.
3	Bare soil.
4	Potatoes, bintje.
5	Maize, LG 11.
6	Oats, leanda.
7	Barley, audley.
8	Potatoes, bintje.
9	Beans, prelude.
10	Winter wheat, arminda.
11	Winter wheat, okapi.
12	Winter wheat, donjon.
13	Winter wheat, arminda.
14	Winter wheat, durin.